

*Electronic Supplementary Materials for*

**NIR Absorbing Aromatic (Antiaromatic) Vinylogous Carbasapphyrins  
(3.3.1.0.1) with built-in Fused Dipolar Aromatic Hydrocarbon: Synthesis and Characterization**

Sumit Sahoo,<sup>a</sup> Gunasekaran Velmurugan,<sup>b</sup> Buddhadeb Chakraborty,<sup>a</sup> Peter Comba\*<sup>b</sup> and Harapriya Rath\*<sup>a</sup>

<sup>a</sup> School of Chemical Sciences, Indian Association for The Cultivation of Science, 2A/2B Raja S. C. Mullick Road, Jadavpur, Kolkata 700 032, India, E-mail: [ichr@iacs.res.in](mailto:ichr@iacs.res.in)

<sup>b</sup> Heidelberg University, Institute of Inorganic Chemistry and Interdisciplinary Center for Scientific Computing, Im Neuenheimer Feld 270, 69120 Heidelberg, GERMANY. E-mail: peter.comba@aci.uni-heidelberg.de

**Table of Contents**

Materials and Methods	S2-S4
General Synthetic Procedure	S5-S11
Spectroscopic Data	S12-S37
X-ray crystal Data	S38
Theoretical Calculations	S39-S68
X,Y,Z Coordinates	S69-S73

## **Materials and Methods:**

**1.1** Electronic absorption spectra were measured with a Perkin Elmer Lambda 950 UV-visible-NIR spectrophotometer.  $^1\text{H}$  NMR spectra were recorded on a Bruker AVIII 500 MHz spectrometer, Bruker AVIII 400 MHz, Bruker DPX-300 MHz spectrometer and chemical shifts were reported as the delta scale in ppm relative to  $\text{CHCl}_3$  ( $\delta$  = 7.26 ppm) and  $\text{CH}_2\text{Cl}_2$  ( $\delta$  = 5.32 ppm) as internal reference for  $^1\text{H}$  and  $^{13}\text{C}$  NMR  $\text{CHCl}_3$  ( $\delta$  = 77.00 ppm) and  $\text{CH}_2\text{Cl}_2$  ( $\delta$  = 55.00 ppm). MALDI-TOF MS data were recorded using Bruker Daltonics flex Analyser and ESI HR-MS data were recorded using Waters QTOF Micro YA263 spectrometer. All solvents and chemicals were of reagent grade quality, obtained commercially and used without further purification except as noted. For spectral measurements, anhydrous dichloromethane was obtained by refluxing and distillation over  $\text{CaH}_2$ . Dry THF was obtained by refluxing and distillation over pressed Sodium metal. Thin layer chromatography (TLC) was carried out on alumina sheets coated with silica gel 60  $F_{254}$  (Merck 5554) and gravity column chromatography were performed using Merck Silica Gel 230-400 mesh. Aluminum Oxide (Basic) grade II was purchased from Sigma Aldrich.

## **1.2 X-Ray structure determination.**

A specimen of  $\text{C}_{58}\text{H}_{51}\text{N}_2\text{O}_4\text{S}_2$ , approximate dimensions 0.100 mm x 0.100 mm x 0.100 mm, was used for the X-ray crystallographic analysis. The X-ray intensity data were measured ( $\lambda$  = 0.71073 Å).

The total exposure time was 3.63 hours. The frames were integrated with the Bruker SAINT Software package using a narrow-frame algorithm. The integration of the data using an orthorhombic unit cell yielded a total of 47123 reflections to a maximum  $\theta$  angle of 25.50° (0.83 Å resolution), of which 5132 were independent (average redundancy 10.931, completeness = 99.4%,  $R_{\text{int}}$  = 3.17%,  $R_{\text{sig}}$  = 1.53%) and 3828 (88.80%) were greater than  $2\sigma$  ( $F^2$ ). The final cell constants of  $a$  = 22.5989(8) Å,  $b$  = 20.6160(7) Å,  $c$  = 9.7234(3) Å, volume = 4530.1(3) Å<sup>3</sup>, are based upon the refinement of the XYZ-centroids of 9880 reflections above 20  $\sigma$  ( $I$ ) with  $4.560^\circ < 2\theta < 54.14^\circ$ . Data were corrected for absorption effects using the Multi-Scan method (SADABS). The ratio of minimum to maximum apparent transmission was 0.835. The calculated minimum and maximum transmission coefficients (based on crystal size) are 0.9830 and 0.9830. The structure was solved and refined using the Bruker SHELXTL Software Package, using the space group P n m a, with  $Z$  = 4 for the formula unit,  $\text{C}_{58}\text{H}_{51}\text{N}_2\text{O}_4\text{S}_2$ . The final anisotropic full-matrix least-squares refinement on  $F^2$  with 284 variables converged at  $R1$  = 7.08%, for the observed data and  $wR2$  = 19.83% for all data. The goodness-of-fit was 1.060. The largest peak in the final difference electron density synthesis was 0.963 e $^-$ /Å<sup>3</sup> and the largest hole was -0.533 e $^-$ /Å<sup>3</sup> with an RMS deviation of 0.060 e $^-$ /Å<sup>3</sup>. On the basis of the final model, the calculated density was 1.153 g/cm<sup>3</sup> and F (000), 1908 e $^-$ .

To be noted that solvent has been squeezed out since hydrogens on the solvent atoms were leading to non-convergence of the refinement (oscillatory shifts) due to symmetry. The carbonyl group of acetyl substituent is disordered over two sites in 1:3 ratio and the terminal C28 atom resides on the mirror plane hence treated with fixed occupancy of 0.5 (0.25 for each disordered part). However, the B ALERTS and slight high residual densities near C26 atom (part of 6 membered ring) are probably due to disorder, which has not been treated due to the non-convergence of refinement influenced by symmetry.

### 1.3 Theoretical Calculation

The ground-state geometry of the macrocycles were fully optimized at the DFT level using B3LYP<sup>1</sup> with 6-31G (d, p) basis set. These fully optimized stationary points were further characterized by harmonic analysis to ensure that all the structures are minima on the potential energy surface. Over the years, polarized continuum model (PCM)<sup>2</sup> has been reported to be the most successful and cost effective model to examine the solvent effect. We have used dichloromethane as solvent. Further the time dependent density functional theory (TD-DFT)<sup>3</sup> has been used to compute the electronic absorption spectra, singlet vertical excitation energies and oscillator strengths on the ground state optimized geometries. All computations were carried out with Gaussian 16 program package.<sup>4</sup> The quantum theory of atoms in molecules has been computed using AIM200 program.<sup>5</sup> The contribution of various fragments towards their HOMO and LUMO has been analyzed using QMForge Program.<sup>6</sup> The NICS indices are defined as theoretically computed negative values of the absolute magnetic shielding. The difference between NICS(0) and NICS(1) is the point at which the magnetic shielding value is calculated. The NICS(0) value is determined at the geometrical center of the ring under consideration,<sup>7</sup> whereas the NICS(1) value is calculated 1 Å above the center of the mean plane of the ring being studied.<sup>8</sup> Schleyer et al., introduced the summation of the NICS values as a global aromaticity index. As a result, the summation of NICS values for a given polycyclic system produces a single quantity called the “total NICS” ( $\sum \text{NICS}(1)$ ).<sup>9</sup> The NMR shielding tensors were computed, using B3LYP/6-31G (d, p) method, with the Gauge-Independent Atomic Orbital (GIAO) at the center of rings.<sup>10</sup> On the other hand, the harmonic oscillator model of aromaticity (HOMA) index was also used to determine the aromaticity of the proposed compounds.<sup>11</sup> The anisotropy of the current (induced) density (ACID) has been done using ACID plot.<sup>12</sup> Graphical representations of ELF have been visualised in the Multiwfn.<sup>13</sup>

### References:

- 1 (a) A. D. Becke, Density-Functional Thermochemistry. III. The Role of Exact Exchange, *J. Chem. Phys.*, 1993, **98**, 5648–5662; (b) J. P. Perdew, Density-functional approximation for the correlation energy of the inhomogeneous electron gas, *Phys. Rev. B*, 1986, **33**, 8822–8824; (c) A. D. Becke, Density-functional exchange-energy approximation with correct asymptotic behaviour, *Phys. Rev. A.*, 1988, **38**, 3098–3100; (d) C. Lee, W. Yang and R. G. Parr, Development of the Colle-Salvetti correlation-energy formula into a functional of the electron density, *Phys. Rev. B*, 1988, **37**, 785–789.
- 2 (a) M. Cossi, G. Scalmani, N. Rega and V. Barone, New Developments in the Polarizable Continuum Model for Quantum Mechanical and Classical Calculations on Molecules in Solution, *J. Chem. Phys.*, 2002, **117**, 43–54; (b) E. Cancès, B. Mennucci and J. Tomasi, A New Integral Equation Formalism for the Polarizable Continuum Model: Theoretical Background and Applications to Isotropic and Anisotropic Dielectrics, *J. Chem. Phys.*, 1997, **107**, 3032–3041; (c) B. Mennucci and J. Tomasi, Continuum solvation models: A New Approach to the Problem of Solute's Charge Distribution and Cavity Boundaries, *J. Chem. Phys.*, 1997, **106**, 5151–5158.
- 3 (a) E. Runge and E. K. U. Gross, Density-Functional Theory for Time-Dependent Systems, *Phys. Rev. Lett.*, 1984, **52**, 997–1000; (b) R. E. Stratmann, G. E. Scuseria and M. J. Frisch, An efficient implementation of time-dependent density-functional theory for the calculation of excitation energies of large molecules, *J. Chem. Phys.*, 1998, **109**, 8218–8224; (c) R. Bauernschmitt and R. Ahlrichs, Treatment of Electronic Excitations within the Adiabatic Approximation of Time Dependent Density Functional Theory, *Chem. Phys. Lett.*, 1996, **256**, 454–464.
- 4 M. Frisch, G. Trucks, H. Schlegel, G. Scuseria, M. Robb, J. Cheeseman, G. Scalmani, V. Barone, B. Mennucci, G. Petersson, H. Nakatsuji, M. Caricato, X. Li, H. Hratchian, A. Izmaylov, J. Bloino, G. Zheng, J. Sonnenberg, M. Hada, M. Ehara, K. Toyota, R. Fukuda, J. Hasegawa, M. Ishida, T. Nakajima, Y. Honda, O. Kitao, H. Nakai, T. Vreven, J. Montgomery, Jr, J. E. Peralta, F. Ogliaro, M. Bearpark, J. J. Heyd, E. Brothers, K. N. Kudin, V. Staroverov, R. Kobayashi, J. Normand, K. Raghavachari, A. Rendell, J. Burant, S. Iyengar, J. Tomasi, M. Cossi, N. Rega, N. Millam, M. Klene, J. E. Knox, J. B. Cross, V. Bakken, C. Adamo, J. Jaramillo, R. Gomperts, R. Stratmann, O. Yazyev, A. Austin, R. Cammi, C. Pomelli, J. Ochterski, R. L. Martin, K. Morokuma, V. Zakrzewski, G. Voth, P. Salvador, J. Dannenberg, S. Dapprich, A. Daniels, Ö. Farkas, J. Foresman, J. Ortiz, J. Cioslowski, D. Fox, Gaussian 16, revision C. 01, Gaussian, Inc., Wallingford, CT 2010.
- 5 (a) F. Biegler-König and J. Schönbohm, Update of the AIM2000-Program for Atoms in Molecules, *J. Comput. Chem.*, 2002, **23**, 1489; (b) R. Bader, McMaster University, Hamilton, Canada, 2000.

- 6 (a) A. Tenderholt, "QMForge: A Program to Analyze Quantum Chemistry Calculations", Version 2.3.2, <http://qmforge.sourceforge.net>; (b) G. Velmurugan and P. Venuvanalingam, Luminescent Re(I) Terpyridine Complexes for OLEDs: What Does the DFT/TD-DFT Probe Reveal?, *Dalton Trans.*, 2015, **44**, 8529–8542; (c) G. Velmurugan, B. K. Ramamoorthi and P. Venuvanalingam, Are Re(I) Phenanthroline Complexes Suitable Candidates for OLEDs? Answers from DFT and TD-DFT investigations, *Phys. Chem. Chem. Phys.*, 2014, **16**, 21157–21171; (d) G. Velmurugan, S. A. Vedha and P. Venuvanalingam, Computational Evaluation of Optoelectronic and Photophysical Properties of Unsymmetrical Distyrylbiphenyls, *RSC Adv.*, 2014, **4**, 53060–53071.
- 7 P. V. R. Schleyer, C. Maerker, A. Dransfeld, H. Jiao and N. J. R. V. E. Hommes, Nucleus-Independent Chemical Shifts: A Simple and Efficient Aromaticity Probe, *J. Am. Chem. Soc.*, 1996, **118**, 6317–6318.
- 8 K. K. Zborowski, I. Alkorta, J. Elguero and L. M. Proniewicz, Calculation of the HOMA Model Parameters for the Carbon-Boron Bond, *Struct. Chem.*, 2012, **23**, 595–600.
- 9 P. V. R. Schleyer, M. Manoharan, H. Jiao and F. Stahl, The Acenes: Is There a Relationship between Aromatic Stabilization and Reactivity?, *Org. Lett.*, 2001, **3**, 3643–3646.
- 10 K. Wolinski, J. F. Hinton and P. Pulay, Efficient Implementation of the Gauge-Independent Atomic Orbital Method for NMR Chemical Shift Calculations, *J. Am. Chem. Soc.*, 1990, **112**, 8251–8260.
- 11 S. Ostrowski and J. C. Dobrowolski, What Does the HOMA Index Really Measure?, *RSC Adv.*, 2014, **4**, 44158–44161.
- 12 (a) D. Geuenich, K. Hess, F. Köhler and R. Herges, Anisotropy of the Induced Current Density (ACID), a General Method To Quantify and Visualize Electronic Delocalization, *Chem. Rev.*, 2005, **105**, 3758–3772; b) R. Herges and D. Geuenich, Delocalization of Electrons in Molecules, *J. Phys. Chem. A*, 2001, **105**, 3214–3220.
- 13 T. Lu and F. Chen, Multiwfn: A Multifunctional Wavefunction Analyzer, *J. Comput. Chem.*, 2012, **33**, 580–592.

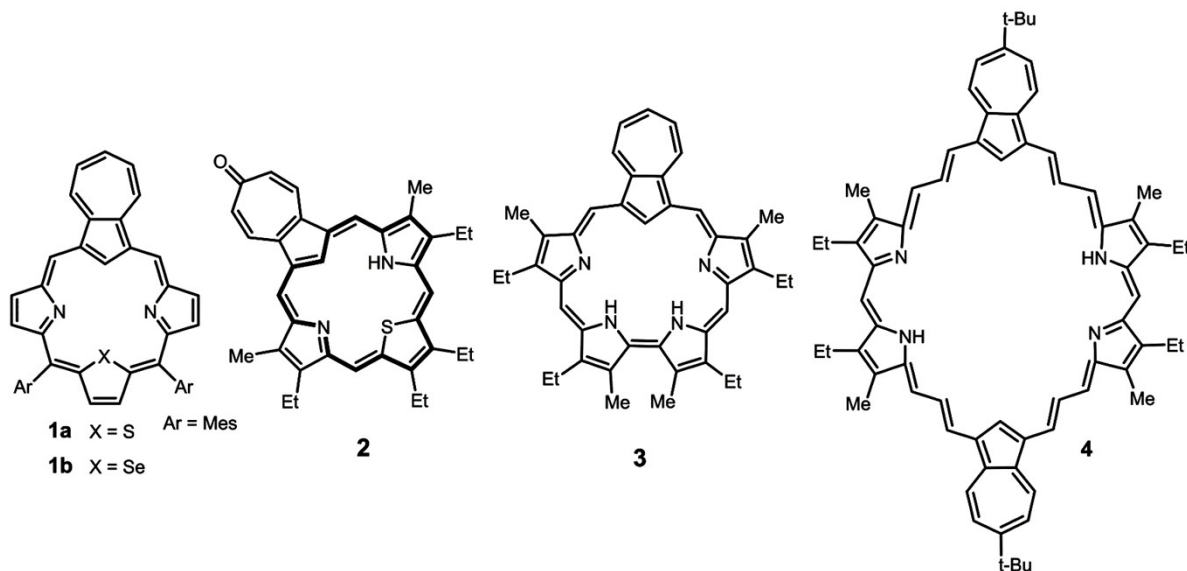
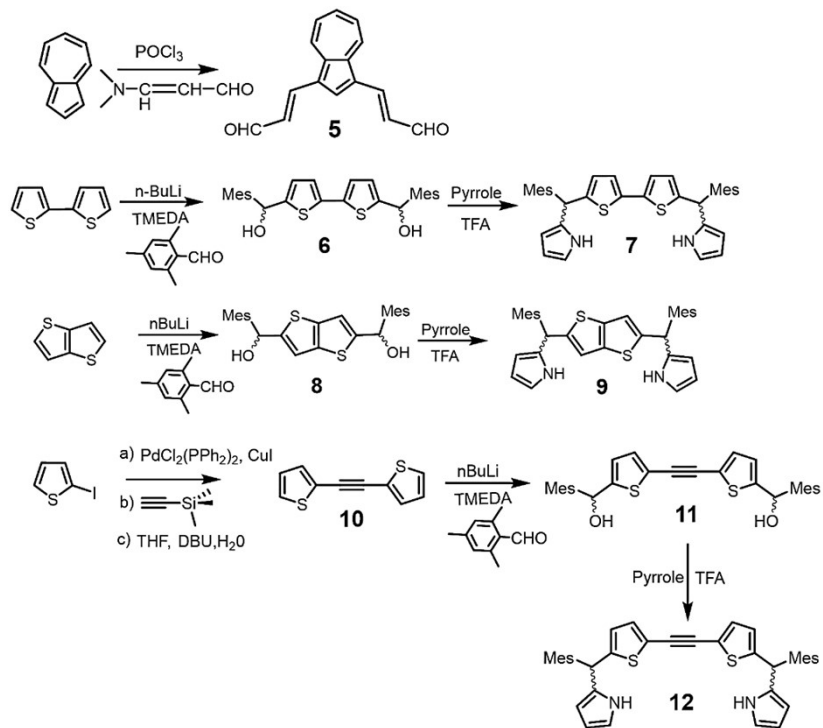
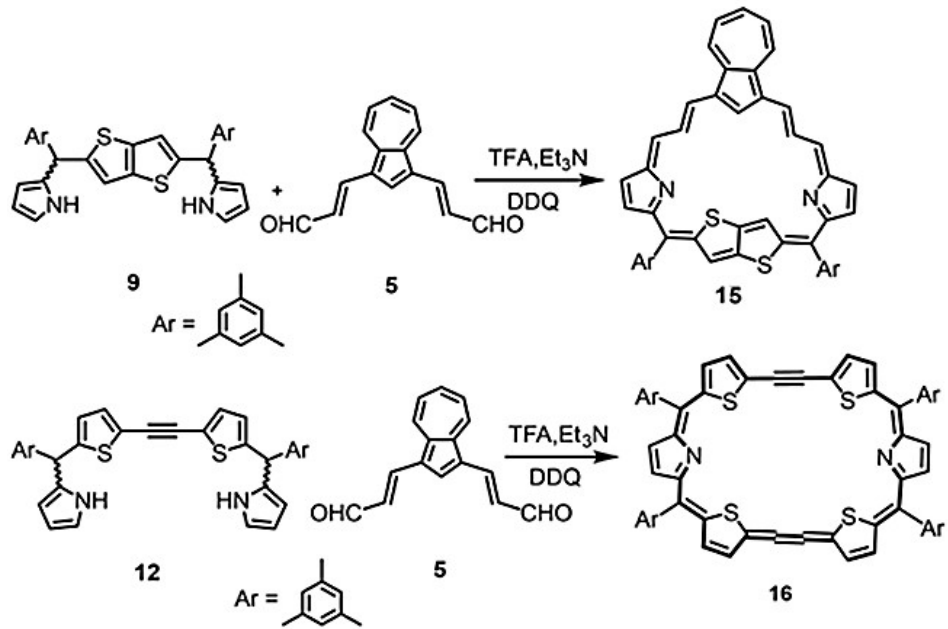


**Chart S1.** Representative examples of azuli porphyrinoids and vinylogous azuli porphyrinoids

#### 1.4 Synthesis:



**Scheme S1.** Synthesis of all precursors used for the macrocycles reported in the manuscript



**Scheme S2.** Synthesis of porphyrinoids **15/16** reported in the manuscript

**Synthesis of 5:** Phosphorus oxychloride (0.45 g, 2.96 mmol) was added dropwise to a stirred solution of azulene (200 mg; 1.56 mmol) and 3-dimethylaminoacrolein (0.5 mL; 5.15 mmol) in dichloroethane (40 mL) while maintaining the temperature below 10°C. The reaction mixture was stirred under reflux overnight. 2.5 M sodium hydroxide solution (20 mL) was added and the biphasic mixture was stirred for

an additional 10 min. After cooling to room temperature, the mixture was extracted with chloroform and washed with water. The solvent was removed on a rotary evaporator. The residue was run through a silica gel column eluting with chloroform to give the desired compound **5** as a dark brown powder. Yield 310 mg (83%).  $R_f$  0.4 (Hexane/EtOAc = 4:1). Mp 228-230°C

HR-ESI-TOF MS (*m/z*) 237.0916 [M+H]<sup>+</sup> (236.0837 calc. for [C<sub>16</sub>H<sub>12</sub>O<sub>2</sub>]<sup>+</sup>). Elemental analysis: Calc. for C<sub>16</sub>H<sub>12</sub>O<sub>2</sub>: C, 81.34; H, 5.12. Found: C, 81.36; H, 5.15.

<sup>1</sup>H NMR (300 MHz, CDCl<sub>3</sub>, 300 K, δ [ppm]): 9.79 (2H, d, J = 7.5 Hz), 8.64 (d, 2H, J = 10 Hz), 8.53 (1H, s), 8.03 (d, 2H, J = 15.5 Hz), 7.88 (t, 1H, J = 10 Hz), 7.57 (t, 2H, J = 10 Hz), 6.87 (d, 2H). <sup>13</sup>C NMR (75 MHz, CDCl<sub>3</sub>, 300 K, δ [ppm]): 31.06, 125.23, 127.59, 128.62, 133.96, 135.15, 141.05, 142.47, 142.77, 193.47.

**Synthesis of 6:** To a solution of 2, 2'-bithiophene (0.5 g, 3 mmol) in 20 mL of n-hexane containing N,N,N',N'-tetramethylenediamine (1.35 mL, 9.02 mmol) under argon atmosphere, n-butyl lithium (1.6 M) (5.6 mL, 9.02 mmol) was added slowly and was stirred at room temperature for two hours and later refluxed for two hours. The reaction was then allowed to attain room temperature. Mesitaldehyde (1.33 mL, 9.02 mmol) was dissolved in 20 mL of tetrahydrofuran (THF) and was added drop wise to the reaction mixture in ice-cold condition. After the addition, the reaction mixture was allowed to attain the room temperature and was stirred for an additional two hours. The reaction was quenched with saturated ammonium chloride solution and was stirred for half an hour. This was then extracted with ethyl acetate (100 mL). The organic layer was washed with brine and dried over anhydrous sodium sulphate. The crude product obtained on evaporation of the solvent was recrystallized from toluene. The solid obtained was identified as **6**. Yield ~790 mg (57%).  $R_f$  0.29 (Hexane/EtOAc = 9:1), Mp 137°C (decomposed).

HR-ESI-TOF MS (*m/z*) 445.1558 [M-OH]<sup>+</sup> (462.1687. calc. for [C<sub>28</sub>H<sub>30</sub>O<sub>2</sub>S<sub>2</sub>]<sup>+</sup>). Elemental analysis: Calc. for C<sub>28</sub>H<sub>30</sub>O<sub>2</sub>S<sub>2</sub>: C, 72.69; H, 6.54. Found: C, 72.72; H, 6.56.

<sup>1</sup>H NMR (300 MHz, CDCl<sub>3</sub>, 300 K, δ [ppm]): 6.91 (d, 2H, J = 10.4 Hz), 6.86 (s, 4H), 6.51 (d, 2H, J = 10.4 Hz), 6.39 (br, 2H), 2.33 (s, 12H), 2.28 (s, 6H). <sup>13</sup>C NMR (75 MHz, CDCl<sub>3</sub>, 300 K, δ [ppm]): 20.62, 21.02, 69.45, 123.17, 124.4, 130.28, 135.52, 136.97, 137.07, 137.87, 146.52.

**Synthesis of 7:** Compound **6** (1 g, 2.16 mmol) was dissolved in pyrrole (30 mL, 0.432 mol). The solution was stirred for 45 min under nitrogen atmosphere at room temperature. Trifluoroacetic acid (0.1 mL) was added and stirred for 1 h. The reaction mixture was quenched by dichloromethane; product was neutralized by NaOH (aq) solution, extracted by dichloromethane, dried over Na<sub>2</sub>SO<sub>4</sub>, and dried in rotary evaporator to give yellow oil. The crude product was purified by silica gel chromatography using ethyl acetate–hexane (10:90) solution. Compound **7** was obtained as light-yellow foam.

Yield 0.604 g (50%).  $R_f$  0.4 (Hexane/EtOAc = 4:1). HR-ESI-TOF MS (*m/z*) 559.7001 [M<sup>+</sup>] (560.2320. calc. for [C<sub>36</sub>H<sub>36</sub>N<sub>2</sub>S<sub>2</sub>]<sup>+</sup>). Elemental analysis: Calc. for C<sub>36</sub>H<sub>36</sub>N<sub>2</sub>S<sub>2</sub>: C, 77.1; H, 6.47; N, 5. Found: C, 77.12; H, 6.49; N, 4.98.

<sup>1</sup>H NMR (300 MHz, CDCl<sub>3</sub>, 300 K, δ [ppm]): 2.14 (s, 12H,-Me), 2.28 (s, 6H, -Me), 6.02 (s, 2H,-CH), 6.10 (br, 2H, β-H pyrrole), 6.16 (dd, 2H, β-H pyrrole), 6.67 (d, 2H, J = 4.5, β-H pyrrole), 6.71 (d, 2H, thiophene), 6.87 (s, 4H,-CH), 6.91 (d, 2H, β-H thiophene), 7.86 (br, 2H, -NH). <sup>13</sup>C NMR (75 MHz, CDCl<sub>3</sub>, 300 K,

$\delta$  [ppm]): 20.95, 29.45, 40.66, 107.13, 108.67, 116.51, 122.76, 126.30, 130.51, 131.94, 135.58, 136.28, 136.94, 137.54.

**Synthesis of 8:** To a 250 mL round-bottomed flask equipped with a magnetic bar, thieno [3, 2-b] thiophene (1 g, 7.13 mmol) was placed followed by dry THF (40 mL). The reaction mixture was stirred under inert atmosphere. N, N, N', N'-Tetramethyl ethylenediamine (3.2 mL, 0.021 mol) was added followed by stirring for half an hour at room temperature. Afterward, n-BuLi in hexane (1.6 M) (13.04 mL, 0.021 mol) was added through rubber septa drop wise, yellow turbidity started forming. The reaction mixture was stirred at room temperature for 2 hours and then heated to 66°C for 1 hour. The reaction mixture was brought room temperature after which it was brought to ice cold temperature. At ice cold temperature, Mesitaldehyde (2.62 mL, 0.017 mol) in dry THF (40 mL) was then added drop wise to the reaction mixture, the reaction mixture was stirred for 2 hours. The reaction mixture was quenched by saturated NH<sub>4</sub>Cl (aq) solution, product was extracted by diethyl ether, dried over Na<sub>2</sub>SO<sub>4</sub>. The crude product was precipitated out by hexane and purified by silica gel column chromatography using ethyl acetate-hexane (1:4) solution. The solvent was evaporated and light-yellow solid was obtained.

Yield 2.09 g (67%). R<sub>f</sub> 0.2 (Hexane/EtOAc = 9:1). Mp 156°C.

HR-ESI-TOF MS (*m/z*) 459.02 [M + Na]<sup>+</sup> (436.63. calc. for [C<sub>26</sub>H<sub>28</sub>O<sub>2</sub>S<sub>2</sub>]<sup>+</sup>). Elemental analysis: Calc. for C<sub>26</sub>H<sub>28</sub>O<sub>2</sub>S<sub>2</sub>: C, 71.52; H, 6.46. Found: C, 71.54; H, 6.48.

<sup>1</sup>H NMR (500 MHz, CDCl<sub>3</sub>, 300 K,  $\delta$  [ppm]): 2.28 (s, 6H), 2.33 (s, 12H), 6.46 (s, 2H), 6.71 (s, 2H), 6.87 (s, 4H). <sup>13</sup>C NMR (125 MHz, CDCl<sub>3</sub>, 300 K,  $\delta$  [ppm]): 20.66, 29.84, 69.82, 116.41, 130.92, 135.36, 137.02, 137.92, 138.30, 148.88.

**Synthesis of 9:** Compound 8 (1g, 2.29 mmol) was dissolved in pyrrole (15 mL, 0.19 mol). The solution was stirred for 45 minutes under nitrogen atmosphere at room temperature. Trifluoroacetic acid (0.05 mL, 0.22 mmol) was added and stirred for 1 hour. The reaction mixture was quenched by dichloromethane; product was neutralized by NaOH (aq) solution, extracted by dichloromethane, dried over Na<sub>2</sub>SO<sub>4</sub> and dried in rotary evaporator to give yellow oil. The crude product was purified by silica gel chromatography using 10% ethylacetate-hexane mixture. Compound 9 was obtained as light yellow foam. Yield 0.702 g (57%). R<sub>f</sub> 0.3 (Hexane/EtOAc = 4:1).

HRMS (*m/z*) 534.4229 [M<sup>+</sup>] (534.78 calc. for C<sub>34</sub>H<sub>34</sub>N<sub>2</sub>S<sub>2</sub>). Elemental analysis: Calc. for C<sub>34</sub>H<sub>34</sub>N<sub>2</sub>S<sub>2</sub>: C, 76.36; H, 6.41; N, 5.24. Found: C, 76.38; H, 6.43; N, 5.23.

<sup>1</sup>H NMR (500 MHz, CDCl<sub>3</sub>, 300K,  $\delta$  [ppm]): 2.03 (s, 6H, -Me), 2.29-2.35 (s, 12H, -Me), 4.24 (s, 2H,-CH), 6.03 (br, 1H,  $\beta$ -H of pyrrole), 6.13 (s, 1H,  $\beta$ -H of thienothiophene), 6.23 (d, 1H, J = 4.5 Hz,  $\beta$ -H of pyrrole), 6.30 (d, 1H, J = 4.5 Hz,  $\beta$ -H of pyrrole), 6.54 (br, 1H,  $\beta$ -H of pyrrole), 6.69 (s, 1H,  $\beta$ -H of thienothiophene), 6.70-6.71 (m, 1H,  $\beta$ -H of pyrrole), 6.72-6.73 (m, 1H,  $\beta$ -H of pyrrole), 6.86 (s, 2H, Mesityl-CH), 6.92 (s, 2H, Mesityl-CH), 7.99 (br, 1H, -NH), 8.50 (br, 1H, -NH). <sup>13</sup>C NMR (125 MHz, CDCl<sub>3</sub>, 300 K,  $\delta$  [ppm]): 20.15, 20.74, 20.97, 21.11, 22.90, 30.85, 41.24, 107.47, 108.56, 109.26, 109.43, 117.01, 117.47, 118.91, 124.71, 126.35, 129.29, 130.68, 133.32, 134.03, 135.96, 136.44, 136.52, 136.87, 137.00, 137.15, 137.18, 137.53, 145.55.

**Synthesis of 10:** To an oven-dried 25 mL round-bottom flask were added Pd(PPh<sub>3</sub>)<sub>2</sub>Cl<sub>2</sub> (67.4 mg, 6 mol %), CuI (30.5 mg, 10 mol %), and 2-iodothiophene (0.17 mL, 1.6 mmol), and the flask was purged with argon. Argon-purged anhydrous toluene (8 mL) and DBU (1.43 mL, 6 equiv) were added successively by syringe. Ice-chilled trimethylsilyl ethyne (104.5  $\mu$ L, 0.50 equiv) was then added by syringe, followed immediately by distilled water (11.5  $\mu$ L, 40 mol %). The reaction flask was covered by aluminum foil and stirred for 18 hours at RT. Then the reaction mixture was partitioned in ethyl ether and distilled water (50 mL each). The organic layer was washed with 10% HCl (3  $\times$  75 mL) and saturated aqueous NaCl (75 mL) and dried over MgSO<sub>4</sub>. The crude product was purified by silica gel column chromatography (eluent: EtOAc/petroleum ether). Yield: 130.9 mg, 86%. R<sub>f</sub> 0.16 (Hexane). Mp 98–100°C.

HRMS (m/z) 190.1130 [M]<sup>+</sup> (189.99 calc. for C<sub>10</sub>H<sub>6</sub>S<sub>2</sub>). Elemental analysis: Calc. for C<sub>10</sub>H<sub>6</sub>S<sub>2</sub>: C, 63.12; H, 3.18. Found: C, 63.14; H, 3.19.

<sup>1</sup>H NMR (400 MHz, CDCl<sub>3</sub>, 300K,  $\delta$  [ppm]): 7.27–7.31 (m, 4H), 7.00–7.02 (m, 2H). <sup>13</sup>C NMR (100 MHz, CDCl<sub>3</sub>, 300K,  $\delta$  [ppm]): 132.2, 127.7, 127.2, 123.0, 86.3.

**Synthesis of 11:** To a 250 mL round-bottomed flask equipped with a magnetic bar, **10** (1.354 g, 7.13 mmol) was placed followed by dry THF (40 mL). The reaction mixture was stirred under inert atmosphere. N,N,N',N'-Tetramethyl ethylenediamine (3.2 mL, 0.021 mol) was added followed by stirring for half an hour at room temperature. Afterward, *n*-BuLi in hexane (1.6 M) (13.04 mL, 0.021 mol) was added through rubber septa drop wise, yellow turbidity started forming. The reaction mixture was stirred at room temperature for 2 hours and then heated to 66 °C for 1 hour. The reaction mixture was brought room temperature after which it was brought to ice cold temperature. At ice cold temperature, Mesitaldehyde (2.62 mL, 0.017 mol) in dry THF (40 mL) was then added drop wise to the reaction mixture, the reaction mixture was stirred for 2 hours. The reaction mixture was quenched by saturated NH<sub>4</sub>Cl (aq) solution, product was extracted by diethyl ether, dried over Na<sub>2</sub>SO<sub>4</sub>. The crude product was precipitated out by hexane and purified by silica gel column chromatography using ethyl acetate-hexane (1:4) solution. The solvent was evaporated and light-yellow solid was obtained. Yield 2.30 g (67%). R<sub>f</sub> 0.48 (Hexane/EtOAc = 9:1). Mp 135–137 °C.

HRMS (m/z): 509.0054 [M+Na]<sup>+</sup> (509.1585 calc. for [C<sub>30</sub>H<sub>30</sub>O<sub>2</sub>S<sub>2</sub>Na]<sup>+</sup>). Elemental analysis: Calc. for C<sub>30</sub>H<sub>30</sub>O<sub>2</sub>S<sub>2</sub>: C, 74.04; H, 6.21. Found: C, 74.06; H, 6.24.

<sup>1</sup>H NMR (500 MHz, CDCl<sub>3</sub>, 300K,  $\delta$  [ppm]): 2.28 (s, 3H), 2.31 (s, 6H), 6.39 (s, 1H); 6.52 (d, 1H, J = 3.5 Hz), 6.86 (s, 2H), 7.05 (d, 1H, J = 3.5 Hz). <sup>13</sup>C NMR (125 MHz, CDCl<sub>3</sub>, 300K,  $\delta$  [ppm]): 20.3, 20.8, 69.3, 86.4, 122.2, 123.5, 130.0, 131.9, 135.3, 136.7, 137.8, 150.2.

**Synthesis of 12:** Compound **11** (1.11 g, 2.29 mmol) was dissolved in pyrrole (15 mL, 0.19 mol). The solution was stirred for 45 minutes under nitrogen atmosphere at room temperature. Trifluoroacetic acid (0.05 mL, 0.22 mmol) was added and stirred for 1 hr. The reaction mixture was quenched by dichloromethane; followed by neutralization with NaOH (aq) solution. The crude product was extracted with dichloromethane, dried over Na<sub>2</sub>SO<sub>4</sub> and dried in rotary evaporator to give yellow oil. The crude product was purified by silica gel chromatography using 10% ethylacetate-hexane mixture. Compound **12** was obtained as light-yellow foam. Yield 0.760 g (57%). R<sub>f</sub> = 0.4 (Hexane/EtOAc = 7:3).

HR-ESI-TOF MS (*m/z*): 584.7821. [M]<sup>+</sup> (584.23 calc. for ([C<sub>38</sub>H<sub>36</sub>N<sub>2</sub>S<sub>2</sub>]<sup>+</sup>). Elemental analysis: Calc. for C<sub>38</sub>H<sub>36</sub>N<sub>2</sub>S<sub>2</sub>: C, 78.04; H, 6.2; N, 4.79. Found: C, 78.06; H, 6.21; N, 4.77.

<sup>1</sup>H NMR (500 MHz, CDCl<sub>3</sub>, 300 K, δ [ppm]): 2.11 (s, 6H, -Me), 2.28 (s, 3H, -Me), 6.06 (s, 2H, -CH), 6.13 (brs, 1H, β-H of pyrrole), 6.177 (s, 1H, β-H of pyrrole), 6.66 (d, 1H, J = 4.5, β-H of pyrrole), 6.74 (d, 1H, J = 4.5, β-H of thiophene), 7.06 (d, 1H, β-H of thiophene), 7.84 (brs, 1H, -NH). <sup>13</sup>C NMR (125 MHz, CDCl<sub>3</sub>, 300K, δ [ppm]): 20.7, 40.6, 86.2, 107.0, 108.5, 116.5, 121.4, 125.6, 130.4, 131.4, 131.6, 135.2, 136.9, 137.3, 148.2.

#### General Synthesis of 13/14:

Tetrapyrrole **7** (0.280 g, 0.5 mmol) was taken in a round bottom flask; to it 250 mL of dry DCM was added and stirred for 15 minutes under nitrogen atmosphere to get a clear solution. Azulene-1, 3-bisacrylaldehyde **5** (0.118 g, 0.5 mmol) was added to the reaction mixture and stirred for 15 minutes under dark condition. To this, 0.192 mL (2.5 mmol) CF<sub>3</sub>COOH was added and reaction mixture was stirred under nitrogen atmosphere in dark for overnight. The reaction mixture was then neutralised with 0.348 mL (2. 5 mmol) triethylamine followed by oxidation with 283 mg (1.25 mmol) of DDQ in open air. After complete removal of solvent from crude mixture by rotary evaporator, the compound was purified using basic alumina grade III where a violet colour band was eluted using dichloromethane as eluent and a deep violet colour band using 5% EtOAc- dichloromethane as eluent was obtained. These two fractions were further purified by repeated PTLCs. The desired macrocycles were isolated as extra pure crystalline solids upon further recrystallization.

Compound **13**: Yield. ~75 mg (20%). R<sub>f</sub> = 0.1 (CH<sub>2</sub>Cl<sub>2</sub>/ Hexane = 9:1). Mp > 350°C

HR-ESI-TOF MS (*m/z*): 759.2862 [M]<sup>+</sup> (759.2865 calc. for ([C<sub>52</sub>H<sub>42</sub>N<sub>2</sub>S<sub>2</sub>]<sup>+</sup>). Elemental analysis: Calc. for C<sub>52</sub>H<sub>42</sub>N<sub>2</sub>S<sub>2</sub>: C, 82.28; H, 5.58; N, 3.69. Found: C, 82.31; H, 5.59; N, 3.68.

<sup>1</sup>H NMR (500 MHz, CDCl<sub>3</sub>, 298 K, δ [ppm], TMS): 1.03 (t, 2H, <sup>3</sup>J = 15 Hz, inner *meso* CH), 2.09 (s, 12H, -CH<sub>3</sub>), 2.17 (s, 1H, inner azulene CH), 2.58 (s, 6H, -CH<sub>3</sub>), 7.26 (s, 4H, mesityl- CH), 7.52-7.54 (m, 1H, azulene-CH), 7.59 (t, <sup>3</sup>J =10 Hz, 2H, azulene-CH), 7.67 (d, <sup>3</sup>J =4.9 Hz, 2H, thiophene β-CH), 8.38-8.41 (m, 2H, pyrrole β-CH and 2H, azulene CH), 9.43- 9.46 (m, 2H, thiophene β -CH and 2H, pyrrole β -CH), 9.61 (d, 2H, <sup>3</sup>J =12 Hz, outer *meso* CH), 10.1 (d, 2H, <sup>3</sup>J =15 Hz, outer *meso* CH). <sup>1</sup>H NMR (500 MHz, CDCl<sub>3</sub>, 263 K, δ [ppm], TMS): 0.61 (t, 2H, <sup>3</sup>J =15 Hz, inner *meso* CH), 2.07 (s, 12H, -CH<sub>3</sub>), 2.19 (s, 1H, inner azulene CH), 2.59 (s, 6H, - CH<sub>3</sub>), 7.26 (s, 4H, mesityl- CH), 7.53-7.55 (m, 1H, azulene-CH), 7.65 (t, <sup>3</sup>J = 10 Hz, 2H, azulene-CH), 7.76 (d, <sup>3</sup>J =4.5 Hz, 2H, thiophene β -CH), 8.48-8.51 (m, 2H, pyrrole β- H and 2H, azulene CH), 9.52 (d, <sup>3</sup>J =4.5 Hz, 2H, pyrrole β-H), 9.58 (d, <sup>3</sup>J =5.5 Hz 2H, thiophene β-CH), 9.78 (d, 2H, <sup>3</sup>J =12 Hz, outer *meso* CH), 10.26 (d, 2H, <sup>3</sup>J =15 Hz, outer *meso* CH). UV-vis (CH<sub>2</sub>Cl<sub>2</sub>, λ [nm], ([ε [M<sup>-1</sup> cm<sup>-1</sup>×10<sup>4</sup>]] 298K) 464.31 (30.5), 504.17 (27.7), 531.16 (sh), 569.12 (26.6), 678.03 (1.2), 817.87 (5.5), 889.49 (5.4), 1111.03 (br).

Compound **14**: Yield. ~118 mg (30%). R<sub>f</sub> = 0.3 (EtOAc/CH<sub>2</sub>Cl<sub>2</sub> = 1:9). Mp > 350°C. HR-ESI-TOF MS (*m/z*): 789.2609 [M-CH<sub>3</sub>]<sup>+</sup> (805.2922 calc. for [C<sub>53</sub>H<sub>44</sub>N<sub>2</sub>O<sub>2</sub>S<sub>2</sub>]<sup>+</sup>). Elemental analysis: Calc. for C<sub>53</sub>H<sub>44</sub>N<sub>2</sub>S<sub>2</sub>O<sub>2</sub>: C, 79.07; H, 5.51; N, 3.48. Found: C, 79.08; H, 5.53; N, 3.47.

<sup>1</sup>H NMR (400 MHz, CD<sub>2</sub>Cl<sub>2</sub>, 298 K, δ [ppm], TMS): -2.77 (t, 1H, inner *meso* CH), -2.52 (s, 1H, inner OH), -2.38 (t, 1H, inner *meso* CH), -2.07 (s, 1H, -NH), 2.03 (s, 6H, -CH<sub>3</sub>), 2.05 (s, 6H, -CH<sub>3</sub>), 2.81 (s, 3H, -CH<sub>3</sub>), 2.83 (s, 3H, -CH<sub>3</sub>), 2.85 (s, 3H, keto-Me), 6.99 (s, 2H, mesityl-CH), 7.0 (br, 1H, pyrrole β-H), 7.17 (br, 1H, pyrrole β-H), 7.41 (d, 1H, <sup>3</sup>J = 4.4 Hz, thiophene β -CH), 7.49 (br, 1H, pyrrole β-H), 7.55 (m, 1H, pyrrole β-H), 7.57 (s, 2H, mesityl-CH), 7.7 (d, 1H, <sup>3</sup>J = 4.4 Hz, thiophene β -CH), 8.05 (br, 1H, thiophene β-CH), 8.47 (m, 1H, Benzene), 9.26 (br, 1H, thiophene β -CH), 9.43 (d, 1H, <sup>3</sup>J = 7.6 Hz, Benzene CH), 9.76 (s, 1H, Benzene CH), 10.23 (br, 1H, outer *meso* CH), 10.59 (br, 1H, outer *meso* CH), 11.47 (br, 1H, outer *meso* CH), 12.03 (br, 1H, outer *meso* CH). <sup>13</sup>CNMR (100 MHz, CD<sub>2</sub>Cl<sub>2</sub>, 300 K, δ [ppm]): 192.67, 167.67, 152.22, 152.05, 147.75, 147.68, 147.51, 142.96, 139.46, 139.45, 138.79, 138.70, 137.60, 136.10, 136, 135.54, 135.22, 132.65, 132.54, 131.54, 131.01, 131.00, 128.86, 128.85, 128.61, 128.18, 128.13, 124.84, 124.83, 124.05, 123.59, 121.79, 121.76, 119.09, 119.08, 115.93, 113.88, 113.87, 107.13, 65.59, 64.59, 33.92, 32.05, 30.19, 29.81, 22.81.

UV-vis-NIR λ [nm], (ε [M<sup>-1</sup> cm<sup>-1</sup> × 10<sup>4</sup>]), 298K: 419.18 (35.21), 537.41 (85.1), 587.87 (42.49), 687.94 (15.78), 992.64(5.94), 1082.9 (5.12).

General Synthesis of **15**: Tripyrrane **9** (0.267 g, 0.5 mmol) was taken in a round bottom flask; to it 250 mL of dry DCM was added and stirred for 15 minutes under nitrogen atmosphere to get a clear solution. Azulene-1, 3-bisacrylaldehyde **5** (0.118 g, 0.5 mmol was added to the reaction mixture and stirred for 15 minutes under dark condition. To this, 0.192 mL (2. 5 mmol) CF<sub>3</sub>COOH was added and reaction mixture was stirred under nitrogen atmosphere in dark for overnight. The reaction mixture was then neutralised with 0.348 mL (2.5 mmol) triethylamine followed by oxidation with 283 mg (1.25 mmol) of DDQ in open air. After complete removal of solvent from crude mixture by rotary evaporator, the compound was purified using basic alumina grade III where a reddish colour band using dichloromethane as eluent were obtained. After repeated PTLCs chromatography the compound **15** was obtained as green solid using dichloromethane as eluent.

Yield. ~92 mg (25%). R<sub>f</sub> = 0.3 (CH<sub>2</sub>Cl<sub>2</sub>/Hexane = 4:1). Mp > 350°C.

MALDI-TOF MS (*m/z*): 732.761 [M]<sup>+</sup> (732.26 calc. for ([C<sub>50</sub>H<sub>40</sub>N<sub>2</sub>S<sub>2</sub>]<sup>+</sup>). Elemental analysis: Calc. for C<sub>50</sub>H<sub>40</sub>N<sub>2</sub>S<sub>2</sub>: C, 81.93; H, 5.5; N, 3.82. Found: C, 81.96; H, 5.52; N, 3.81.

<sup>1</sup>H NMR (400 MHz, CD<sub>2</sub>Cl<sub>2</sub>, 298 K, δ [ppm], TMS): 1.1 (s, 1H, outer thiophene β -CH), 1.75 (s, 12H, -CH<sub>3</sub>), 1.78 (s, 2H, outer *meso*-CH), 1.88 (s, 2H, outer *meso*-CH), 2.05 (s, 6H, -CH<sub>3</sub>), 3.8 (br, 2H, pyrrole β-CH), 3.9 (br, 2H, pyrrole β-CH), 6.3 (s, 1H, inner β-H thiophene), 6.4 (br, 4H, *m*- CH), 6.9 (s, 1H), 7.55 (m, 2H), 7.75 (m, 3H), 8.5 (br, 2H, inner *meso* CH).

UV-vis (CH<sub>2</sub>Cl<sub>2</sub>, λ [nm], ([ε [M<sup>-1</sup> cm<sup>-1</sup> × 10<sup>3</sup>]), 298 K) 517.18 (43.79), 658.2(8.56).

General Synthesis of **16**: Tetrapyrrane **12** (0.292 g, 0.5 mmol) was taken in a round bottom flask; to it 250 mL of dry DCM was added and stirred for 15 minutes under nitrogen atmosphere to get a clear solution. Azulene-1, 3-bisacrylaldehyde **5** (0.118 g, 0.5 mmol was added to the reaction mixture and stirred for 15 minutes under dark condition. To this, 0.192 mL (2. 5 mmol) CF<sub>3</sub>COOH was added and reaction mixture was stirred under nitrogen atmosphere in dark for overnight. The reaction mixture was then neutralised with 0.348 mL (2.5 mmol) triethylamine followed by oxidation with 283 mg (1.25 mmol)

of DDQ in open air. After complete removal of solvent from crude mixture by rotary evaporator, the compound was purified using basic alumina grade III a deep violet colour band using 5% EtOAc-dichloromethane as eluent were obtained. After repeated PTLCs chromatography, the macrocycle **16** was obtained violet solid which was further recrystallized.

Yield. ~52 mg (10%).  $R_f = 0.3$  ( $\text{CH}_2\text{Cl}_2/\text{Hexane} = 1:1$ ). Mp > 350°C.

MALDI-TOF MS (*m/z*): 1028.45 [M]<sup>+</sup> (1028.33 calc. for ([C<sub>68</sub>H<sub>56</sub>N<sub>2</sub>S<sub>4</sub>]<sup>+</sup>)). Elemental analysis: Calc. for C<sub>68</sub>H<sub>56</sub>N<sub>2</sub>S<sub>4</sub>: C, 79.34; H, 5.48; N, 2.72. Found: C, 79.37; H, 5.46; N, 2.7. UV-vis ( $\text{CH}_2\text{Cl}_2$ ,  $\lambda$  [nm], ( $\epsilon$  [ $\text{M}^{-1}$  cm<sup>-1</sup> × 10<sup>5</sup>]), 298K): 540 (3.79), 577 (3.81), 800 (1.16), 950 (0.001).

## **2. Supplementary Data:**

### **2.1 Mass Spectra**

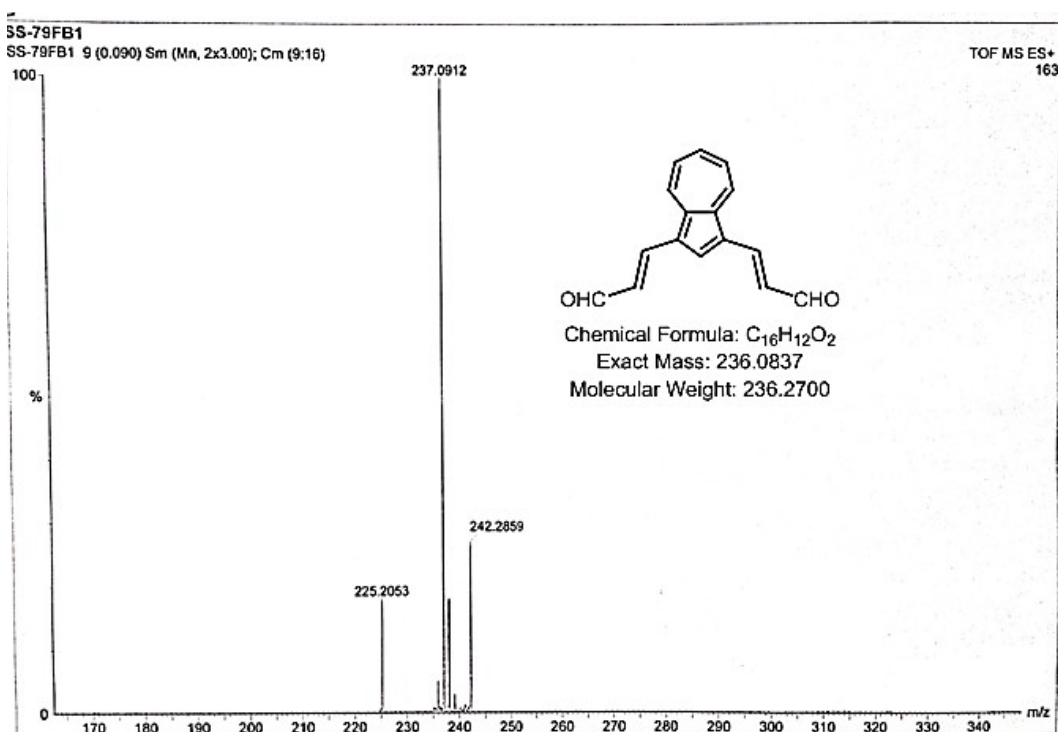


Fig. S1 HRMS Spectra of **5**

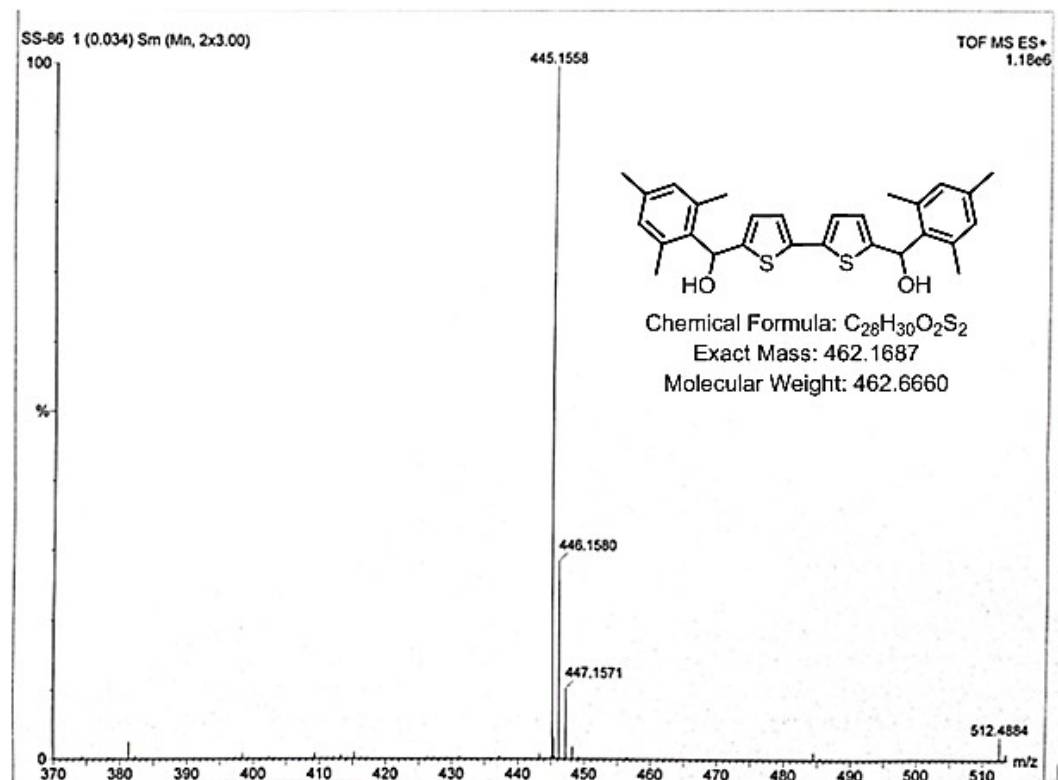


Fig. S2 HRMS Spectra of **6**

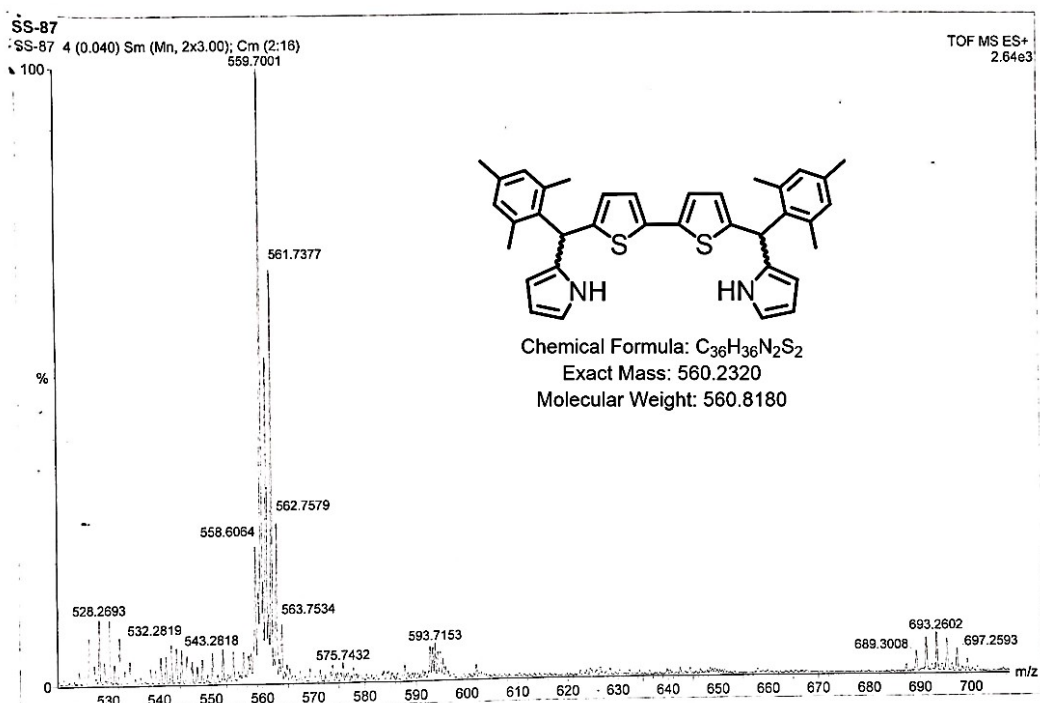


Fig. S3 HRMS Spectra of 7

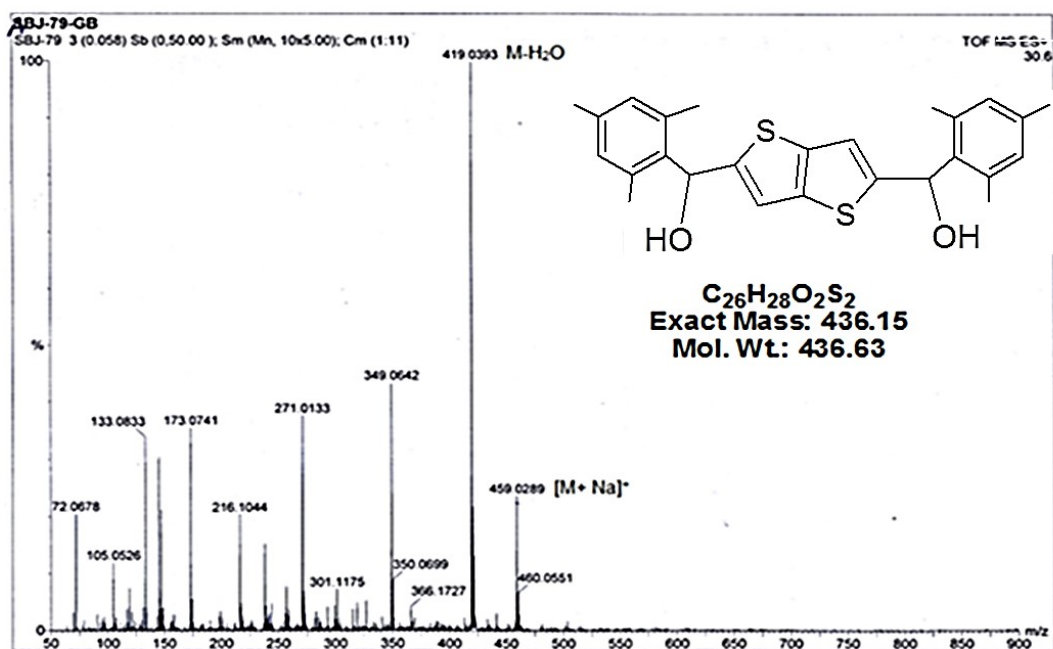


Fig. S4 HRMS Spectra of 8

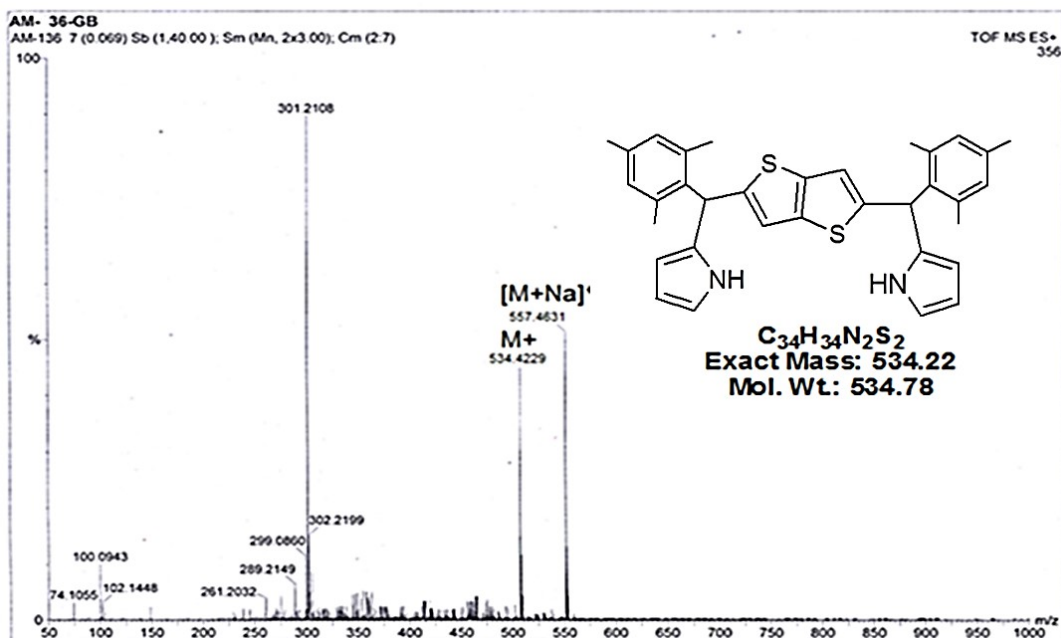


Fig. S5 HRMS Spectra of **9**

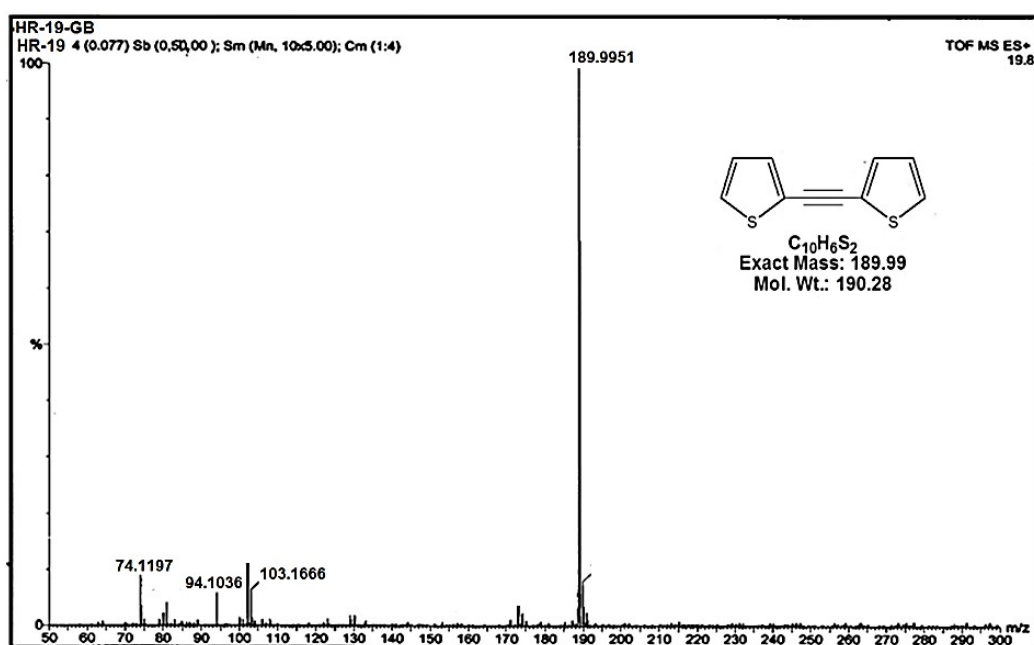


Fig. S6 HRMS Spectra of **10**

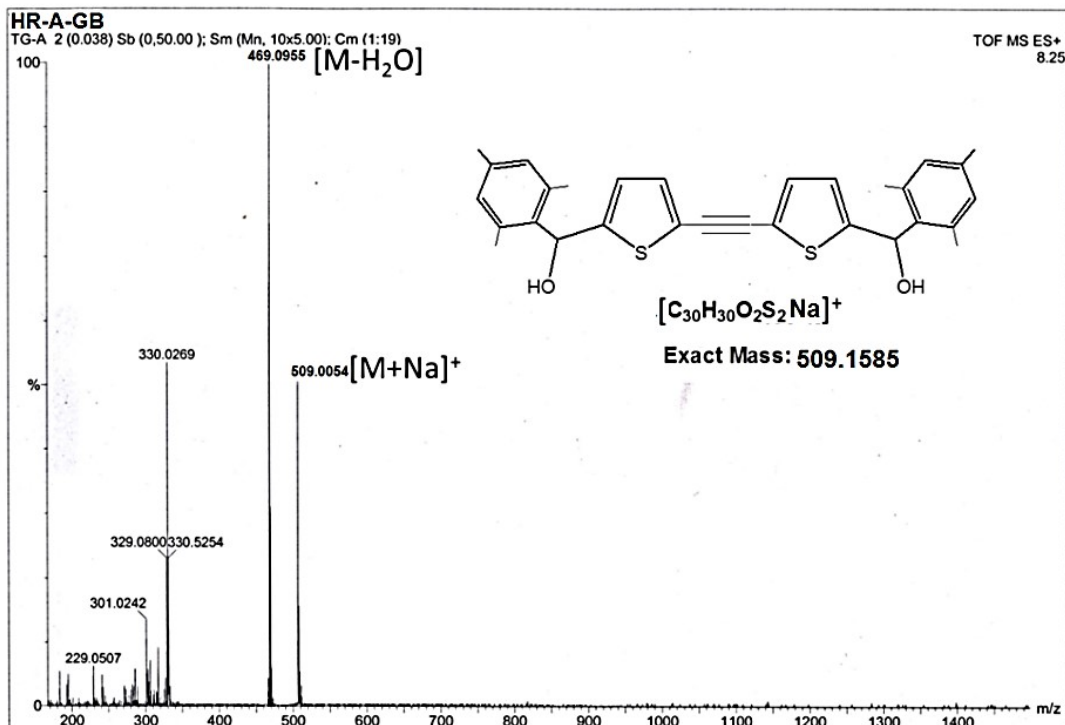


Fig. S7 HRMS Spectra of **11**

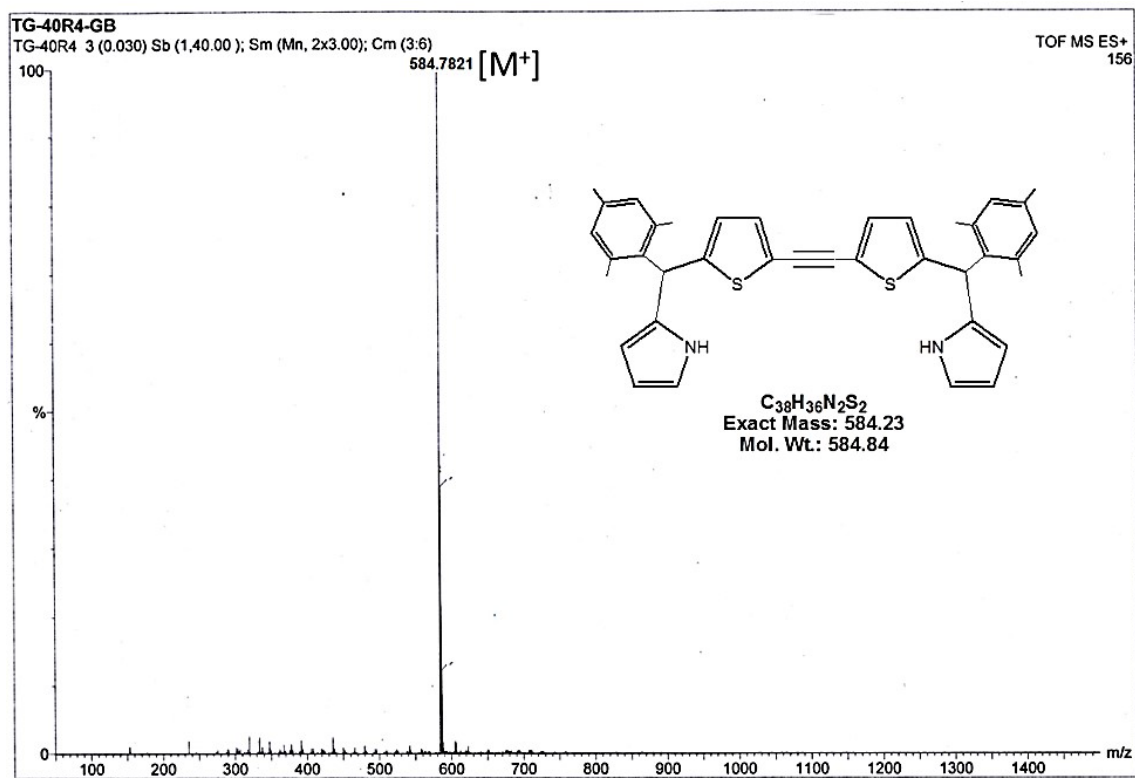


Fig. S8 HRMS Spectra of **12**

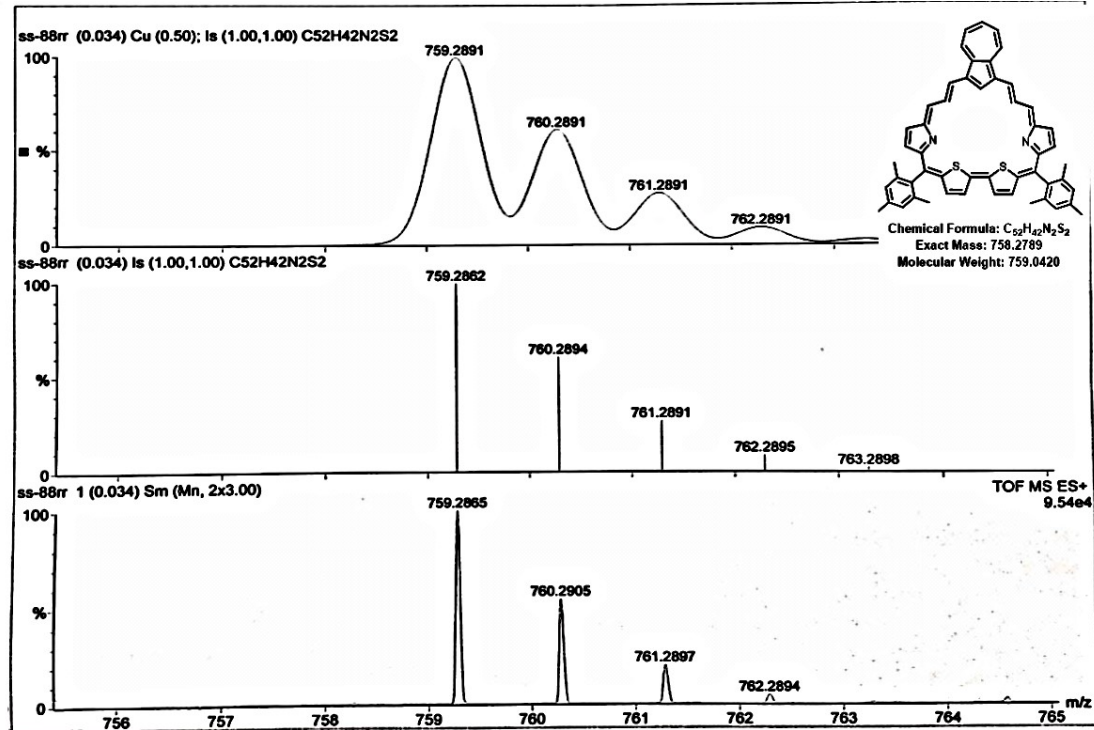


Fig. S9 HRMS Spectra of **13**

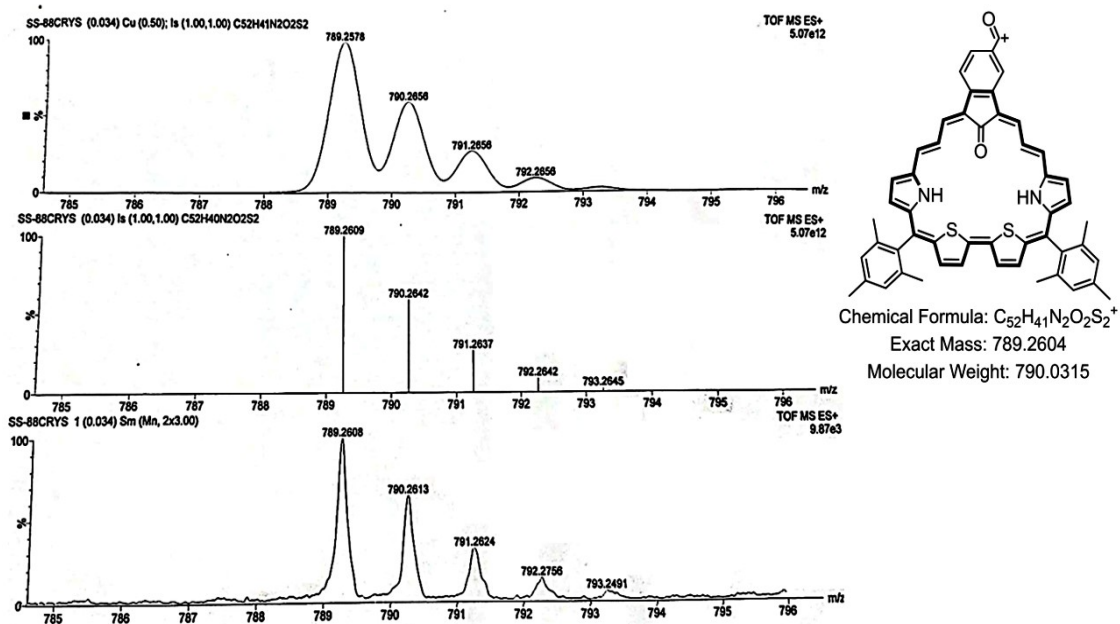


Fig. S10 HRMS Spectra of **14**

Comment 1  
Comment 2

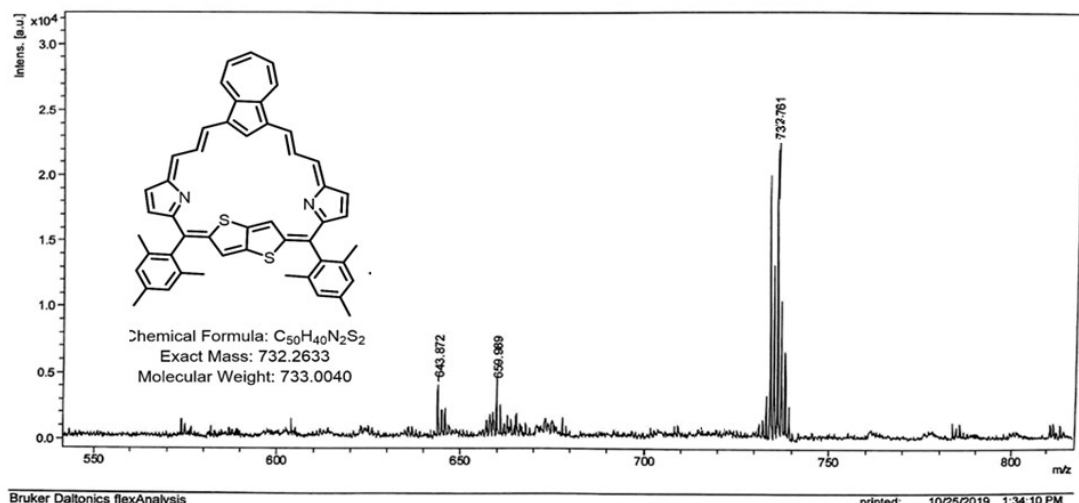


Fig. S11 MALDI-TOF MS Spectra of 15

Comment 1  
Comment 2

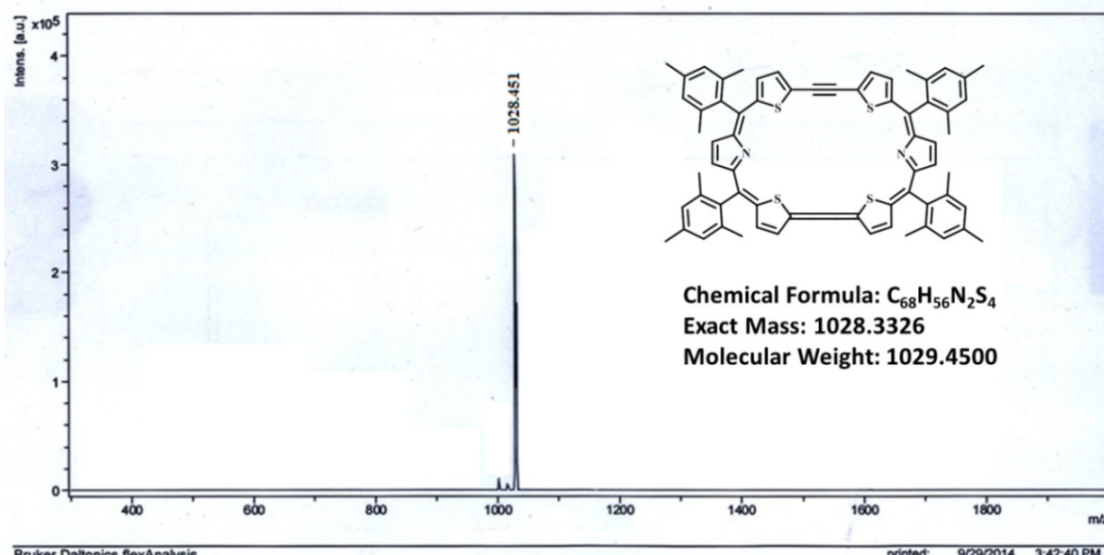


Fig. S12 MALDI-TOF MS Spectra of 16

## 2.2 IR spectra:

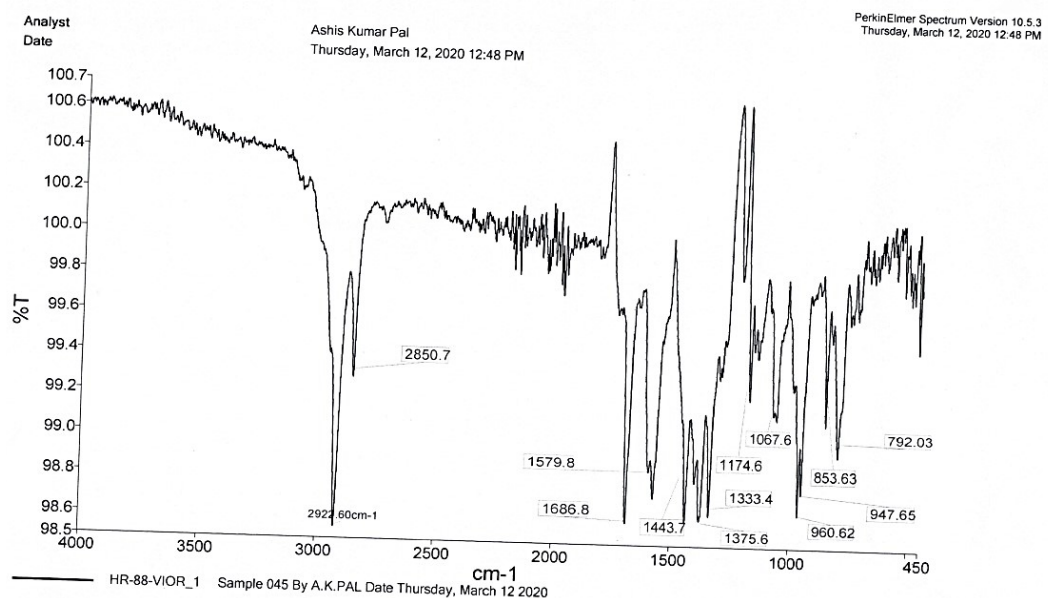


Fig. S13 IR Spectrum of **14**

### 2.3 UV-vis spectra:

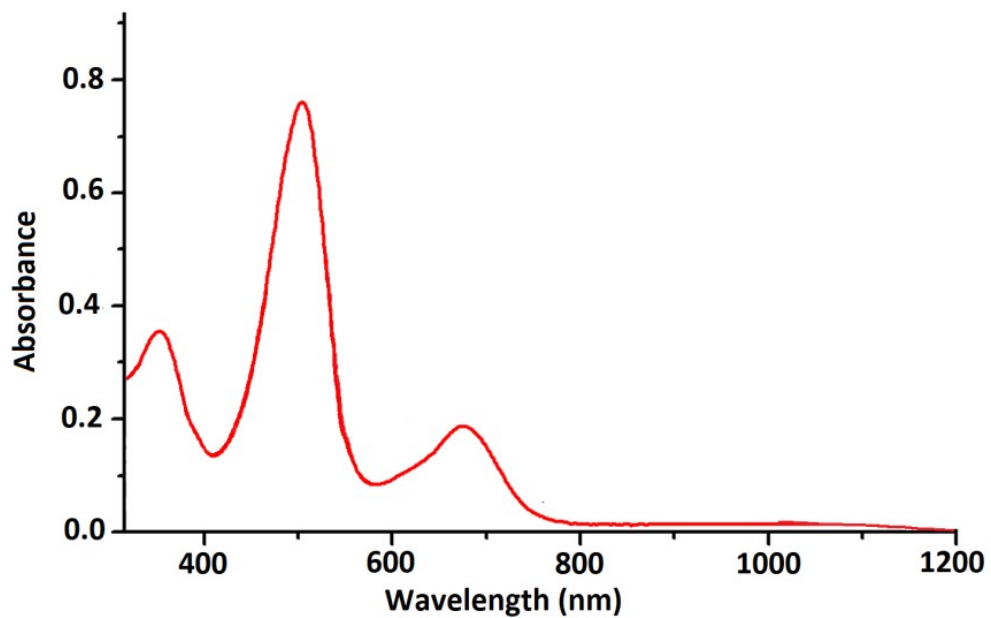


Fig. S14 UV-vis Spectra of **15**

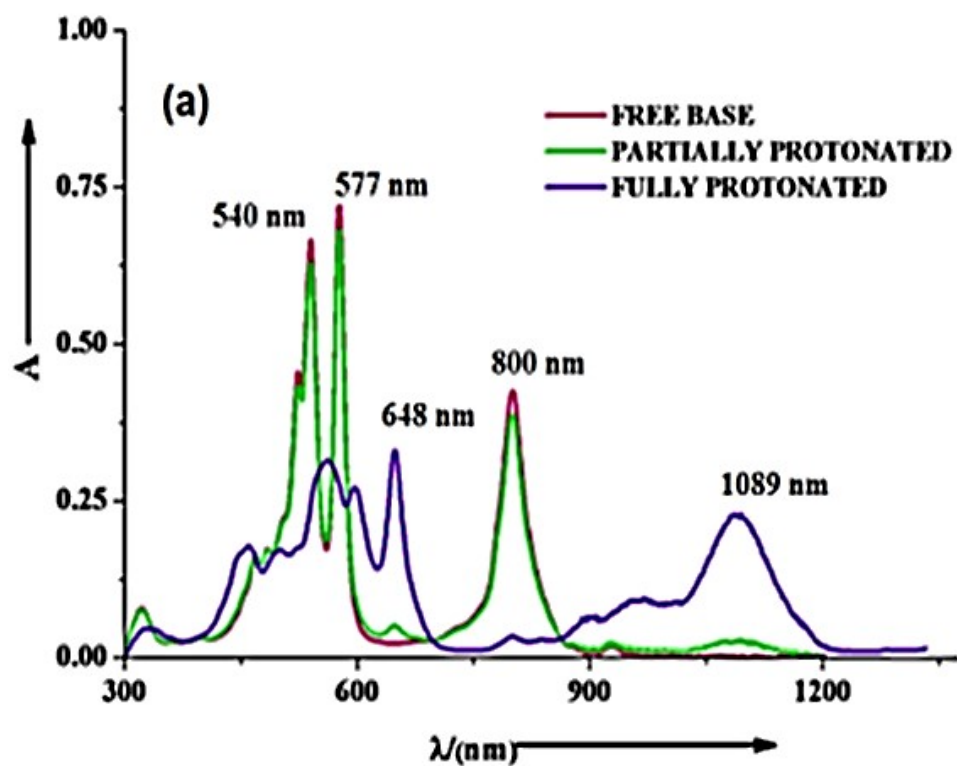


Fig. S15 UV-vis Spectra of **16**

## 2.4 NMR spectra:

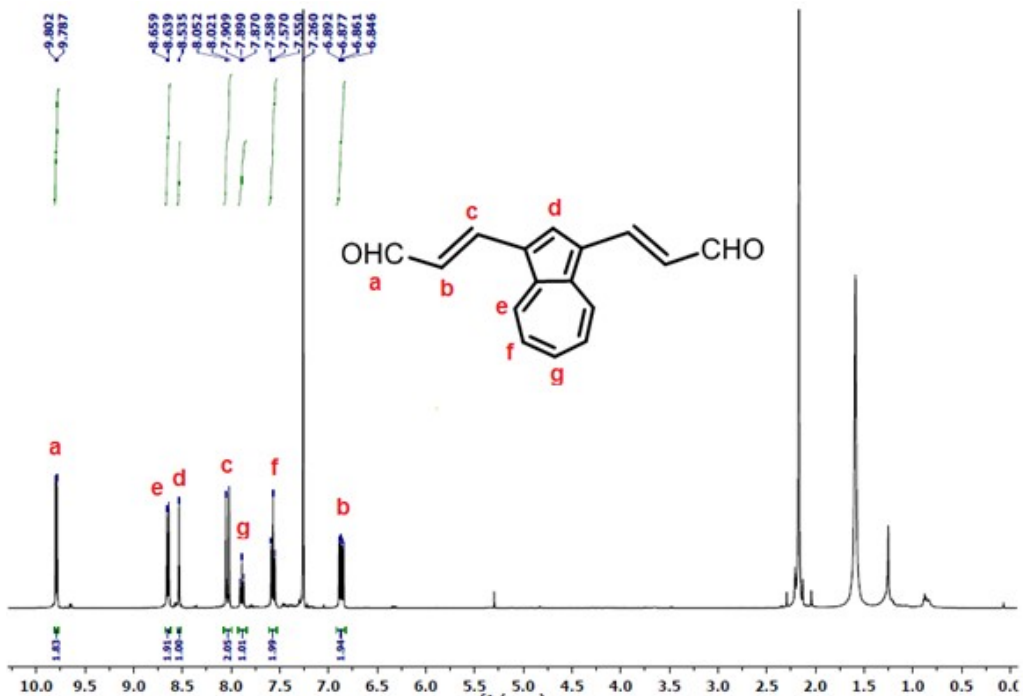


Fig. S16  $^1\text{H}$  NMR spectra of **5** in  $\text{CDCl}_3$  at 298 K

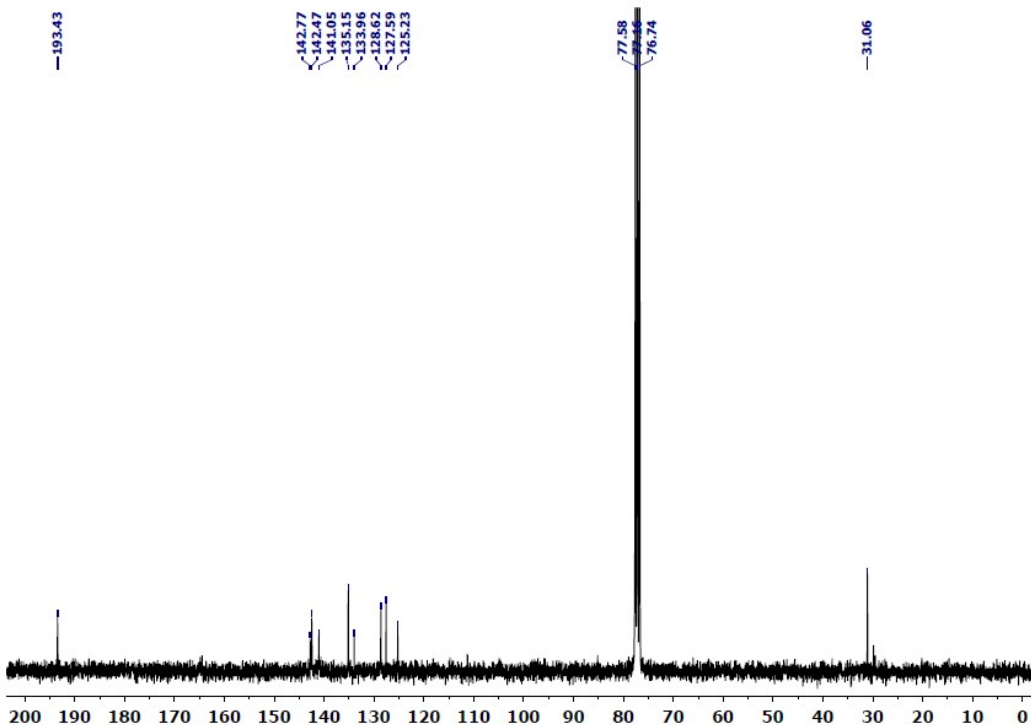


Fig. S17  $^{13}\text{C}$  NMR spectra of **5** in  $\text{CDCl}_3$  at 298 K

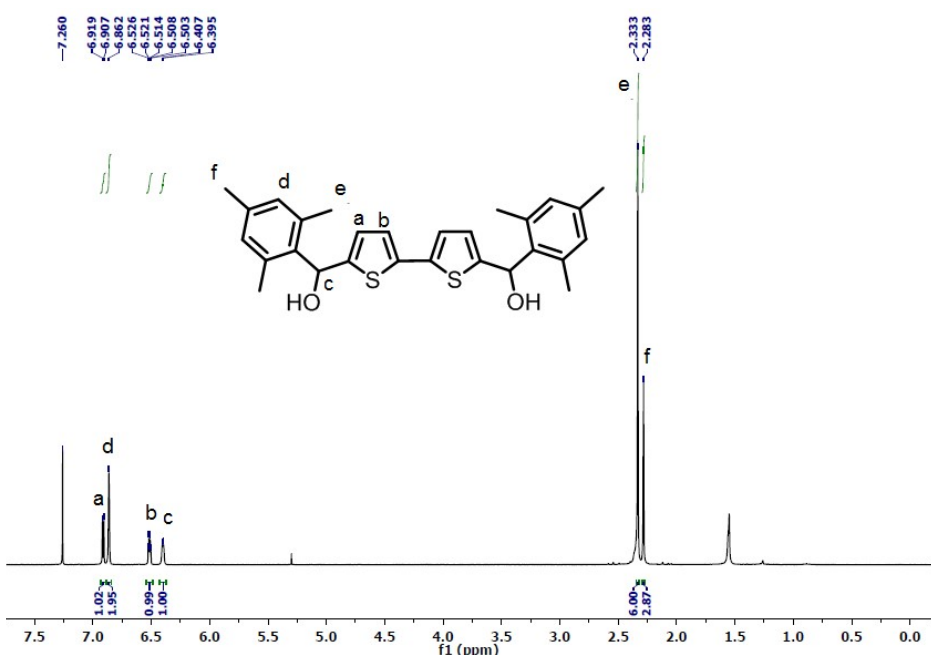


Fig. S18  $^1\text{H}$  NMR spectra of **6** in  $\text{CDCl}_3$  at 298 K

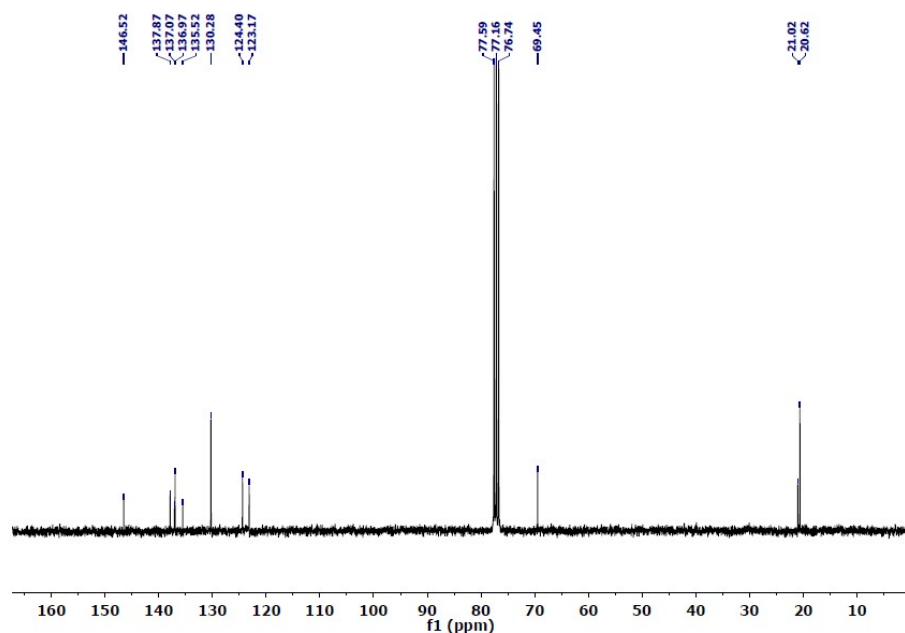


Fig. S19  $^{13}\text{C}$  NMR spectra of **6** in  $\text{CDCl}_3$  at 298 K

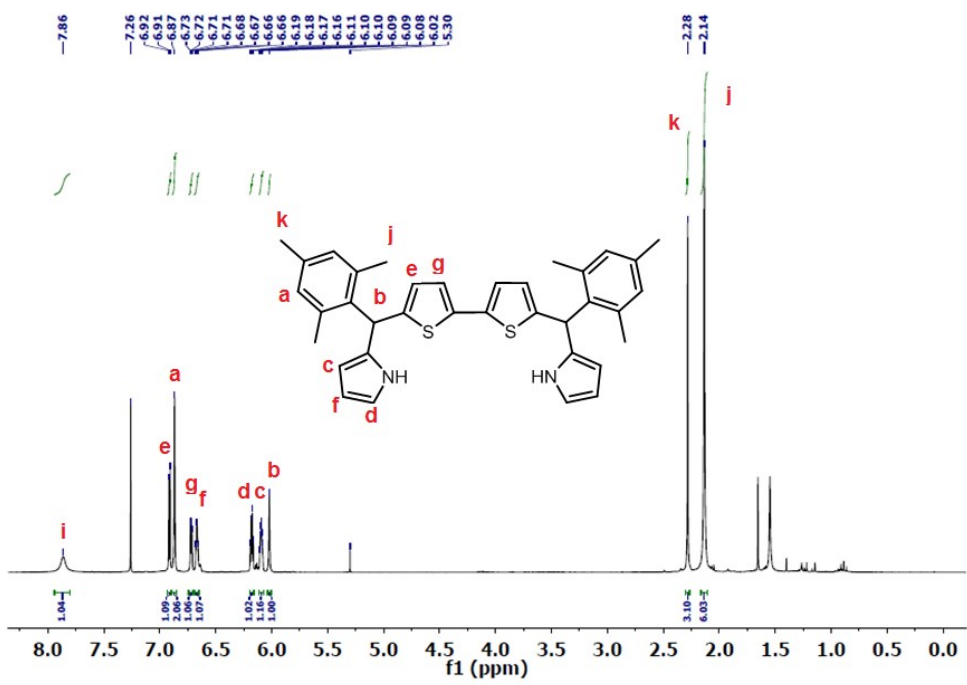


Fig. S20  $^1\text{H}$  NMR spectra of **7** in  $\text{CDCl}_3$  at 298 K

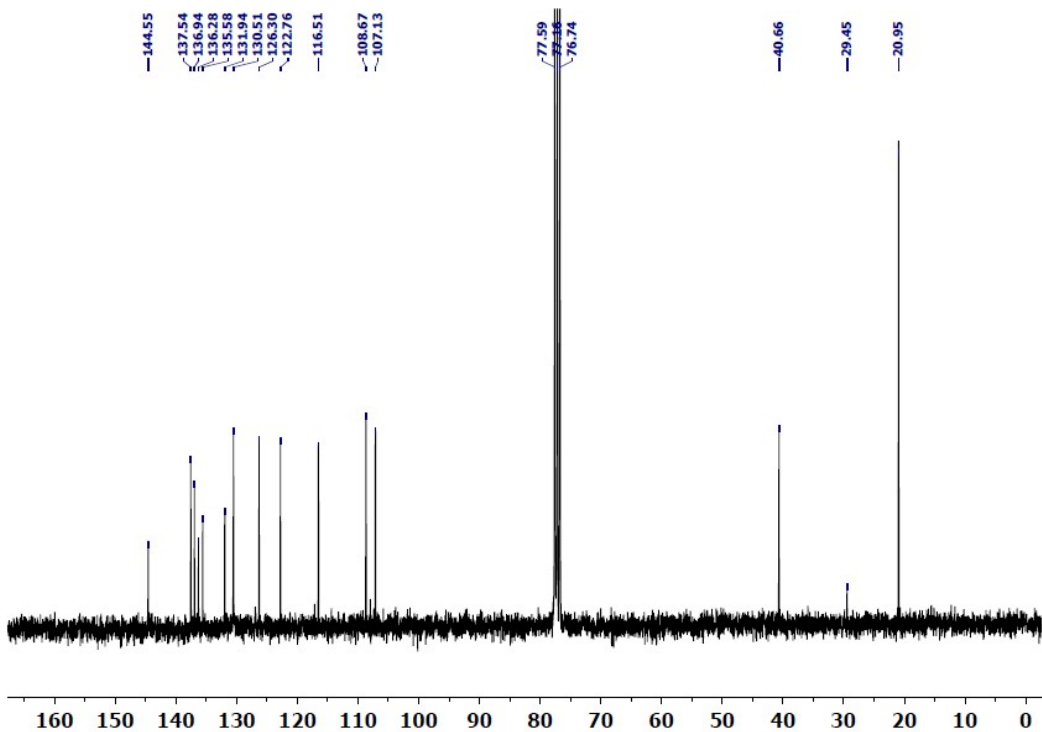


Fig. S21  $^{13}\text{C}$  NMR spectra of **7** in  $\text{CDCl}_3$  at 298 K

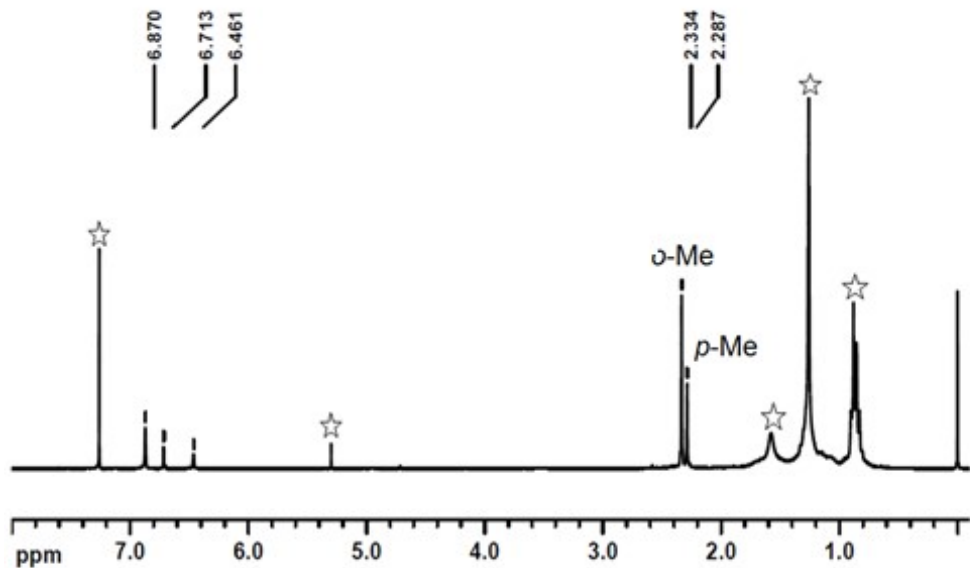


Fig. S22  $^1\text{H}$  NMR spectra of **8** in  $\text{CDCl}_3$  at 298 K

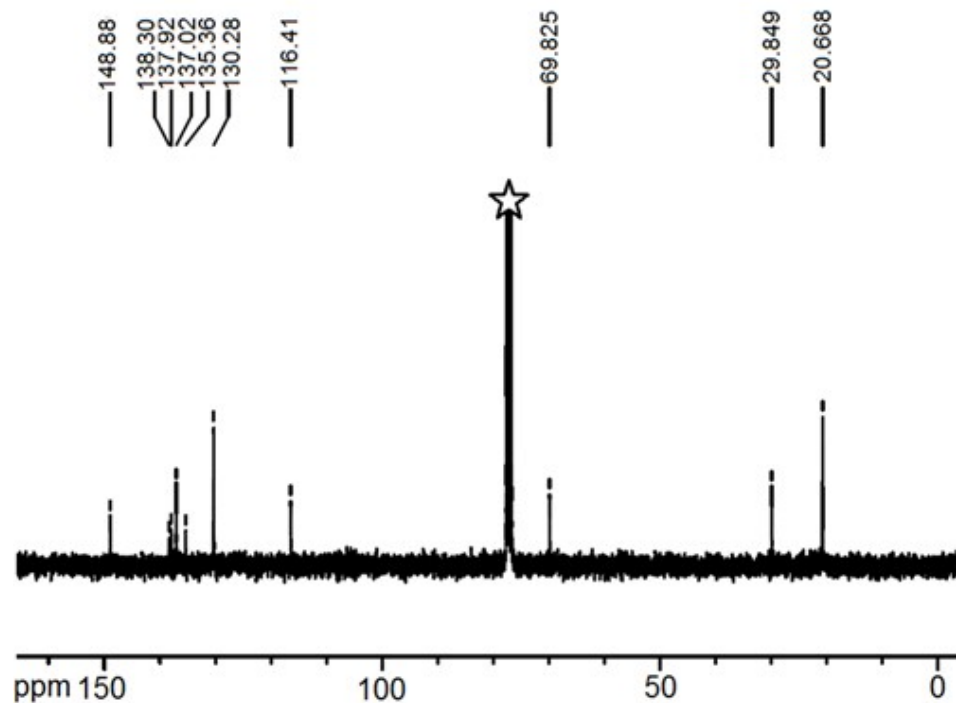


Fig. S23  $^{13}\text{C}$  NMR spectra of **8** in  $\text{CDCl}_3$  at 298 K

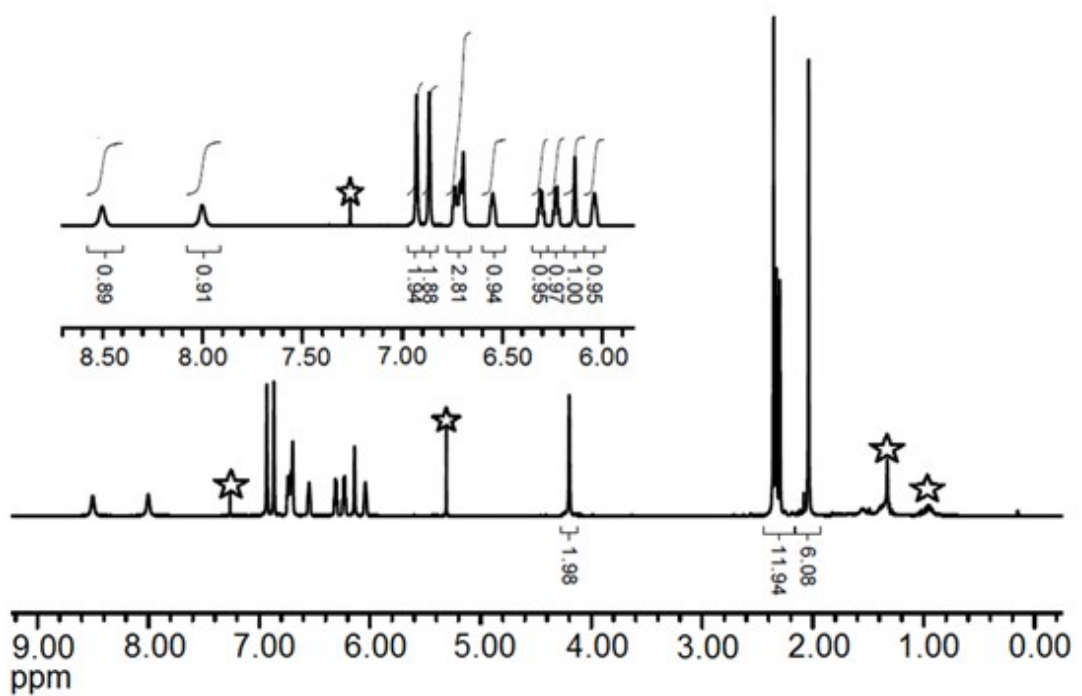


Fig. S24  $^1\text{H}$  NMR spectra of **9** in  $\text{CDCl}_3$  at 298 K

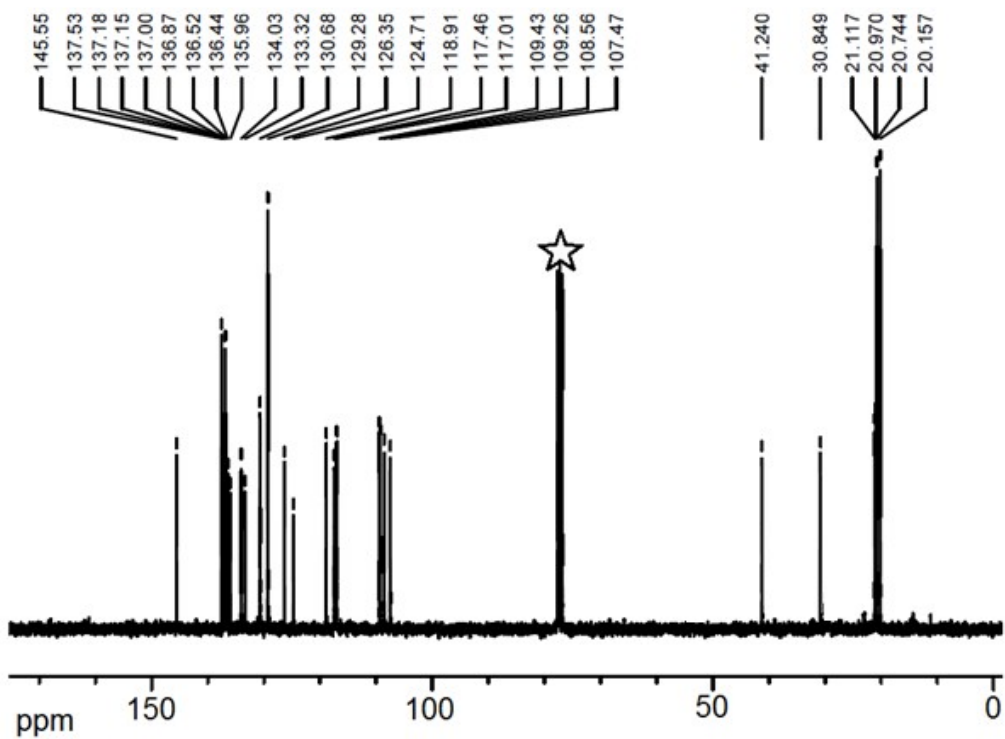


Fig.S25  $^{13}\text{C}$  NMR spectra of **9** in  $\text{CDCl}_3$  at 298 K

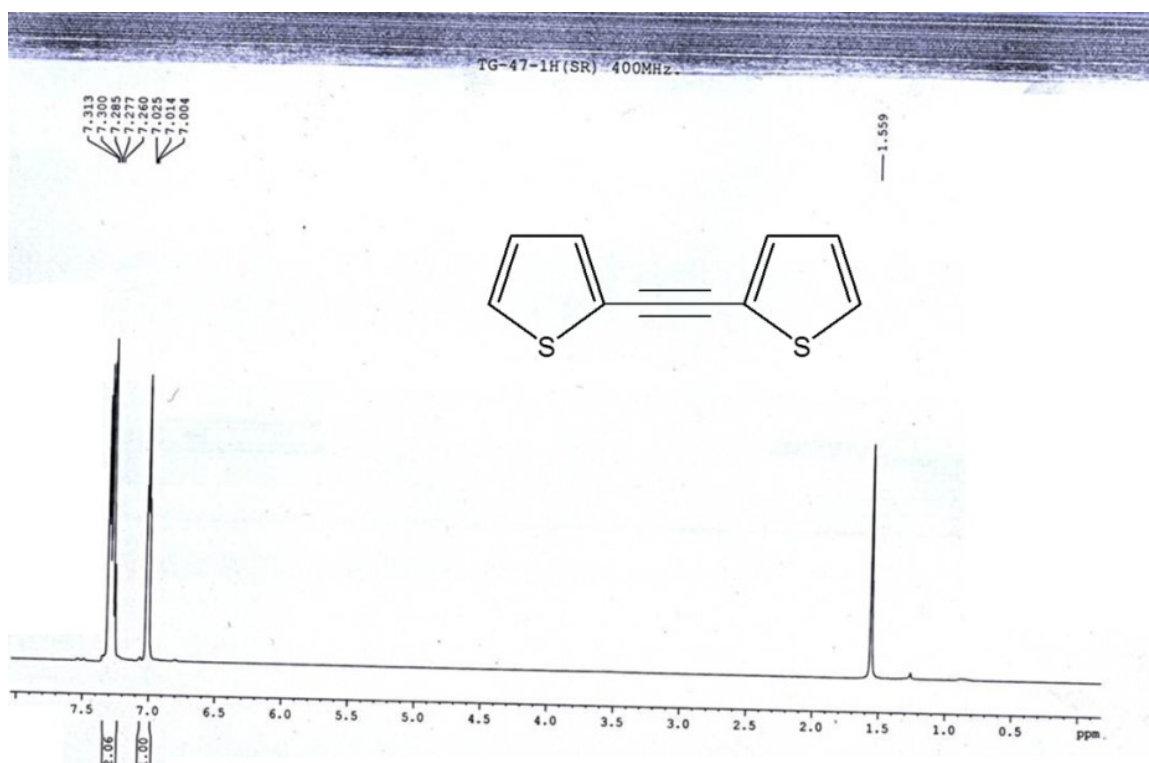


Fig. S26  $^1\text{H}$  NMR spectra of **10** in  $\text{CDCl}_3$  at 298 K

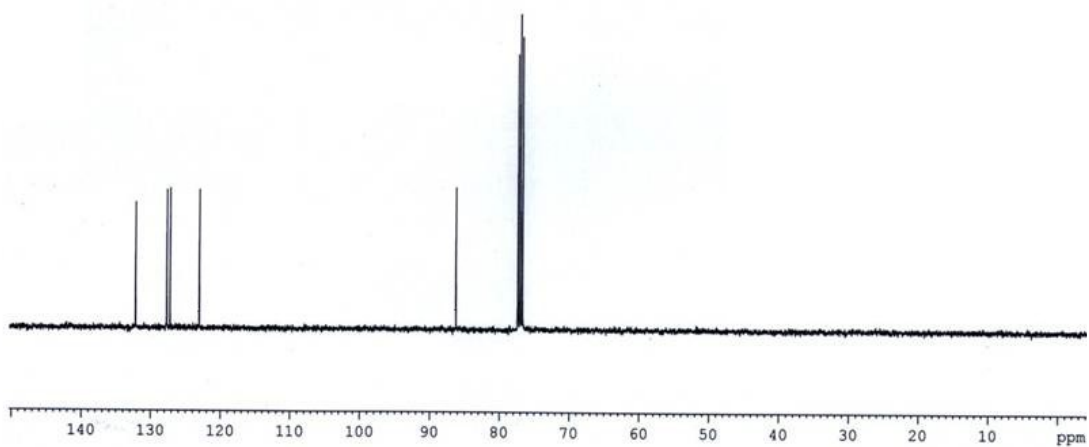


Fig. S27  $^{13}\text{C}$  NMR spectra of **10** in  $\text{CDCl}_3$  at 298 K

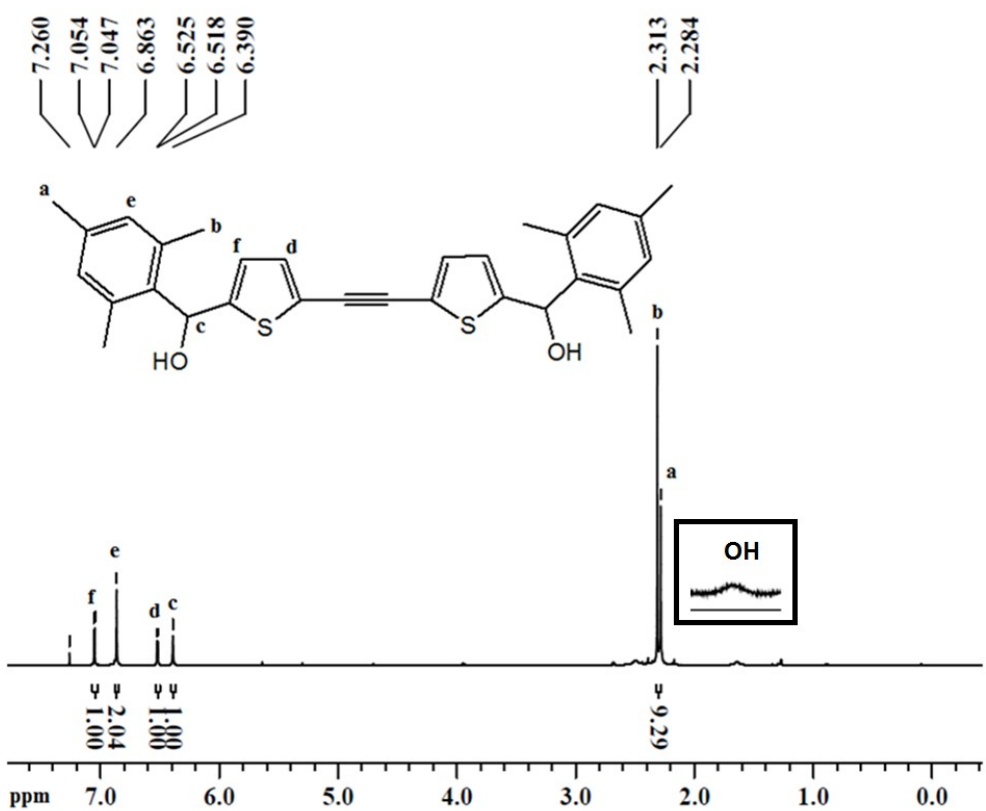


Fig. S28  $^1\text{H}$  NMR spectra of **11** in  $\text{CDCl}_3$  at 298 K

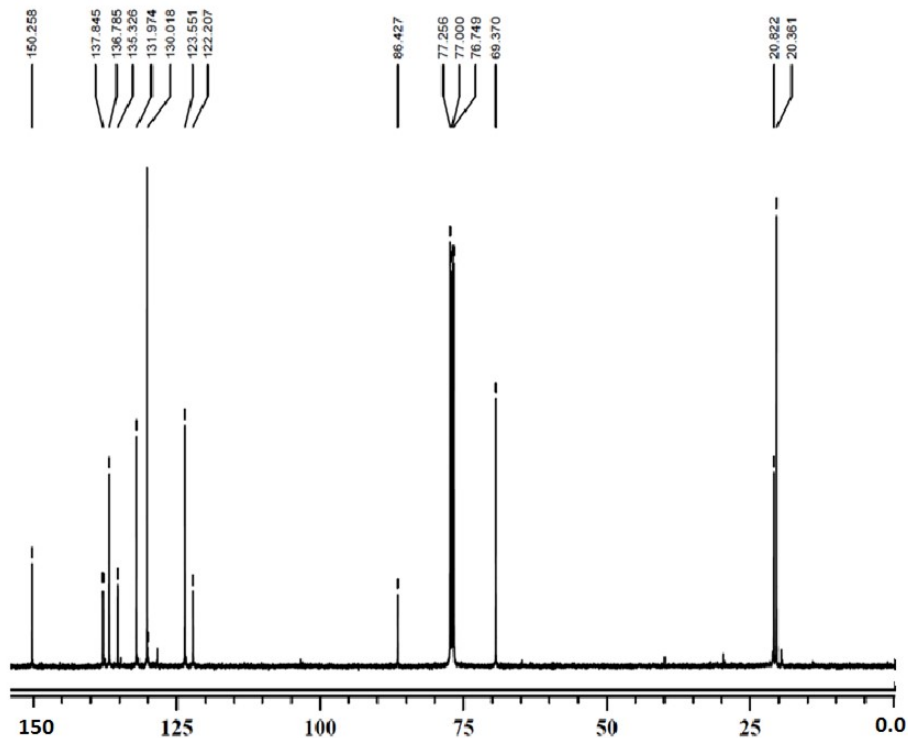


Fig. S29  $^{13}\text{C}$  NMR spectra of **11** in  $\text{CDCl}_3$  at 298 K

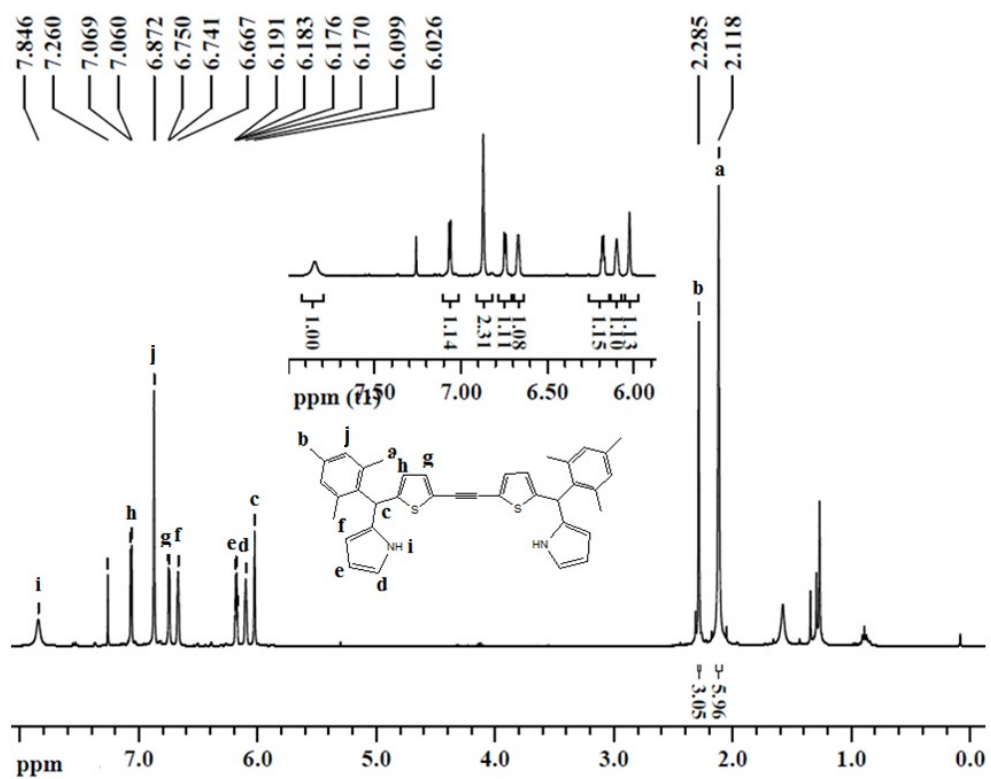


Fig. S30  $^1\text{H}$  NMR spectra of **12** in  $\text{CDCl}_3$  at 298 K

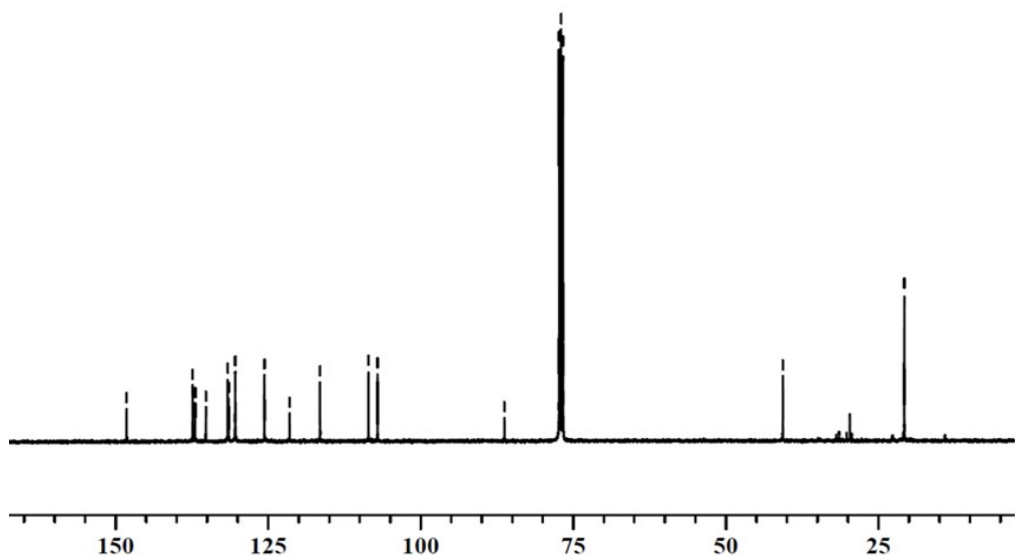


Fig. S31  $^{13}\text{C}$  NMR spectra of **12** in  $\text{CDCl}_3$  at 298 K

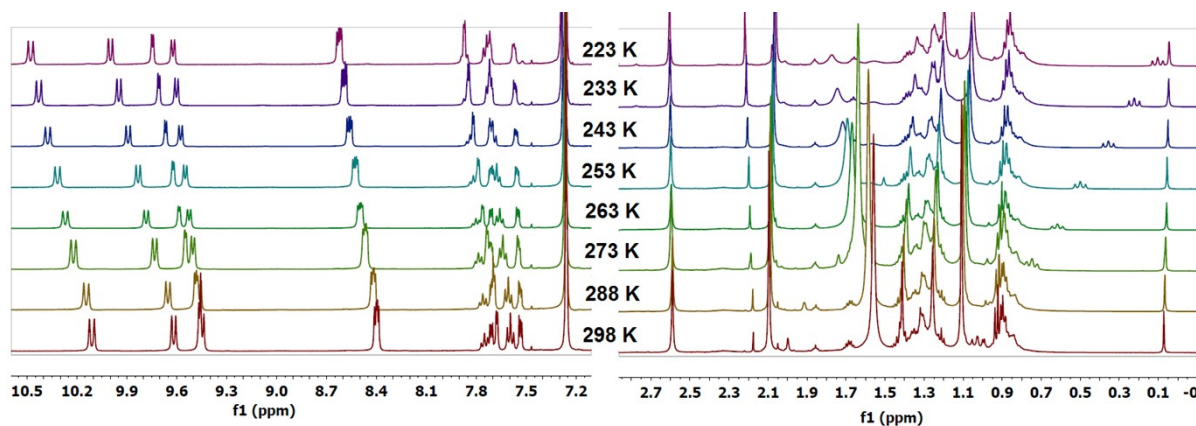


Fig. S32 Low VT <sup>1</sup>H NMR spectra of **13''** in  $\text{CDCl}_3$

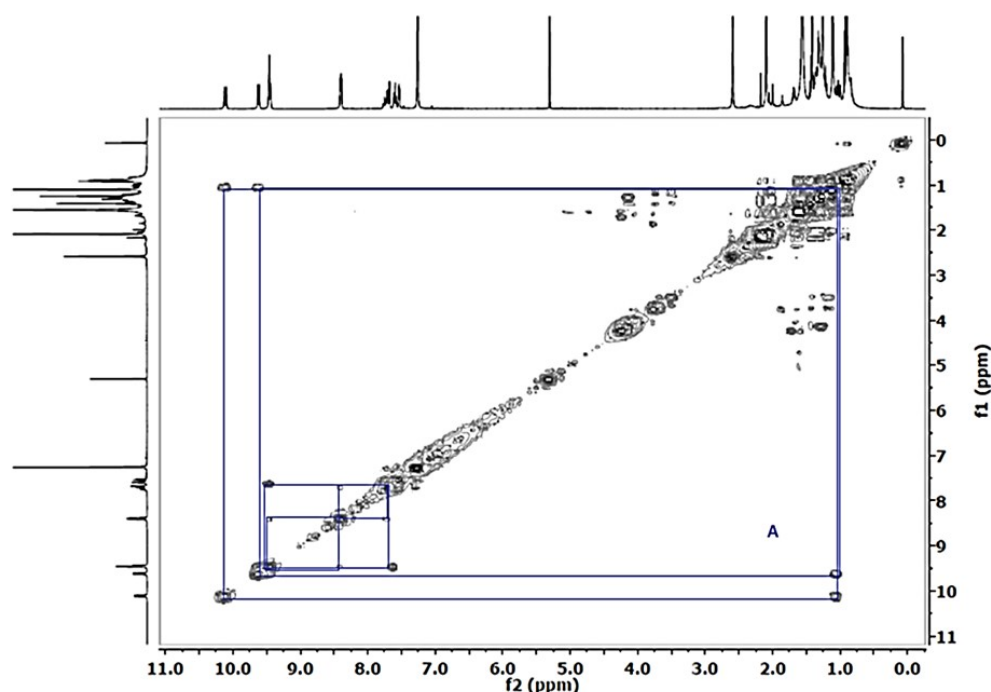


Fig. S33A <sup>1</sup>H-<sup>1</sup>H 2D COSY NMR spectra of **13''** in  $\text{CDCl}_3$  at 298 K

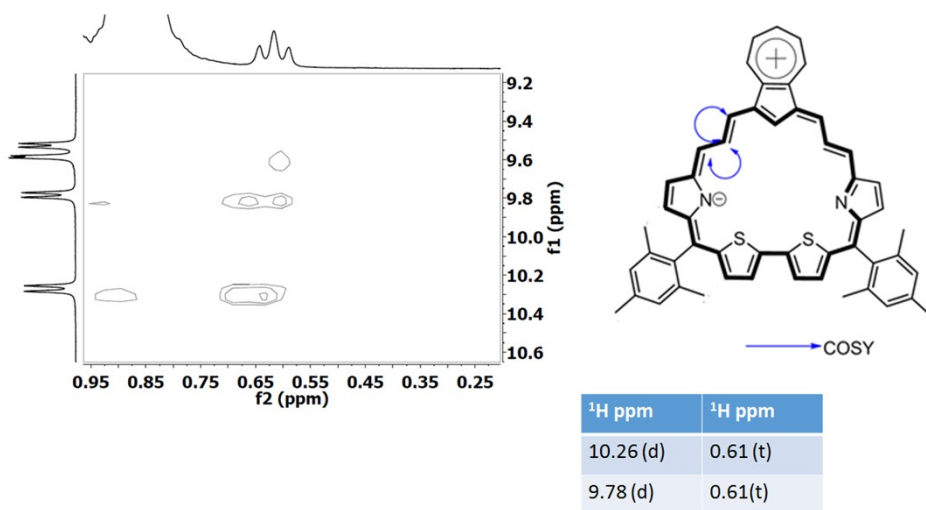


Fig. S33B <sup>1</sup>H-<sup>1</sup>H 2D COSY NMR spectra of **13''** in  $\text{CDCl}_3$  at 263 K

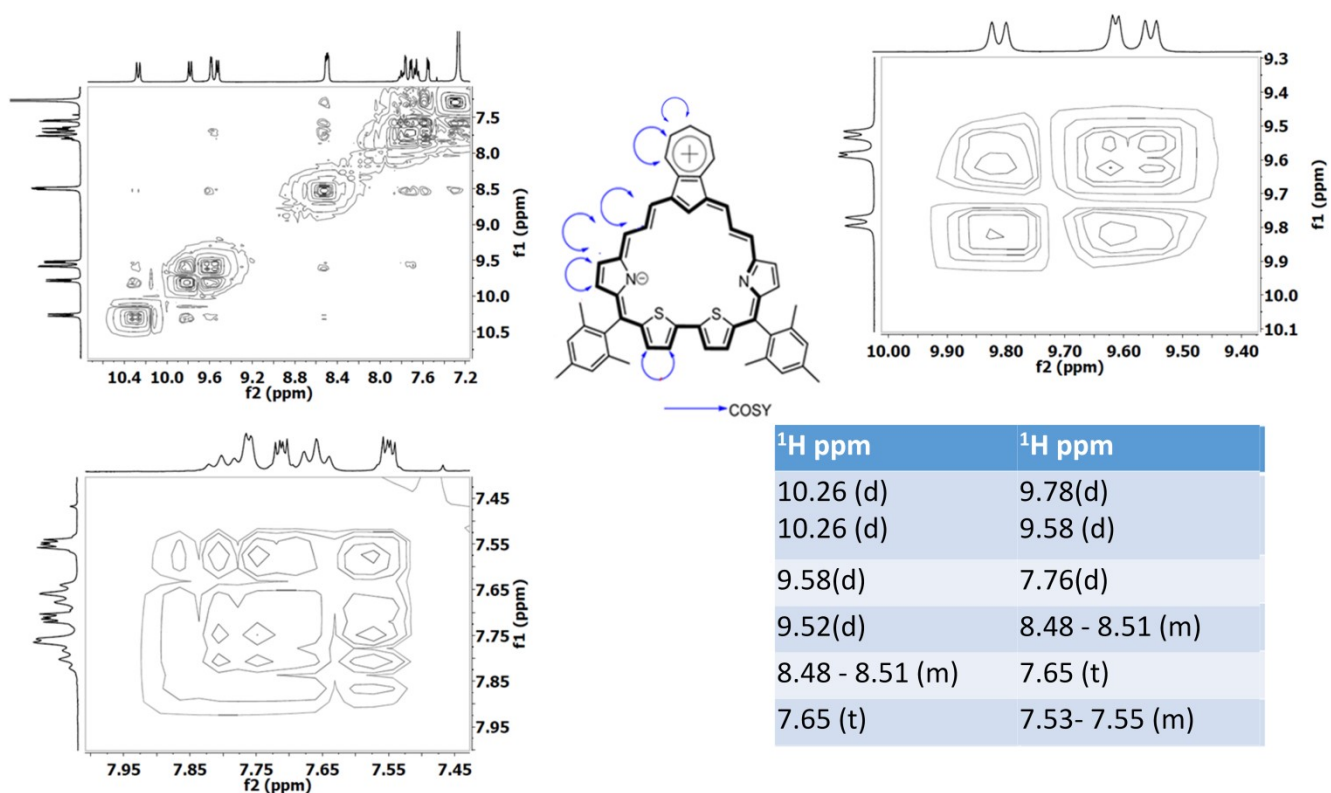


Fig. S33C <sup>1</sup>H -<sup>1</sup>H 2D COSY NMR spectra of **13''** in CDCl<sub>3</sub> at 263 K

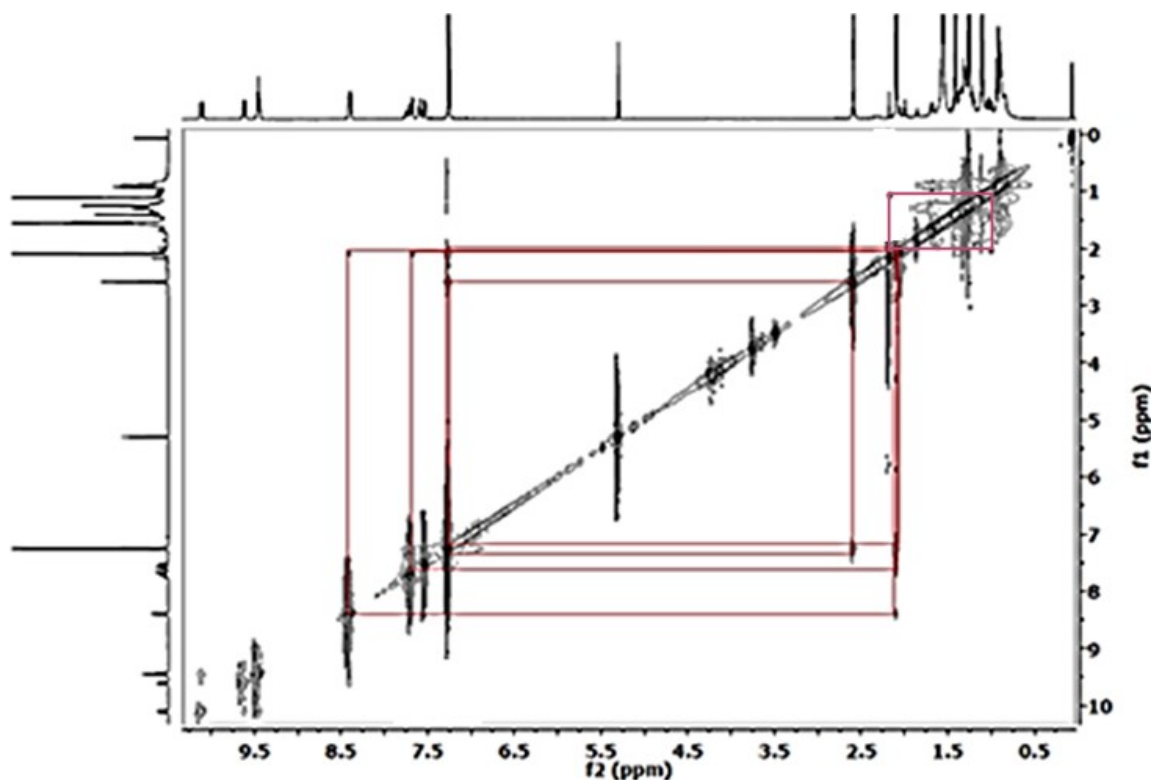


Fig. S34A <sup>1</sup>H -<sup>1</sup>H 2D ROESY NMR spectra of **13''** in CDCl<sub>3</sub> at 298 K

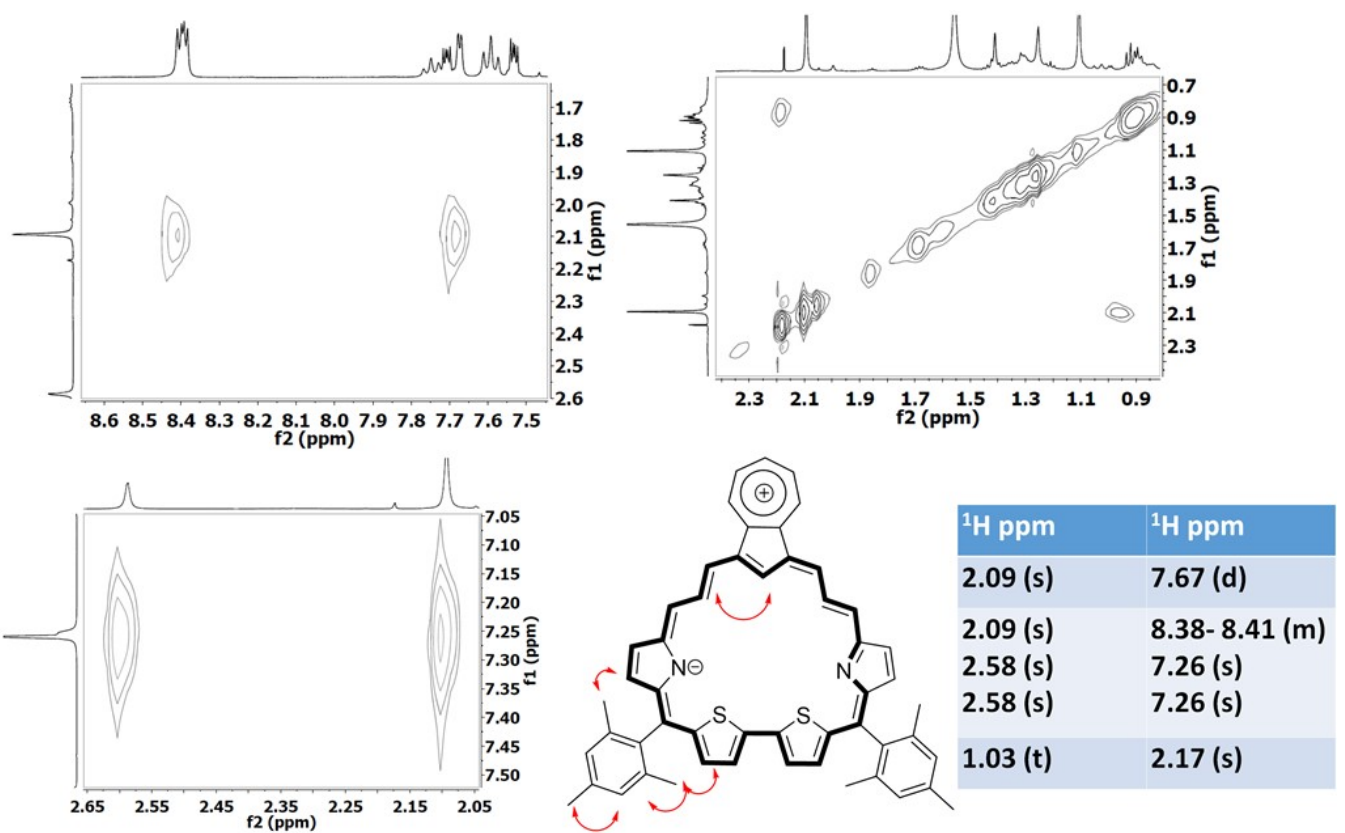


Fig. S34B <sup>1</sup>H -<sup>1</sup>H 2D ROESY NMR spectra of **13''** in CDCl<sub>3</sub> at 298 K

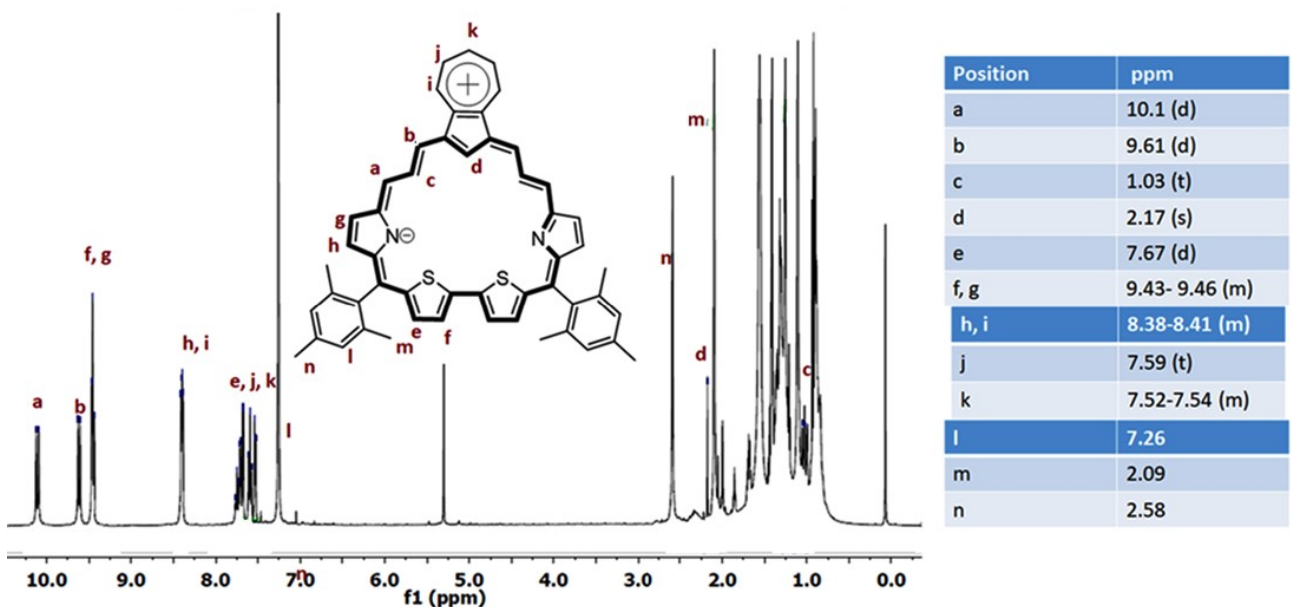


Fig. S35A Complete <sup>1</sup>H NMR spectral assignment of **13''** in CDCl<sub>3</sub> at 298 K

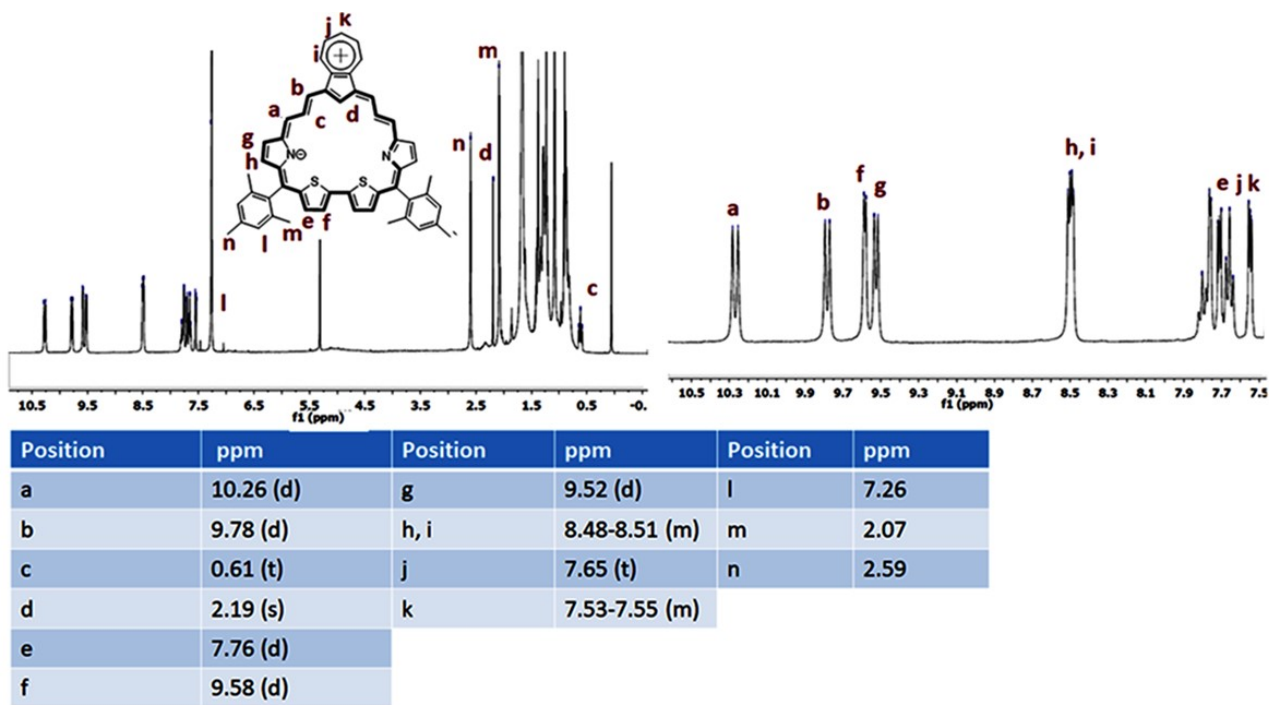


Fig. S35B Complete <sup>1</sup>H NMR spectral assignment of **13''** in CDCl<sub>3</sub> at 263 K

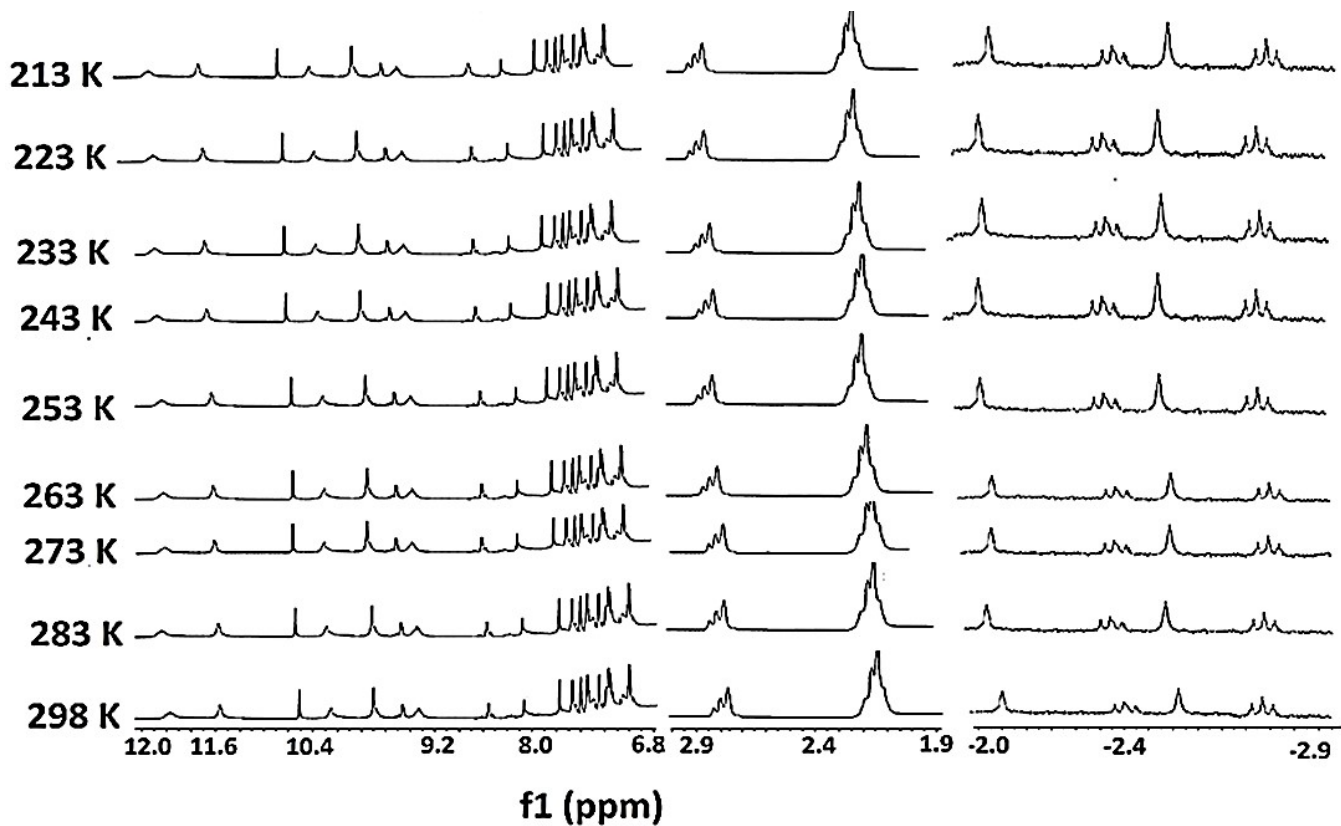


Fig. S36 Low VT <sup>1</sup>H NMR spectra of **14''** in CD<sub>2</sub>Cl<sub>2</sub>

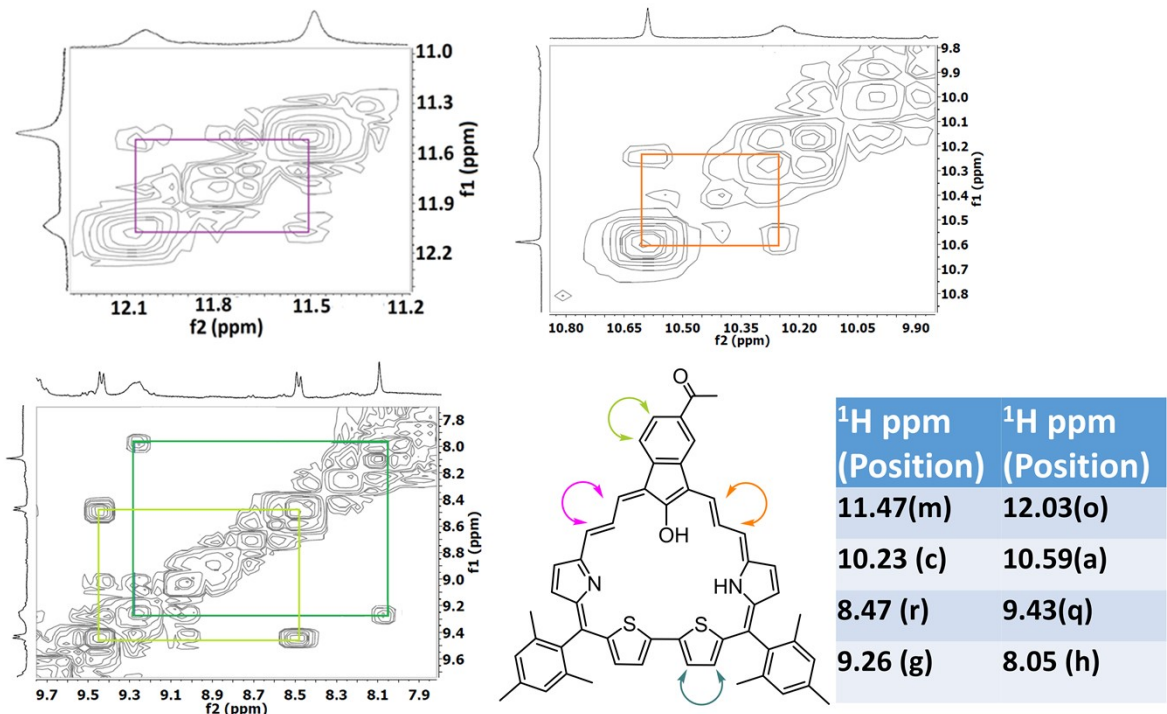


Fig. S37A <sup>1</sup>H -<sup>1</sup>H 2D COSY NMR spectra of **14''** in CD<sub>2</sub>Cl<sub>2</sub> at 298 K

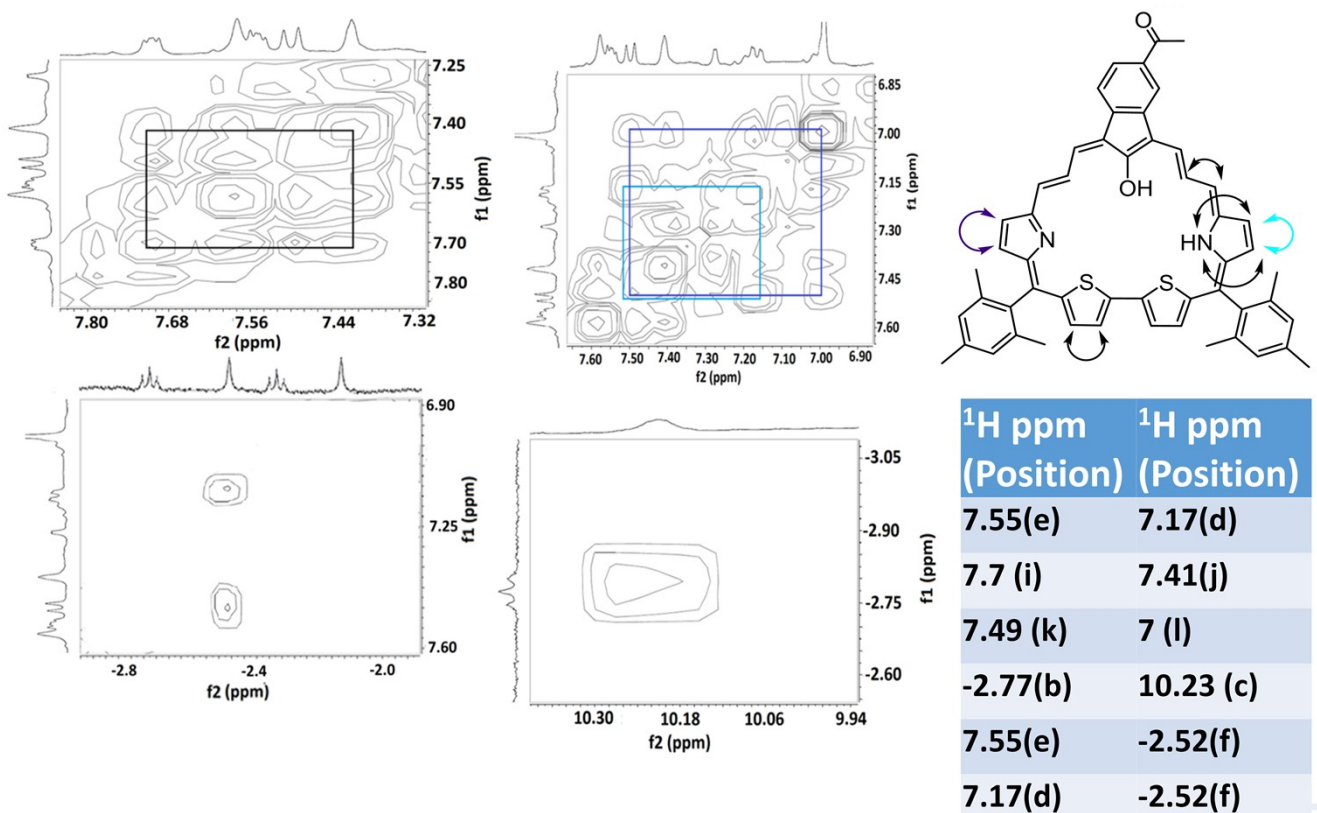


Fig. S37B <sup>1</sup>H -<sup>1</sup>H 2D COSY NMR spectra of **14''** in CD<sub>2</sub>Cl<sub>2</sub> at 298 K

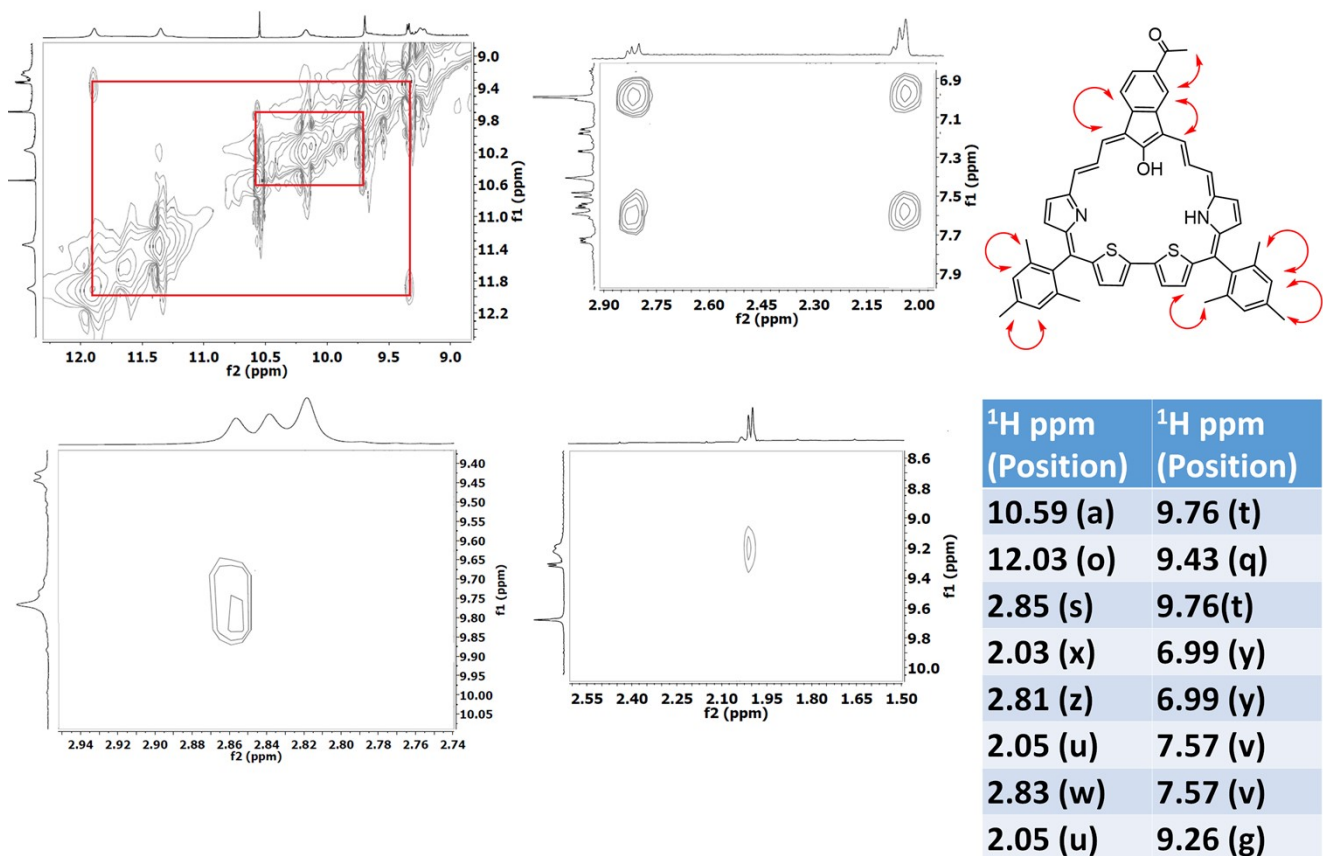


Fig. S38  $^1\text{H}$  - $^1\text{H}$  2D ROESY NMR spectra of **14''** in  $\text{CD}_2\text{Cl}_2$  at 298 K

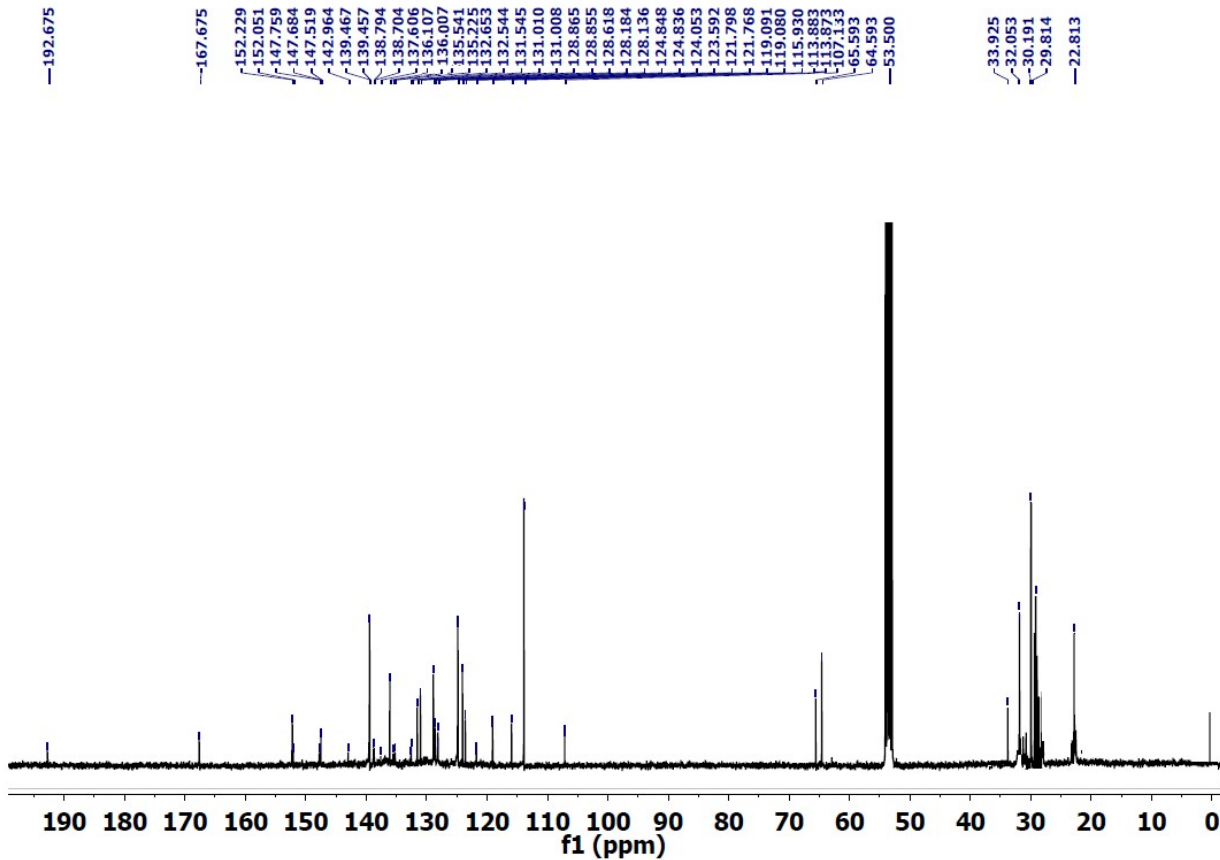
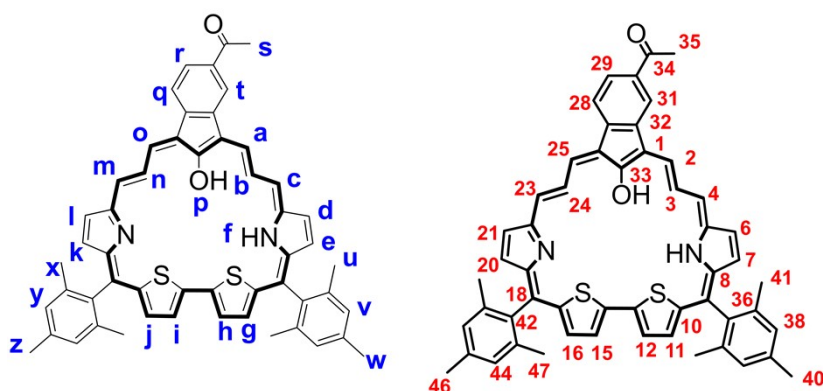
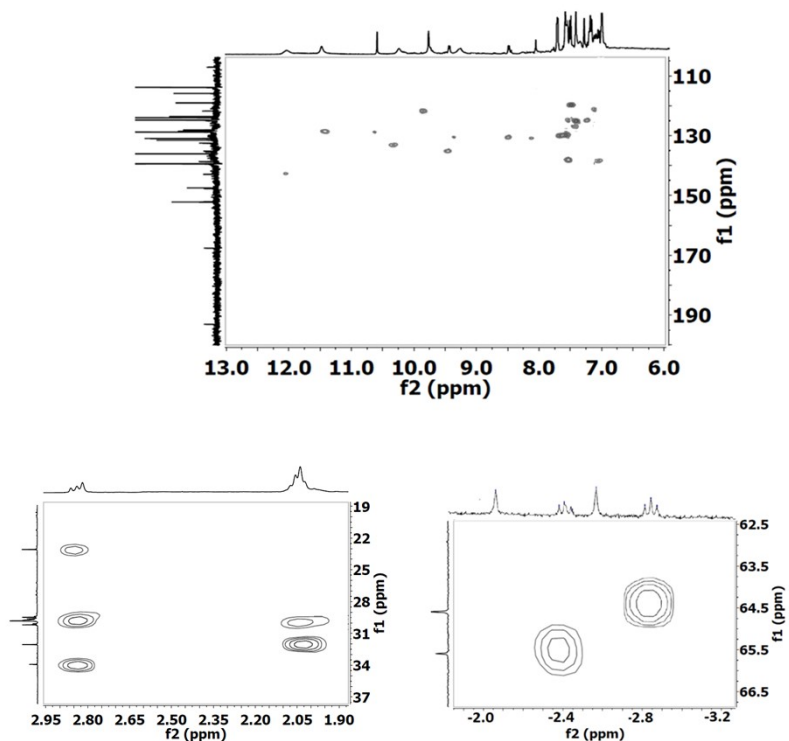


Fig. S39  $^{13}\text{C}$  NMR spectra of **14** in  $\text{CD}_2\text{Cl}_2$  at 298 K



<sup>1</sup> H ppm (Position)	<sup>13</sup> C ppm (Position)
10.59 (a)	128.85 (2)
-2.77 (b)	64.59 (3)
	147.75(1)
10.23 (c)	132.54 (4)
	128.18 (5)
7.17 (d)	124.83 (6)
7.55 (e)	119.08 (7)
-2.52 (f)	
9.26 (g)	131.54 (11)
	128.13 (8)
	135.22 (10)
8.05 (h)	131.01 (12)
	132.65 (13)
	135.54 (14)
7.7 (i)	131 (15)
7.41 (j)	124.05 (16)
	136 (17)
	121.79(19)
7.49 (k)	123.59 (20)
7 (l)	124.84 (21)
	128.86(22)
11.47 (m)	128.61 (23)
-2.38 (n)	65.59 (24)
<sup>1</sup> H ppm (Position)	<sup>13</sup> C ppm (Position)
12.03 (o)	142.96 (25)
-2.07 (p)	
	147.68(26)
	152.05(27)
9.43 (q)	136.1 (28)
8.47 (r)	138.7 (29)
	167.97(30)
	152.22(32)
	107.13(33)
	192.67(34)
2.85 (s)	33.92 (35)
9.76 (t)	121.76 (31)
2.83 (u)	22.81 (41)
7.57 (v)	138.79 (38)
2.05 (w)	29.81 (40)
2.81 (x)	30.19 (47)
6.99 (y)	139.45 (44)
2.03 (z)	22.81 (46)

Fig. S40 HSQC NMR spectra of **14''** in  $\text{CD}_2\text{Cl}_2$  at 298 K

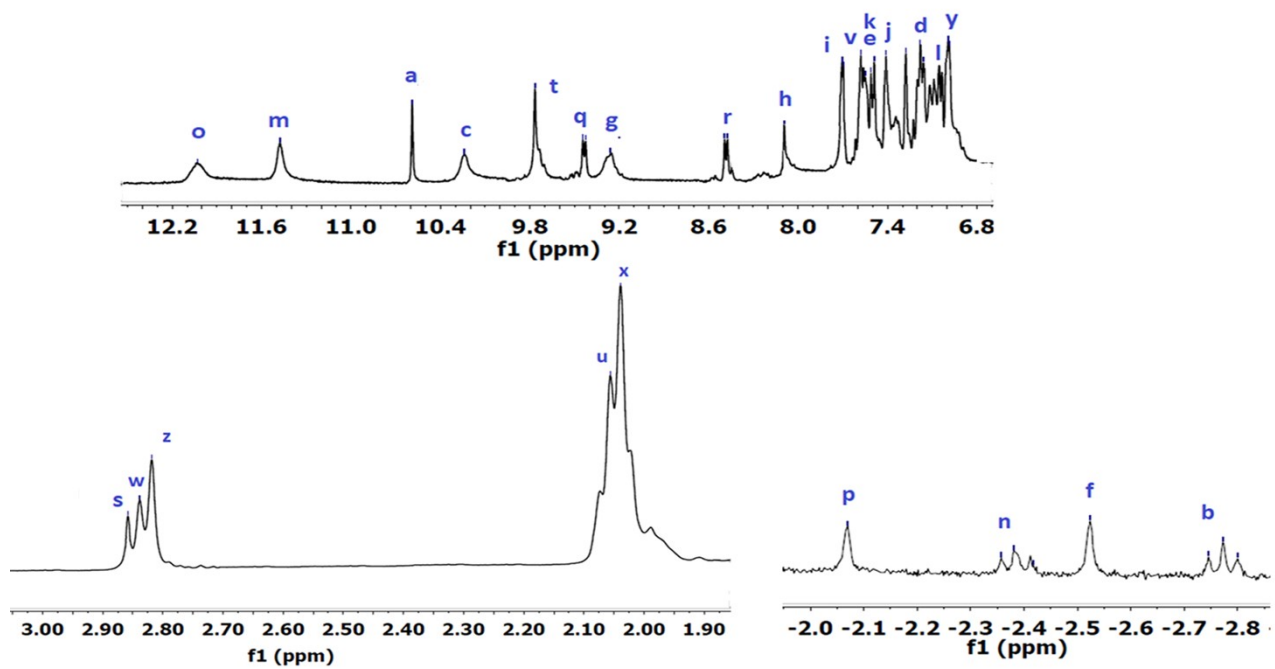


Fig. S41 Complete  $^1\text{H}$  NMR spectral assignment of **14''** in  $\text{CD}_2\text{Cl}_2$  at 298 K

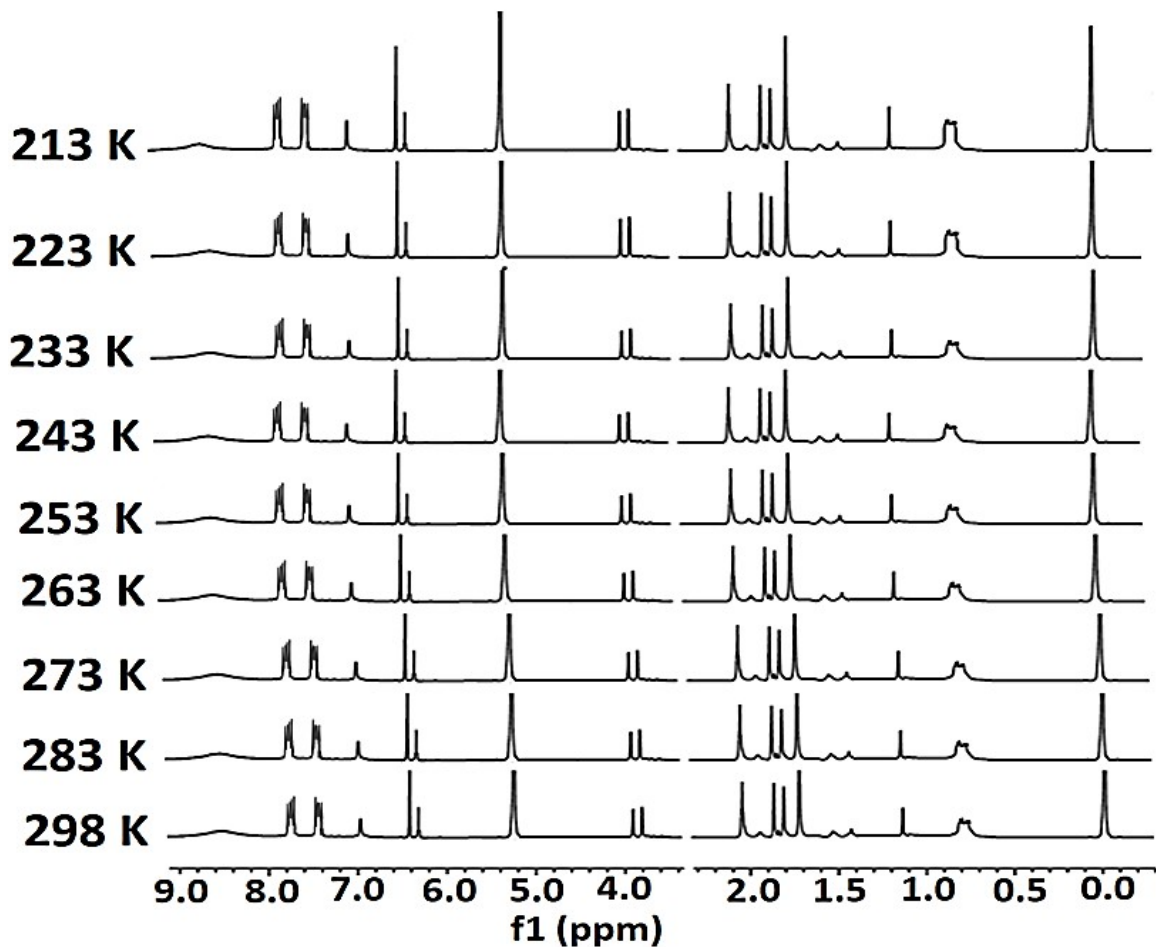


Fig. S42 Low VT  $^1\text{H}$  NMR spectra of **15''** in  $\text{CD}_2\text{Cl}_2$

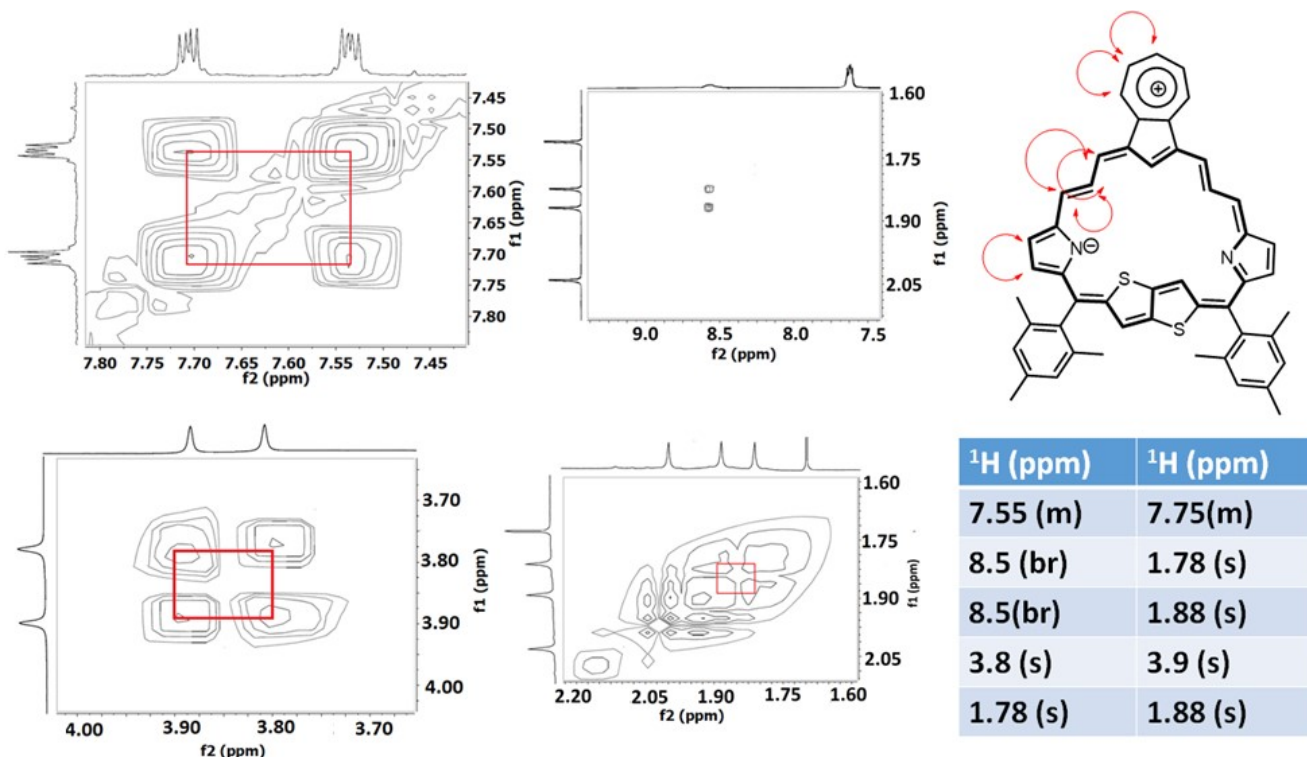


Fig. S43  $^1\text{H}$ - $^1\text{H}$  2D COSY NMR spectra of  $\mathbf{15}''$  in  $\text{CD}_2\text{Cl}_2$  at 298 K

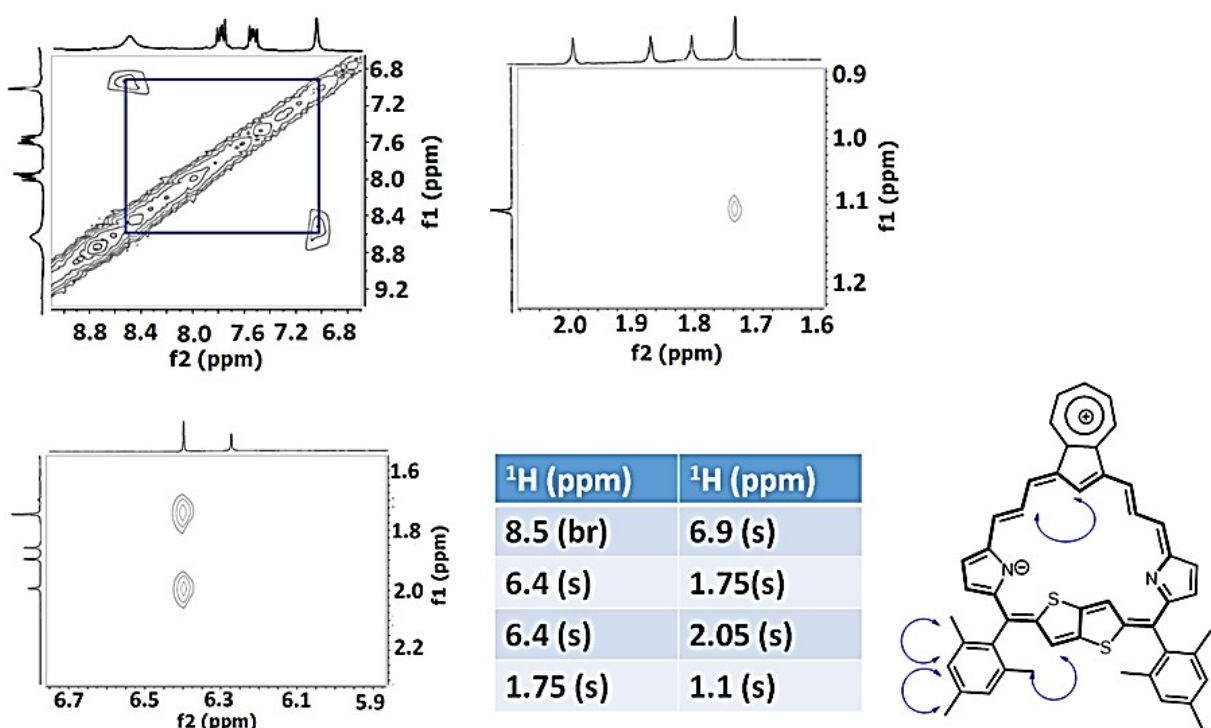


Fig. S44  $^1\text{H}$ - $^1\text{H}$  2D ROESY NMR spectra of  $\mathbf{15}''$  in  $\text{CD}_2\text{Cl}_2$  at 298 K

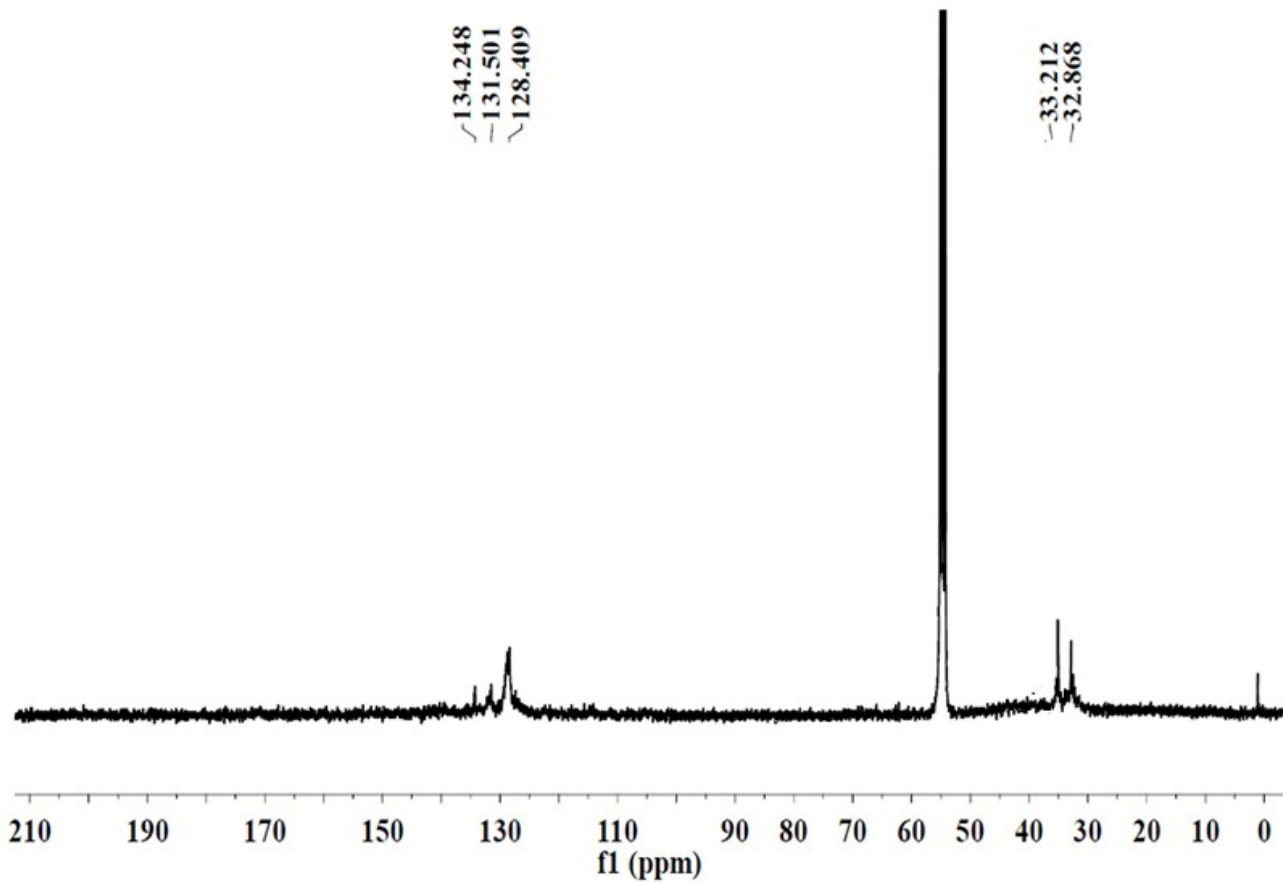


Fig. S45  $^{13}\text{C}$  NMR spectra of **15''** in  $\text{CD}_2\text{Cl}_2$  at 298 K

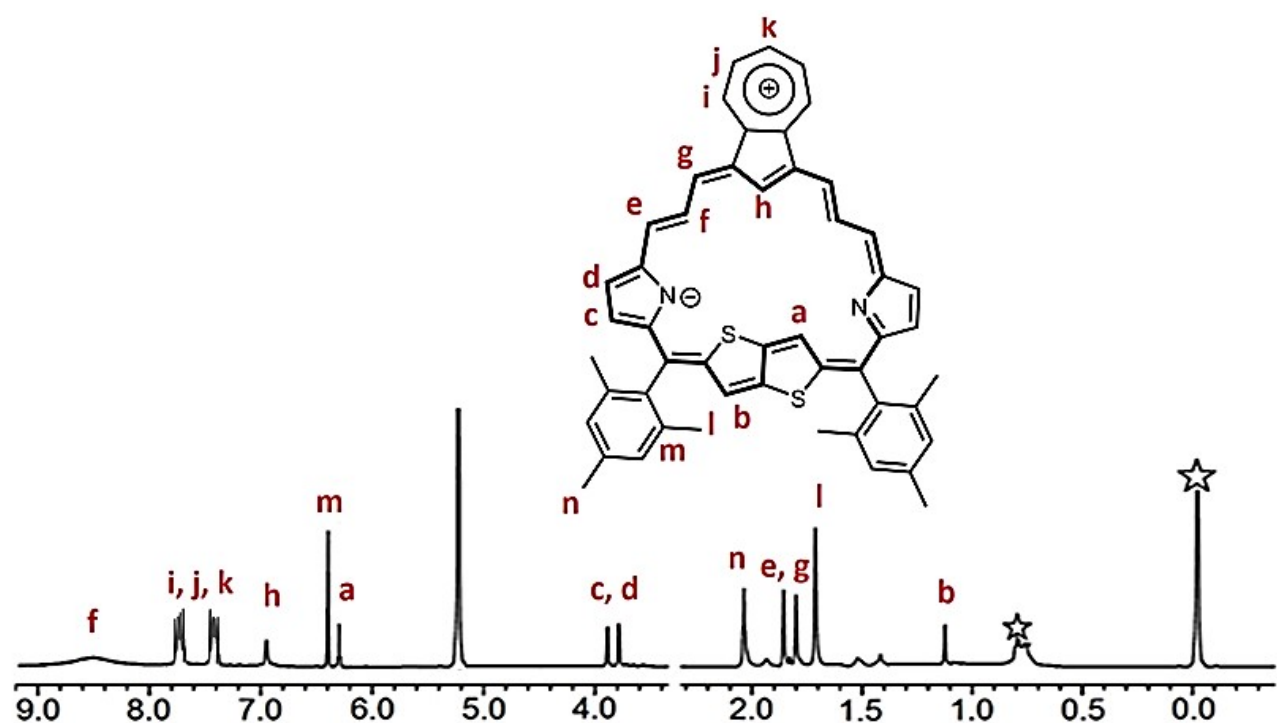


Fig. S46 Completely assigned  $^1\text{H}$  NMR spectra of **15''** in  $\text{CD}_2\text{Cl}_2$  at 298 K

### 3.0 Crystallographic Data

Table S1

Parameters	<b>14</b>
<b>Chemical formula</b>	C <sub>53</sub> H <sub>44</sub> N <sub>2</sub> O <sub>2</sub> S <sub>2</sub>
<b>Formula weight</b>	805.2922
<b>Temperature</b>	100 K
<b>Crystal system</b>	orthorhombic
<b>Space group</b>	P n m a
<b>a (Å); <math>\alpha</math> (°)</b>	22.5989(8); 90
<b>b (Å); <math>\beta</math> (°)</b>	20.6160(7); 90
<b>c (Å); <math>\gamma</math> (°)</b>	9.7234(3); 90
<b>V (Å<sup>3</sup>); Z</b>	4530.1(3); 4
<b><math>\rho</math> (calc.) mg m<sup>-3</sup></b>	1.153
<b><math>\mu</math>(Mo K<math>\alpha</math>) mm<sup>-1</sup></b>	0.157
<b>2<math>\theta</math>max (°)</b>	54.14°
<b>R(int)</b>	3.42%
<b>Completeness to <math>\theta</math></b>	99.4
<b>Data / param.</b>	5132/284
<b>GOF</b>	1.060
<b>R1 [F&gt;4<math>\sigma</math>(F)]</b>	7.08%
<b>wR2 (all data)</b>	19.83%
<b>max. peak/hole (e.Å<sup>-3</sup>)</b>	0.964 / -0.533
<b>CCDC</b>	2116847

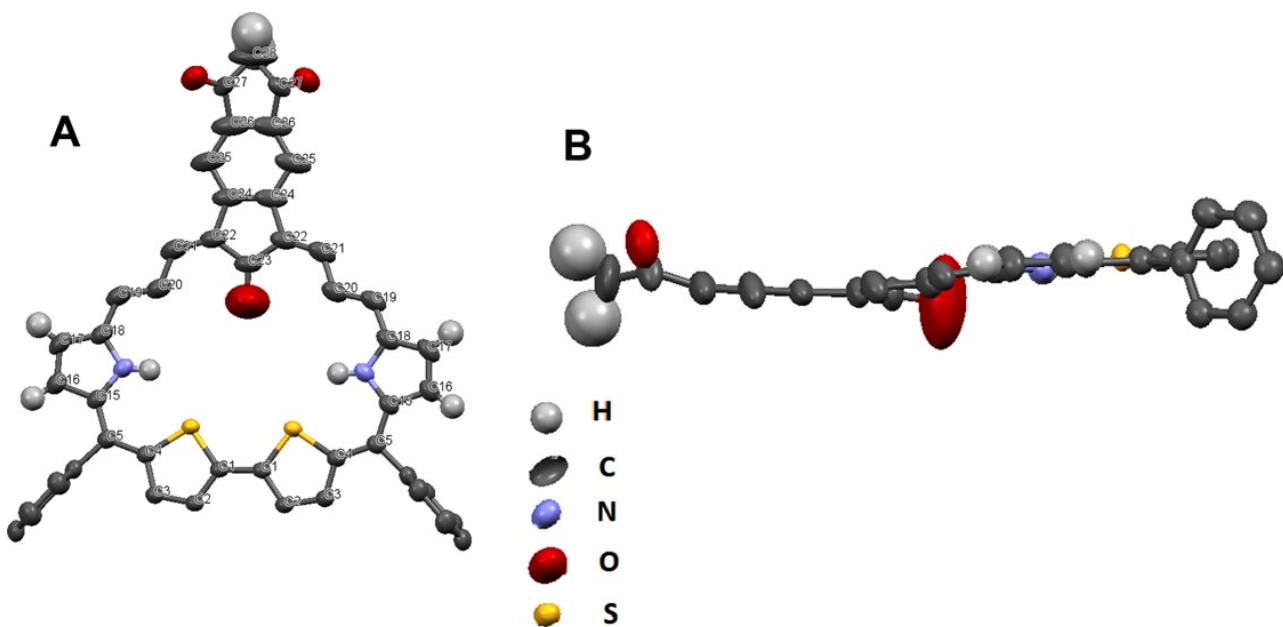


Fig. S47 X-ray crystal structure of **14** (A: Top view, B: side view). The thermal ellipsoids are scaled to 50% probability level

#### 4. Theoretical Calculation

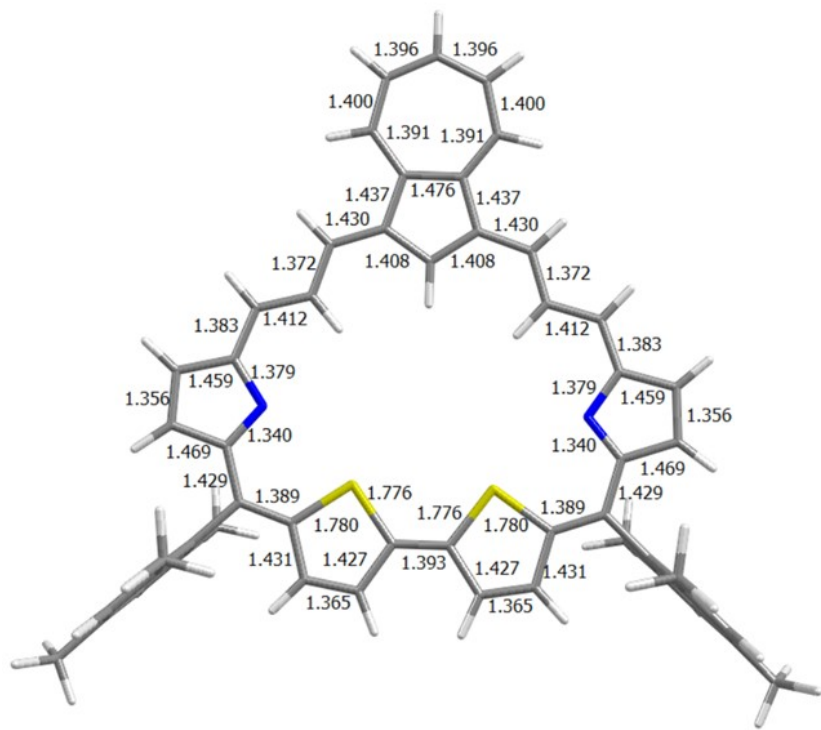


Fig. S48 Optimized geometry of **13** with selected bond length (Å) computed at the B3LYP/6-31G(d,p) level

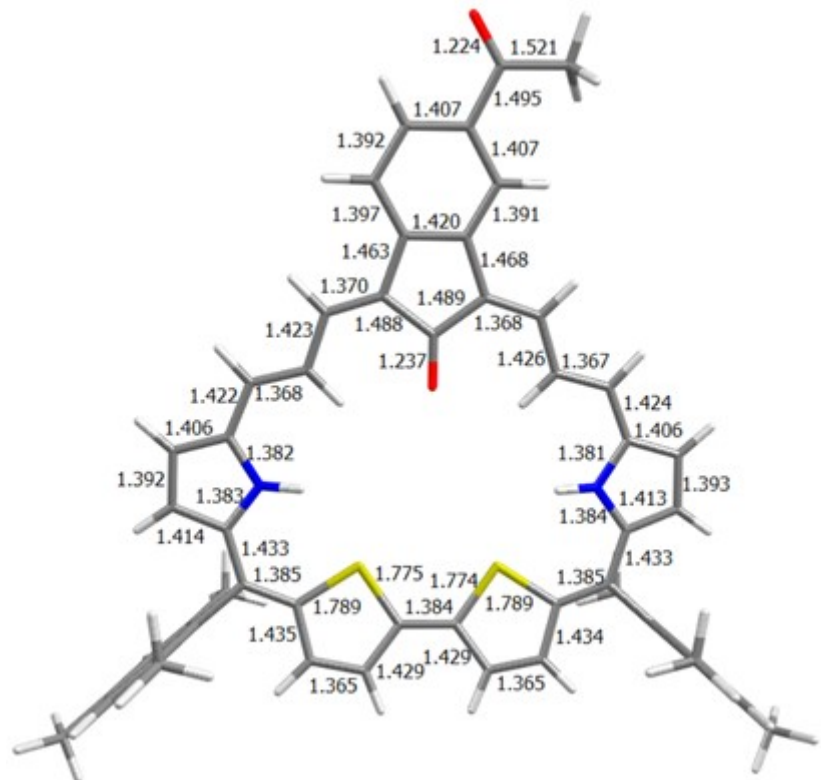


Fig. S49 Optimized geometry of **14** with selected bond length (Å) computed at the B3LYP/6-31G(d,p) level

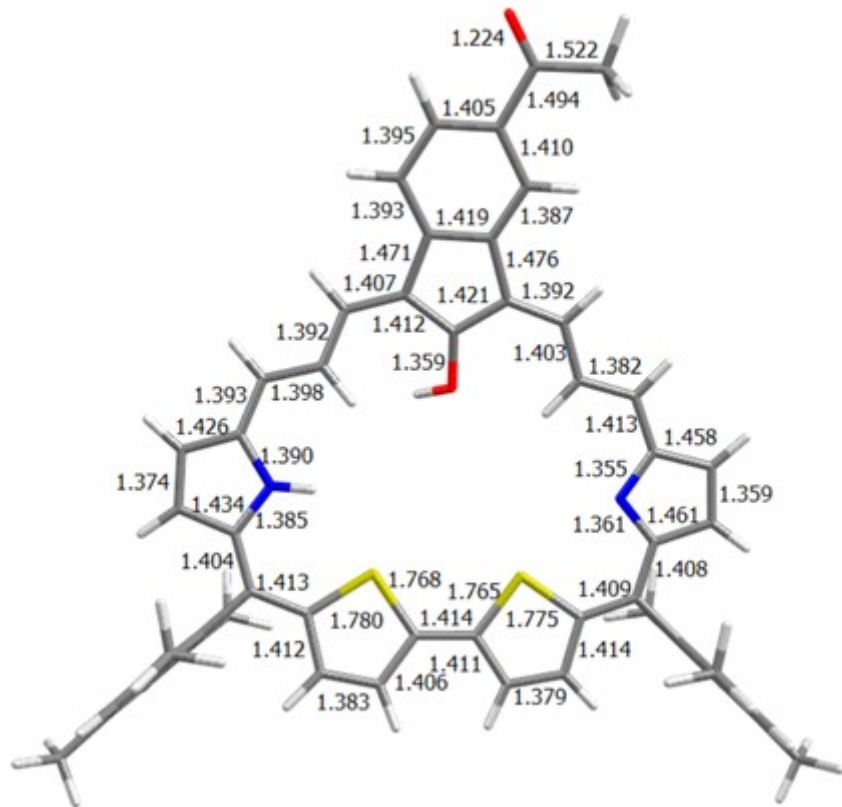


Fig. S50 Optimized geometry of **14'-1** with selected bond length (Å) computed at the B3LYP/6-31G(d,p) level

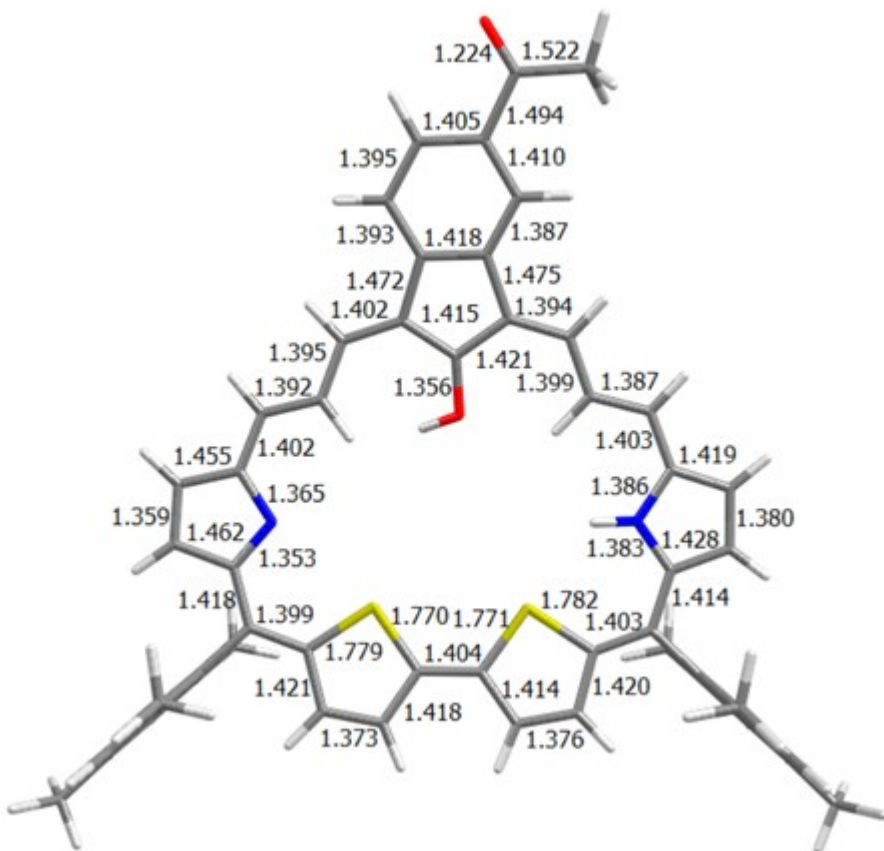


Fig. S51 Optimized geometry of **14"-2** with selected bond length (Å) computed at the B3LYP/6-31G(d,p) level

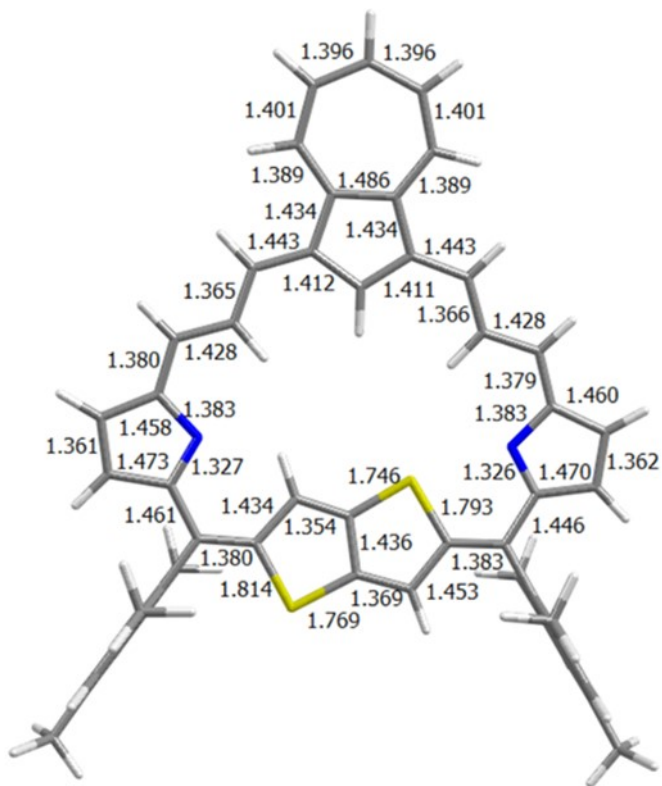


Fig. S52 Optimized geometry of **15** with selected bond length ( $\text{\AA}$ ) computed at the B3LYP/6-31G(d,p) level

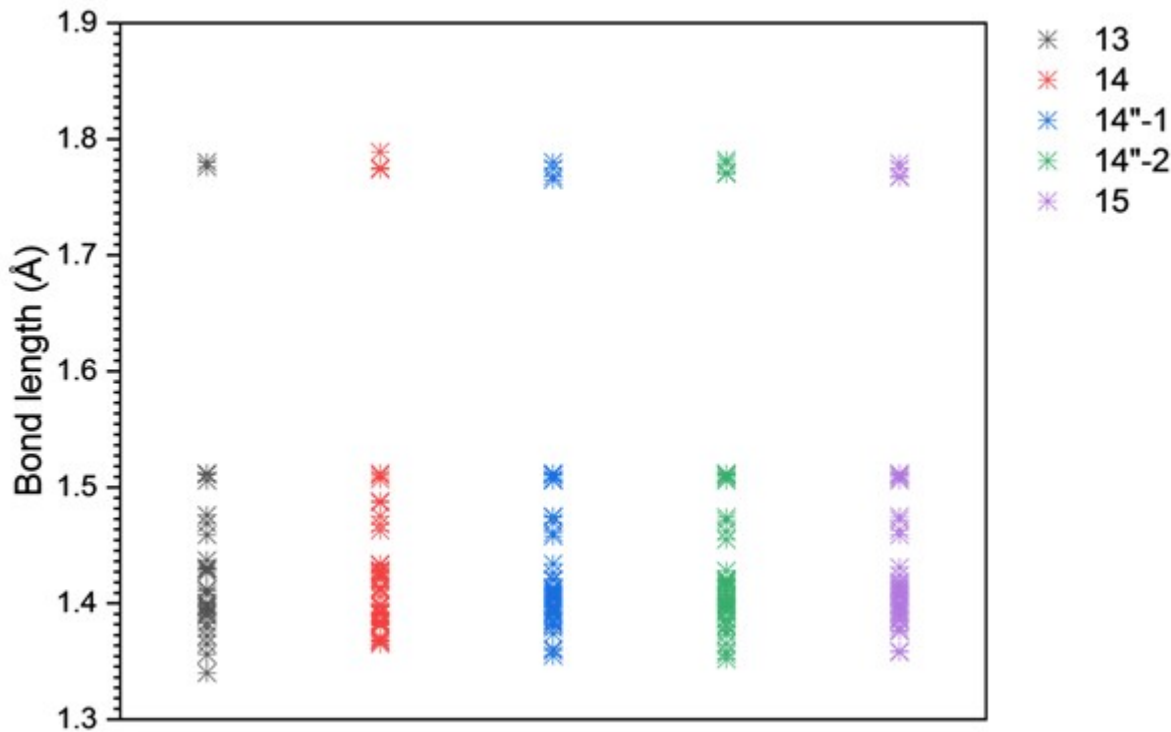


Fig. S53 Illustration of  $\pi$ -delocalization from calculated C-C, C-S and C-N bond lengths of **13**, **14**, **14"-1**, **14"-2** and **15** at the B3LYP/6-31G (d, p) level

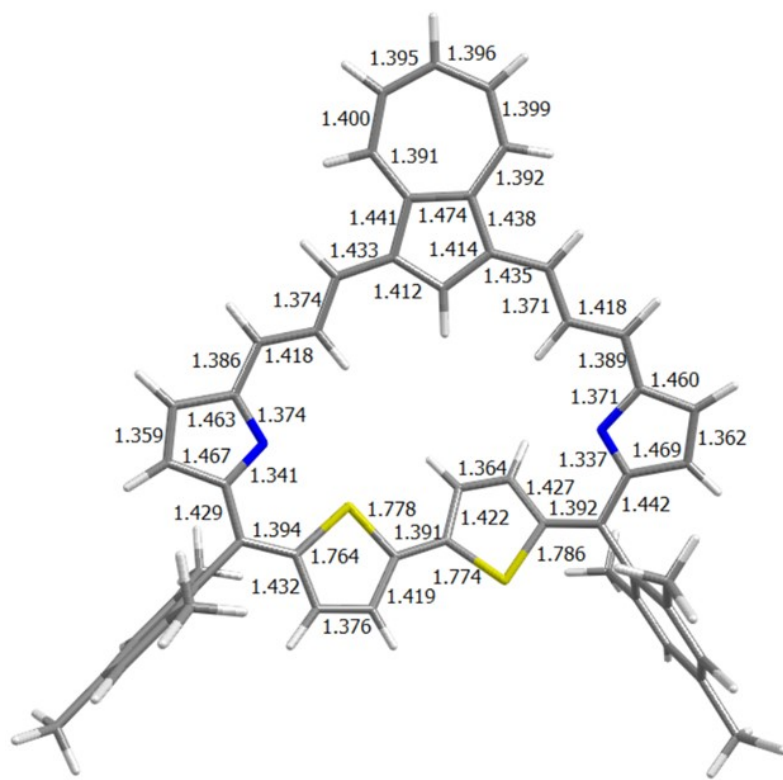


Fig. S54 Optimized geometry of **13**-Conformer-1 with selected bond length (Å) computed at the B3LYP/6-31G(d,p) level

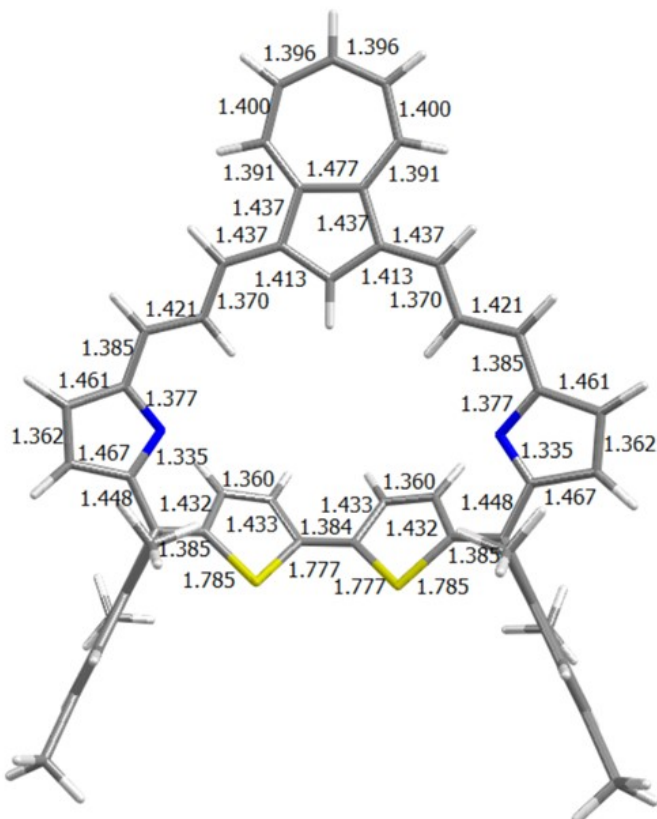


Fig. S55 Optimized geometry of **13**-Conformer-2 with selected bond length (Å) computed at the B3LYP/6-31G (d,p) level

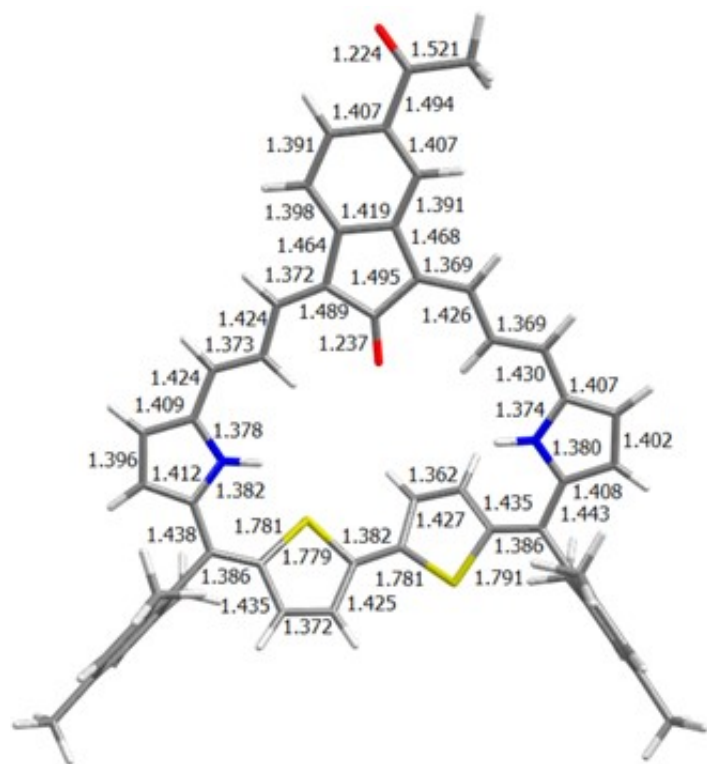


Fig. S56 Optimized geometry of **14**-Conformer-1 with selected bond length (Å) computed at the B3LYP/6-31G(d,p) level

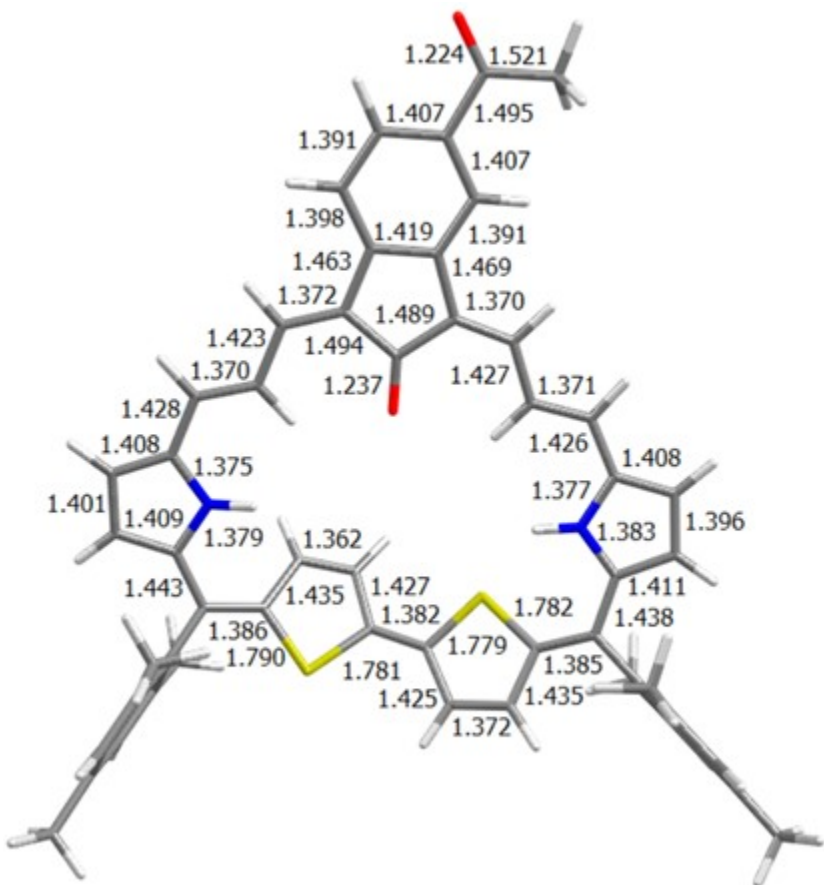


Fig. S57 Optimized geometry of **14**-Conformer-2 with selected bond length (Å) computed at the B3LYP/6-31G(d,p) level

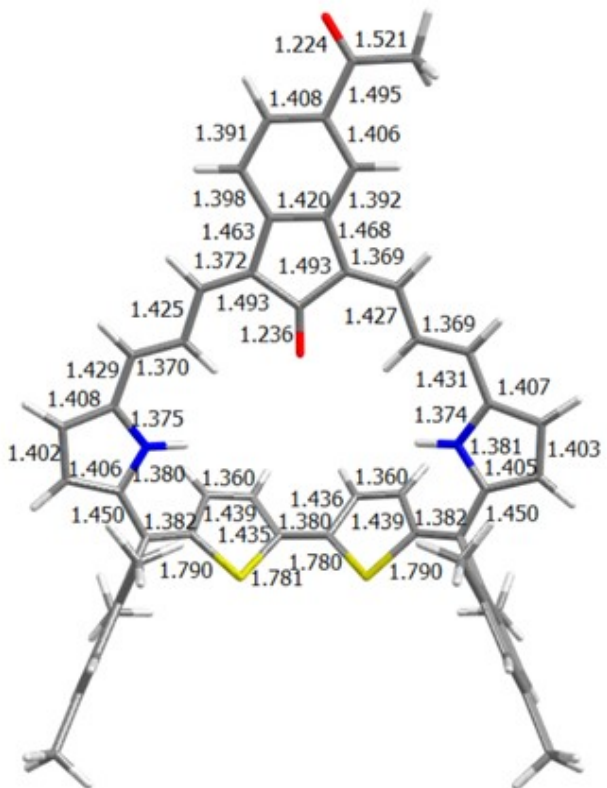


Fig. S58 Optimized geometry of **14**-Conformer-3 with selected bond length ( $\text{\AA}$ ) computed at the B3LYP/6-31G(d,p) level

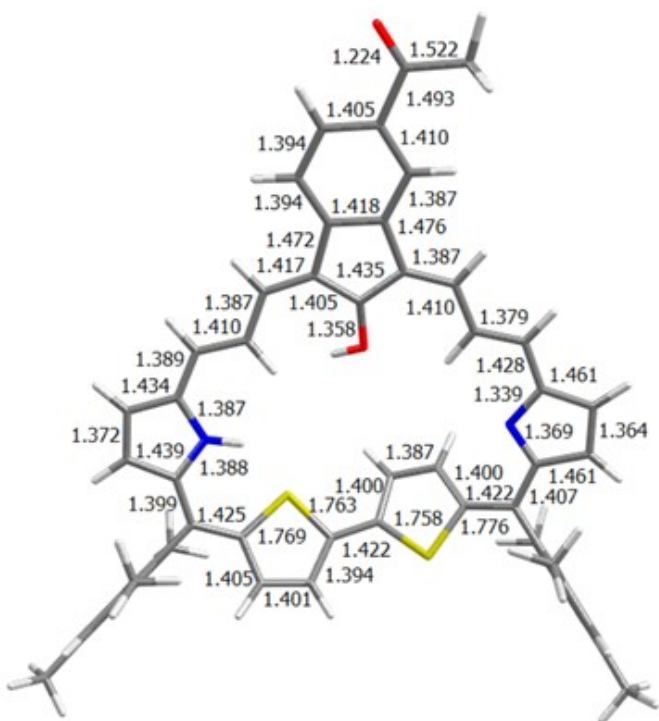


Fig. S59 Optimized geometry of **14"-1** Conformer-1 with selected bond length (Å) computed at the B3LYP/6-31G (d, p) level

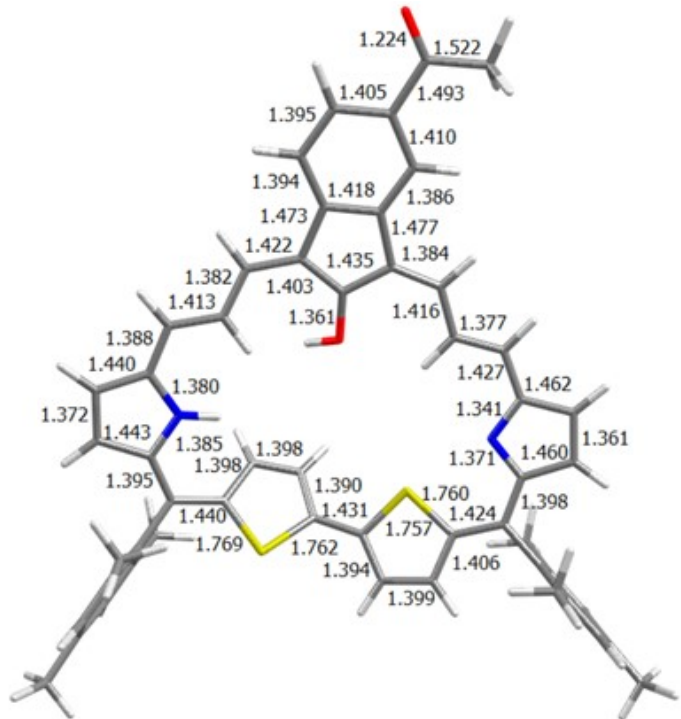


Fig. S60 Optimized geometry of **14''-1** Conformer-2 with selected bond length (Å) computed at the B3LYP/6-31G(d,p) level

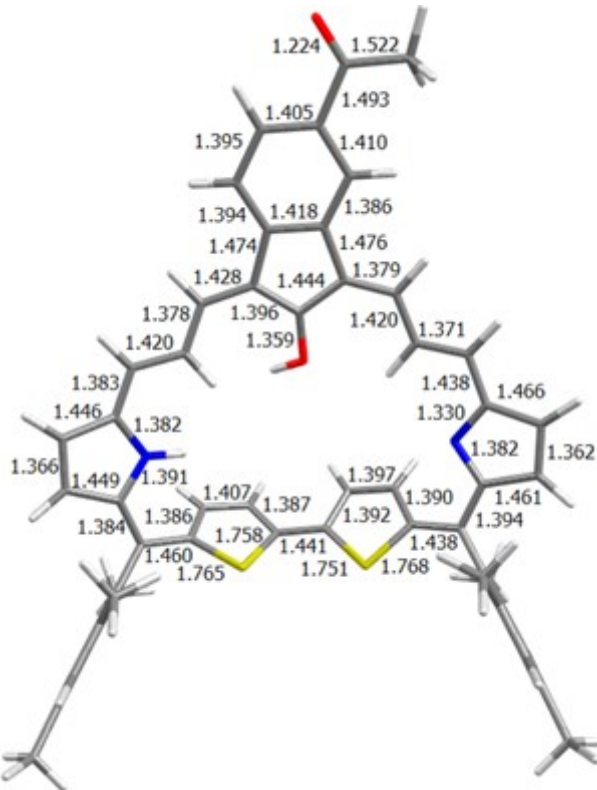


Fig. S61 Optimized geometry of **14''-1** Conformer-3 with selected bond length (Å) computed at the B3LYP/6-31G (d, p) level

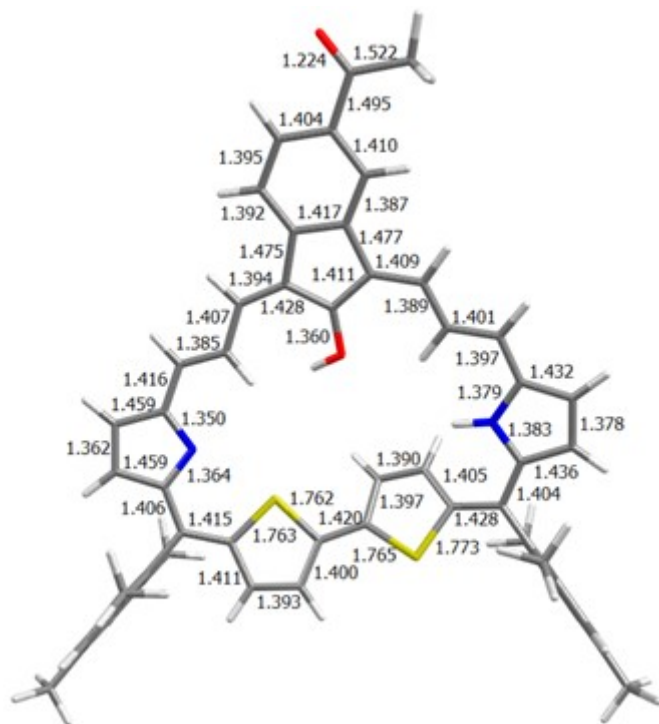


Fig. S62 Optimized geometry of **14"-2** Conformer-1 with selected bond length (Å) computed at the B3LYP/6-31G (d, p) level

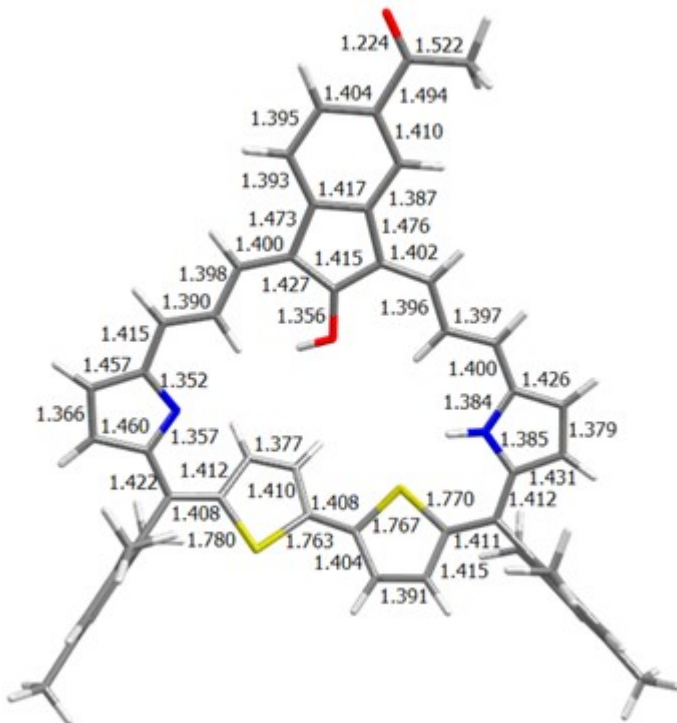


Fig. S63 Optimized geometry of **14"-2** Conformer-2 with selected bond length (Å) computed at the B3LYP/6-31G (d, p) level

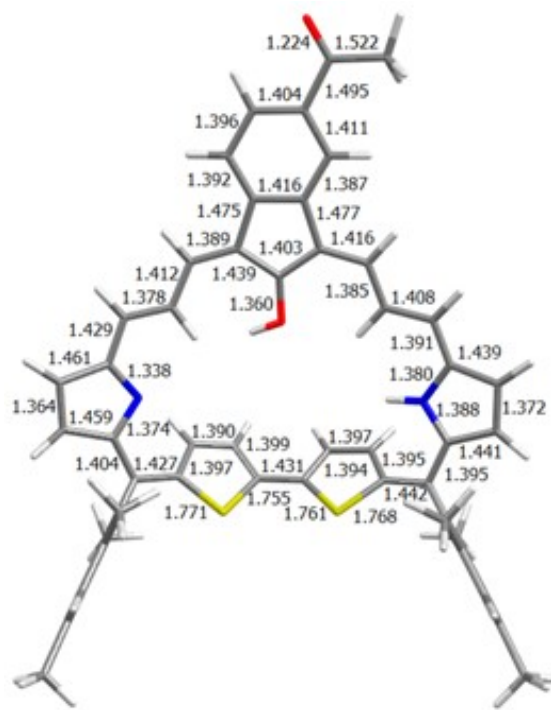


Fig. S64 Optimized geometry of **14''-2** Conformer-3 with selected bond length (Å) computed at the B3LYP/6-31G (d, p) level

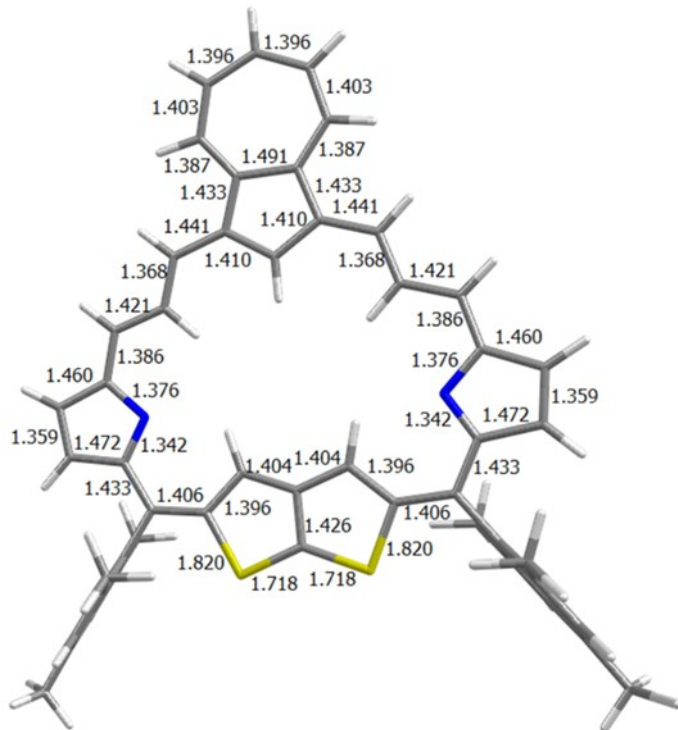


Fig. S65 Optimized geometry of **15**-Conformer-1 with selected bond length (Å) computed at the B3LYP/6-31G (d, p) level

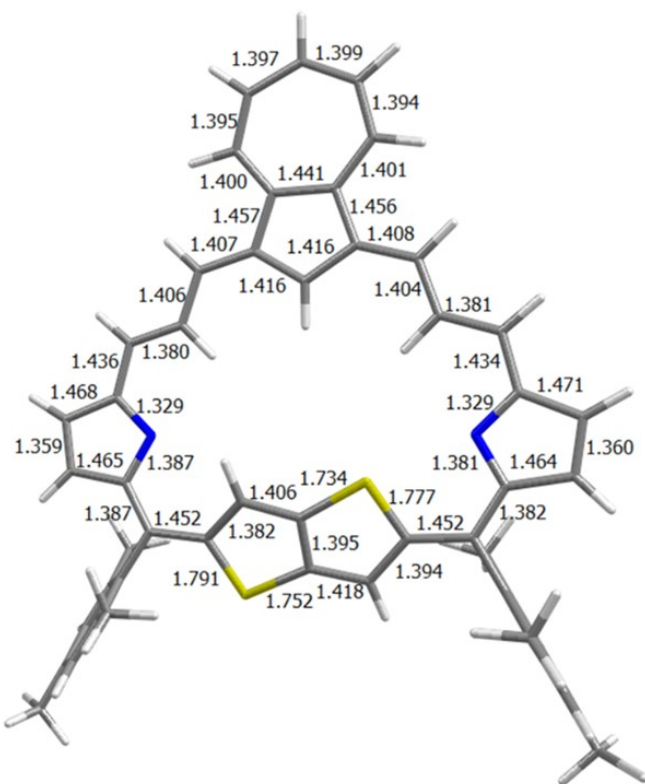


Fig. S66 Optimized geometry of **15**-Conformer-2 with selected bond length (Å) computed at the B3LYP/6-31G (d, p) level

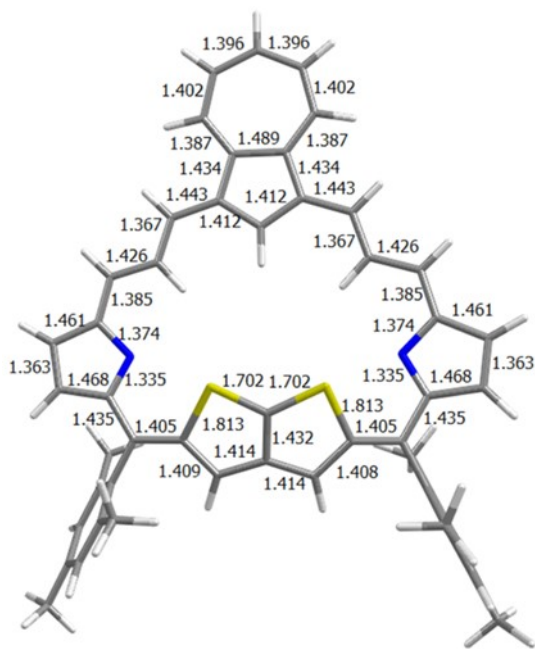


Fig. S67 Optimized geometry of **15**-Conformer-3 with selected bond length (Å) computed at the B3LYP/6-31G (d, p) level

Table S2 Calculated energies of the optimized structures, zero point energy correction (ZPE), free energy corrections (GFE), relative energies ( $\Delta E$ ) and relative Gibbs free energies ( $\Delta G$ ) for plausible isomers of **13**, **14**, **14"-1**, **14"-2** and **15** at the B3LYP/6-31G(d,p) level.

	<b>ZPE (hartree)</b>	<b>GFE (hartree)</b>	<b>Energy (hartree)</b>	<b><math>\Delta E</math> (kJ/mol)</b>	<b><math>\Delta E+ZPE</math> (kJ/mol)</b>	<b><math>\Delta G</math> (kJ/mol)</b>
<b>13</b>	0.782713	0.692921	-2912.698637	0.00	0.00	0.00
<b>13-Conformer-1</b>	0.782262	0.693093	-2912.680814	46.80	45.611	47.25
<b>13-Conformer-2</b>	0.782325	0.694043	-2912.653864	117.55	116.53	120.50
<hr/>						
<b>14</b>	0.820817	0.726417	-3102.543075	0.00	0.00	0.00
<b>14-Conformer-1</b>	0.821078	0.727618	-3102.529016	36.91	37.60	40.06
<b>14-Conformer-2</b>	0.821092	0.727666	-3102.528934	37.12	37.85	40.41
<b>14-Conformer-3</b>	0.821143	0.728206	-3102.50969	87.65	88.51	92.35
<hr/>						
<b>14"-1</b>	0.819331	0.724911	-3102.514288	0.00	0.00	0.00
<b>14"-1-Conformer-1</b>	0.819322	0.72582	-3102.498781	40.71	40.69	42.10
<b>14"-1-Conformer-2</b>	0.819588	0.725851	-3102.501062	34.72	35.40	37.19
<b>14"-1-Conformer-3</b>	0.819362	0.72501	-3102.476037	100.43	100.51	100.68
<b>14"-2</b>	0.819556	0.72517	-3102.518173	0.00	0.00	0.00
<b>14"-2-Conformer-1</b>	0.819454	0.725816	-3102.504887	34.88	34.61	36.58
<b>14"-2-Conformer-2</b>	0.819038	0.725432	-3102.501447	43.91	42.46	44.60
<b>14"-2-Conformer-3</b>	0.819024	0.725138	-3102.478604	103.89	102.49	103.80
<hr/>						
<b>15</b>	0.748596	0.660499	-2835.269661	0.00	0.00	0.00
<b>15-Conformer-1</b>	0.746972	0.659657	-2835.242628	70.97	66.71	68.76
<b>15-Conformer-2</b>	0.746867	0.660638	-2835.236551	86.93	82.39	87.29
<b>15-Conformer-3</b>	0.747269	0.661062	-2835.231737	99.57	96.09	101.05

Table S3. Frontier Molecular Orbital compositions (%) in the ground state for **13**, **14**, **14"-1**, **14"-2**, **15** at the B3LYP/6-31G (d,p) level.

	Orbital	Energy (eV)	Contribution (%)				
			Thiophene	Pyrrole	$\pi$ -bridge	Azulene	Mesitylene
<b>13</b>	HOMO-3	-5.922	19.43	56.51	6.40	9.25	8.41
	HOMO-2	-5.918	12.52	37.47	24.73	18.73	6.56
	HOMO-1	-4.848	19.67	27.47	17.13	34.66	1.07
	HOMO	-4.303	34.85	12.54	21.77	4.36	26.48
	LUMO	-2.842	20.20	13.98	21.95	33.91	9.96
	LUMO+1	-2.517	0.07	0.10	0.08	99.74	0.01
	LUMO+2	-2.219	24.60	30.98	31.90	8.53	4.00
	LUMO+3	-1.798	23.62	12.46	7.51	37.12	19.29
<b>14</b>	HOMO-3	-6.240	0.08	0.61	14.96	84.32	0.03

	HOMO-2	-5.465	18.16	8.95	23.04	36.22	13.63
	HOMO-1	-5.172	24.55	34.87	18.8	20.51	1.27
	HOMO	-4.317	33.03	22.66	7.43	20.54	16.34
	LUMO	-2.720	33.85	18.48	12.65	12.75	22.27
	LUMO+1	-2.359	15.18	16.08	33.03	34.36	1.35
	LUMO+2	-1.617	14.64	15.05	22.63	38.03	9.64
	LUMO+3	-0.915	46.12	18.35	8.82	13.23	13.48
14"-1	HOMO-3	-6.147	17.43	57.3	8.05	11.49	5.74
	HOMO-2	-5.671	9.32	11.53	9.39	65	4.76
	HOMO-1	-4.937	26.08	29.06	16.3	23.21	5.35
	HOMO	-4.582	24.02	16.22	21.94	20.01	17.81
	LUMO	-2.791	29.04	18.93	17.55	16.93	17.54
	LUMO+1	-2.668	24.67	24	30.1	11.31	9.92
	LUMO+2	-1.515	16.02	19.56	20.06	33.89	10.46
	LUMO+3	-0.856	27.29	15.89	13.16	35.9	7.76
14"-2	HOMO-3	-6.184	17.32	58.34	7.85	11.01	5.48
	HOMO-2	-5.662	9.42	11.32	9.6	63.57	6.09
	HOMO-1	-4.963	24.86	30.62	17.01	24.97	2.53
	HOMO	-4.566	26.82	15.23	19.39	18.53	20.04
	LUMO	-2.786	28.81	16.19	17.73	16.31	20.96
	LUMO+1	-2.682	24.77	25.46	32.07	12.79	4.91
	LUMO+2	-1.537	16.62	19.73	20.01	32.53	11.11
	LUMO+3	-0.884	16.01	11.94	9.94	57.05	5.06
15	LUMO	-5.918	83.72	11.48	1.81	1.32	1.67
	LUMO+1	-5.625	28.56	29.36	26.17	12.89	3.02
	LUMO+2	-5.424	13.35	22.65	14.39	32.55	17.07
	LUMO+3	-4.331	24.11	15.36	16.63	21.28	22.62
	LUMO	-2.884	20.92	26.23	35.06	6.45	11.35
	LUMO+1	-2.358	9.79	23.05	19.51	44.22	3.43
	LUMO+2	-2.353	0.11	0.2	0.26	99.39	0.04
	LUMO+3	-1.435	28.99	22.06	14.64	4.98	29.32

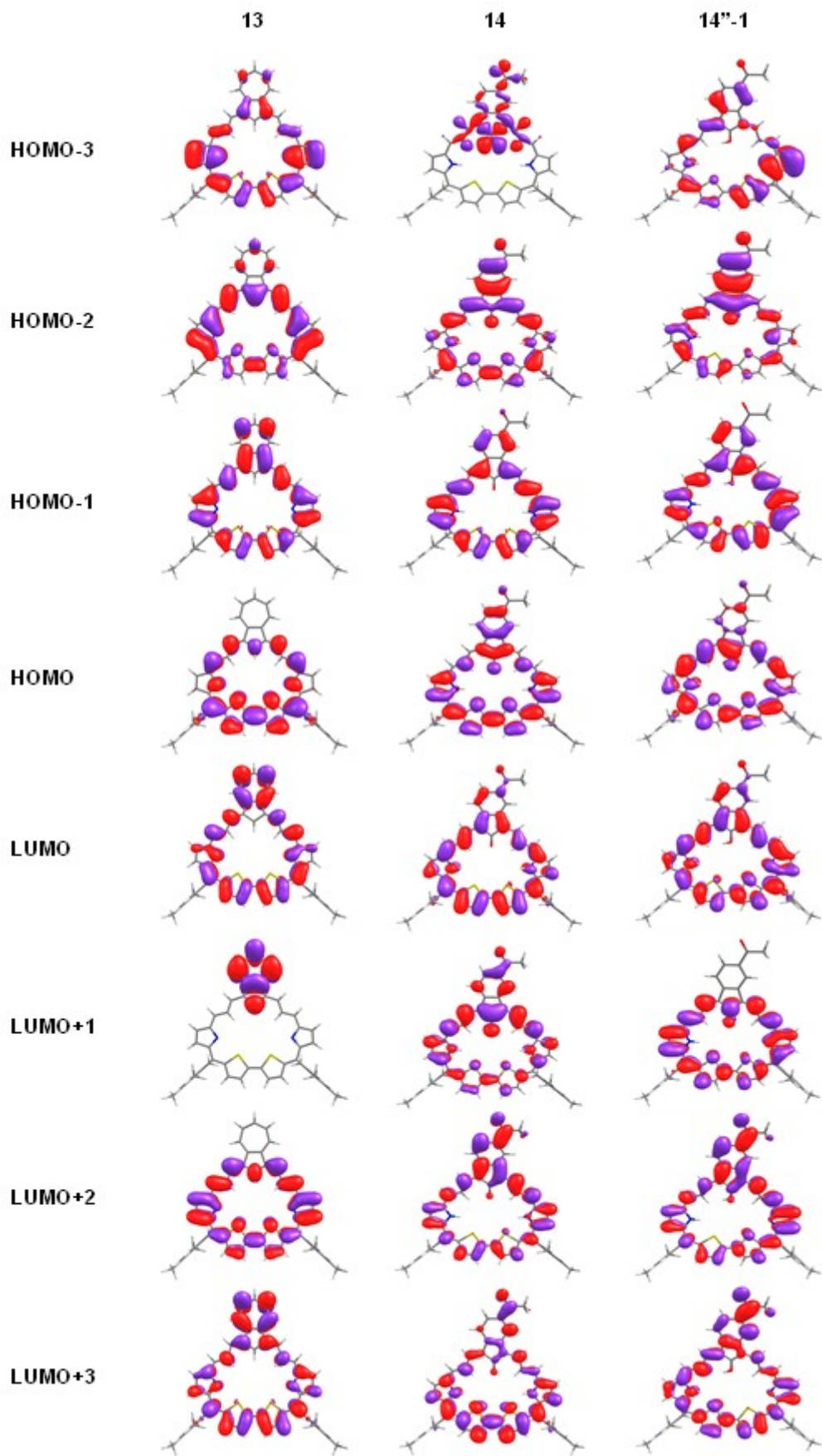


Fig. S68 Highest occupied molecular orbital and lowest unoccupied molecular orbitals of **13**, **14** and **14"-1** at the B3LYP/6-31G(d,p) level

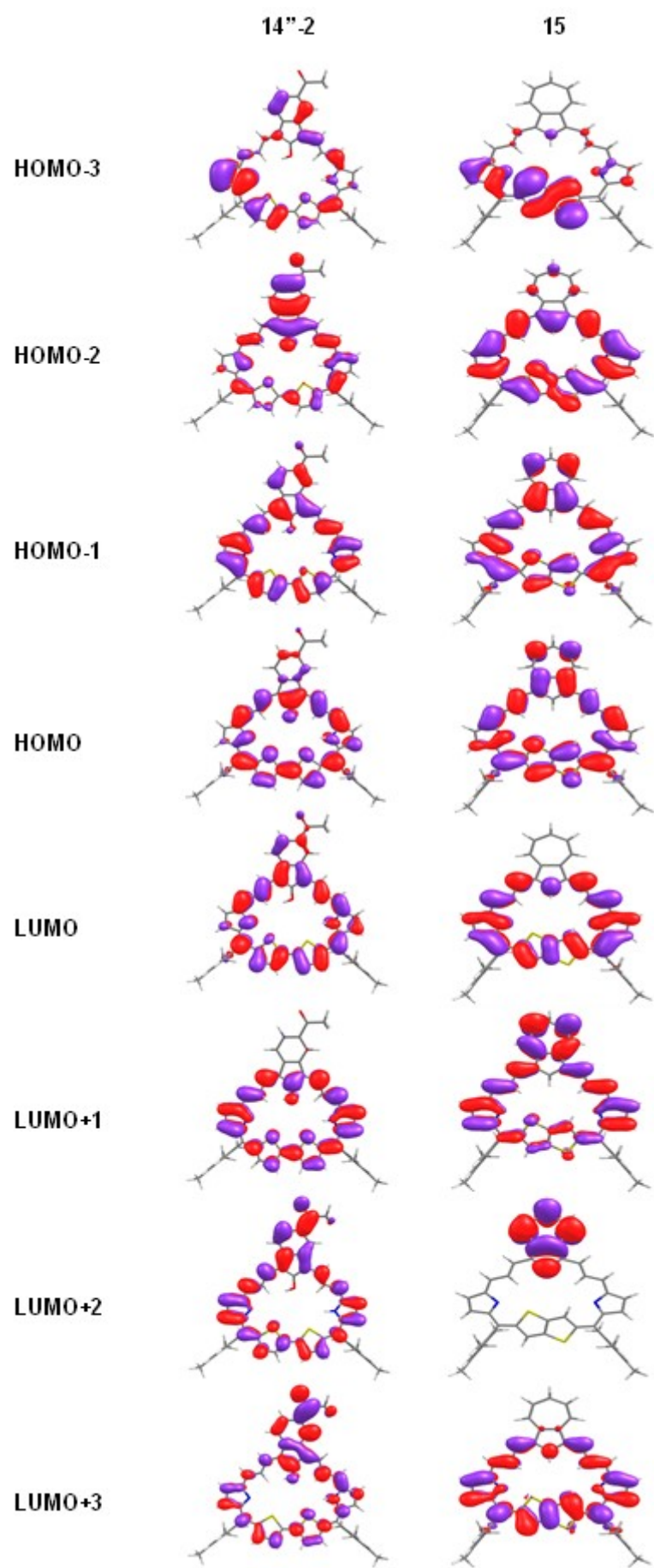


Fig. S69 Highest occupied molecular orbital and lowest unoccupied molecular orbitals of **14"-2** and **15** at the B3LYP/6-31G(d,p) level

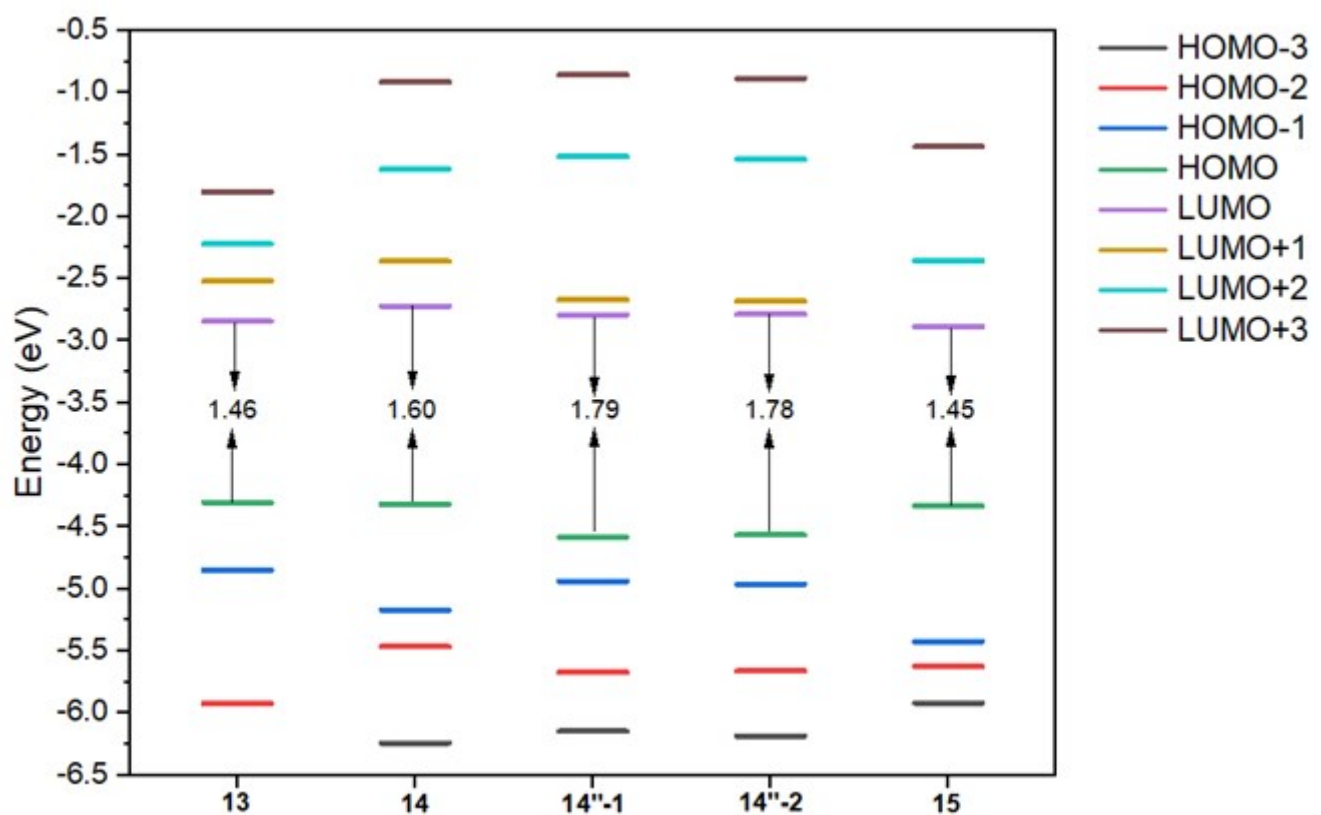


Fig. S70 FMO energy levels of **13**, **14**, **14"-1**, **14"-2** and **15** at the B3LYP/6-31G (d, p) level

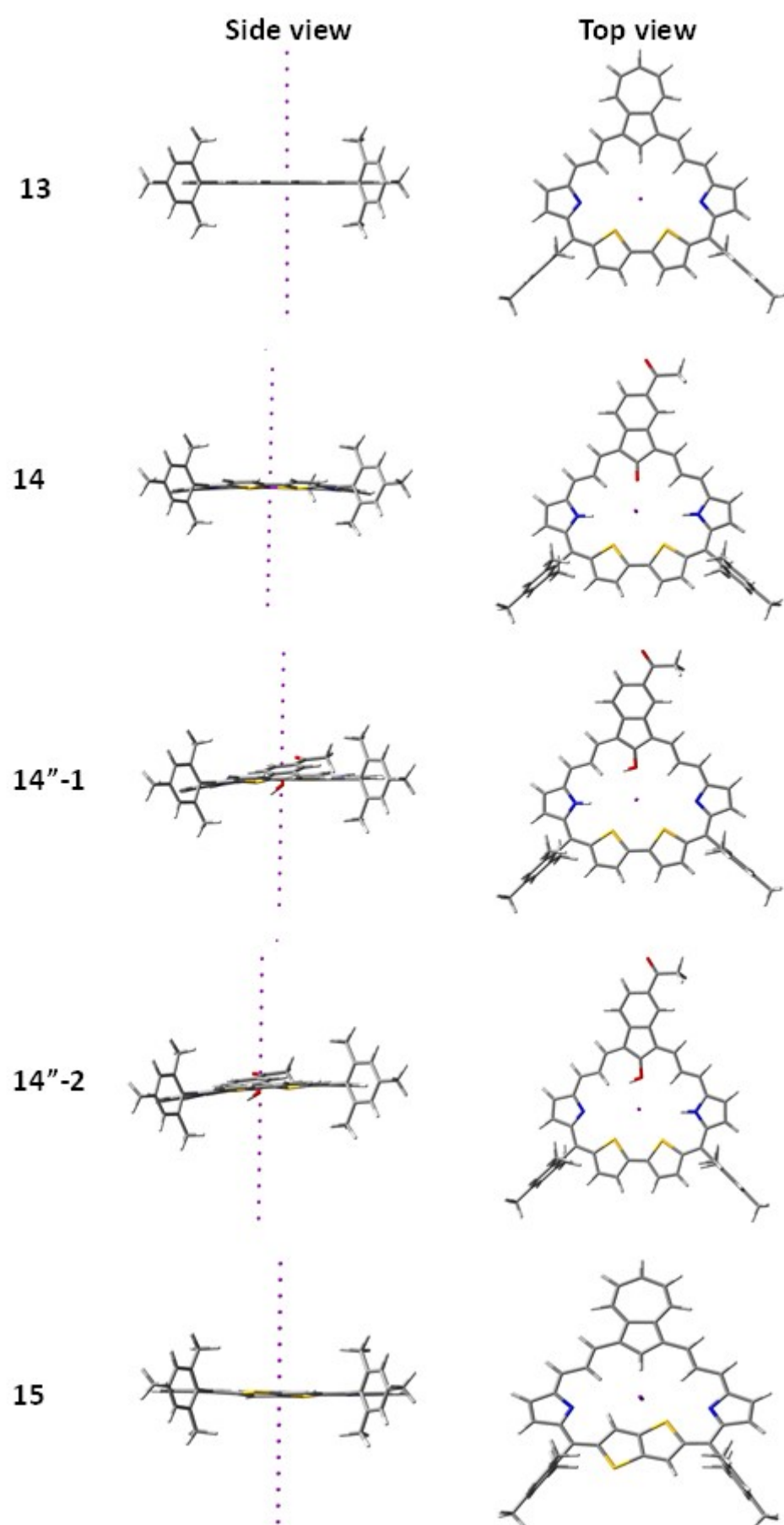


Fig. S71 The centres of macrocycles **13**, **14**, **14"-1**, **14"-2** and **15** for the NICS values were designated at the non-weighted mass of  $\pi$  conjugation pathway of the macrocycles

Table S4. The calculated nucleus-independent chemical shifts (NICS) values for **13**, **14**, **14"-1**, **14"-2** and **15**

Distance (Å)	<b>13</b>	<b>14</b>	<b>14"-1</b>	<b>14"-2</b>	<b>15</b>
-8	-0.923	-0.261	-1.772	-1.767	0.735
-7	-1.203	-0.330	-2.347	-2.342	1.033
-6	-1.582	-0.419	-3.150	-3.148	1.490
-5	-2.088	-0.527	-4.270	-4.275	2.203
-4	-2.734	-0.647	-5.791	-5.812	3.317
-3	-3.484	-0.743	-7.730	-7.776	5.002
-2	-4.206	-0.724	-9.898	-9.973	7.278
-1	-4.730	-0.421	-11.769	-11.882	9.460
0	-4.929	-0.078	-12.511	-12.653	10.299
1	-4.730	-0.439	-11.738	-11.836	9.309
2	-4.207	-0.768	-9.915	-9.964	6.995
3	-3.485	-0.798	-7.744	-7.781	4.781
4	-2.735	-0.696	-5.780	-5.813	3.190
5	-2.088	-0.566	-4.243	-4.272	2.138
6	-1.582	-0.447	-3.120	-3.144	1.459
7	-1.203	-0.351	-2.320	-2.338	1.021
8	-0.923	-0.275	-1.751	-1.764	0.733

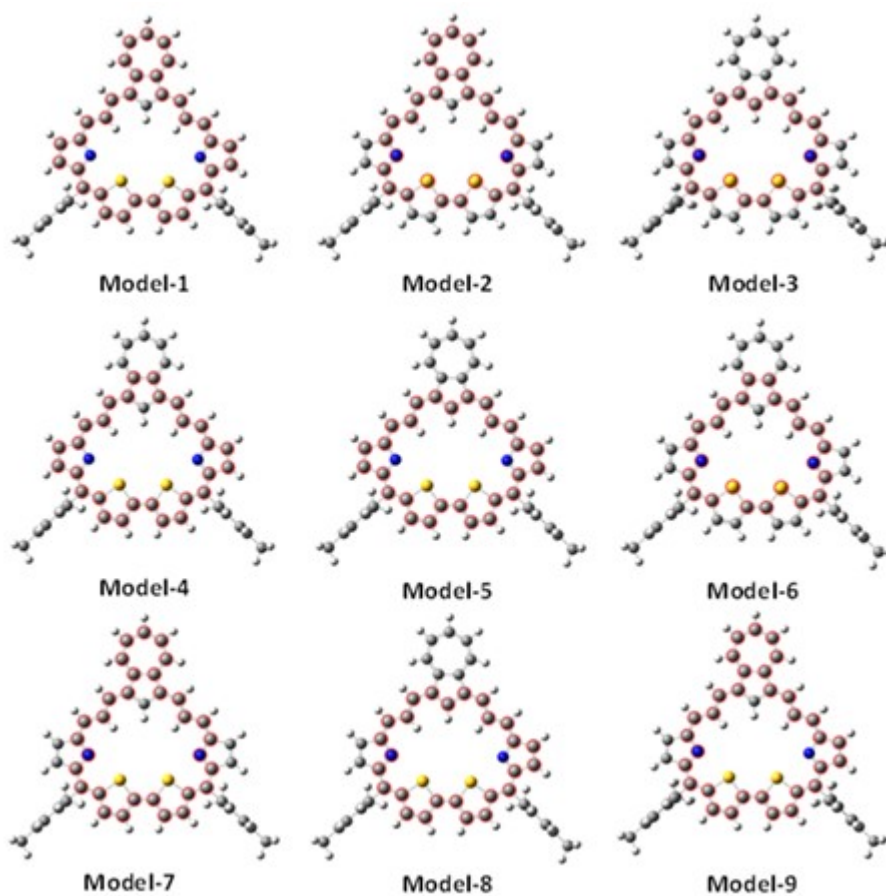


Fig. S72 The different delocalization paths of macrocycles used to calculate HOMA values

Table S5. Harmonic oscillator model of aromaticity (HOMA) values for **13**, **14**, **14"** and **15**

Delocalization paths	<b>13</b>	<b>14</b>	<b>14"-1</b>	<b>14"-2</b>	<b>15</b>
Model-1	0.633	0.723	0.708	0.710	0.450
Model-2	0.729	0.602	0.677	0.679	0.671
Model-3	0.709	0.437	0.762	0.762	0.623
Model-4	0.501	0.682	0.665	0.668	0.246
Model-5	0.595	0.605	0.785	0.787	0.350
Model-6	0.595	0.534	0.623	0.623	0.498
Model-7	0.807	0.693	0.794	0.787	0.629
Model-8	0.697	0.583	0.794	0.881	0.569
Model-9	0.717	0.709	0.712	0.787	0.629

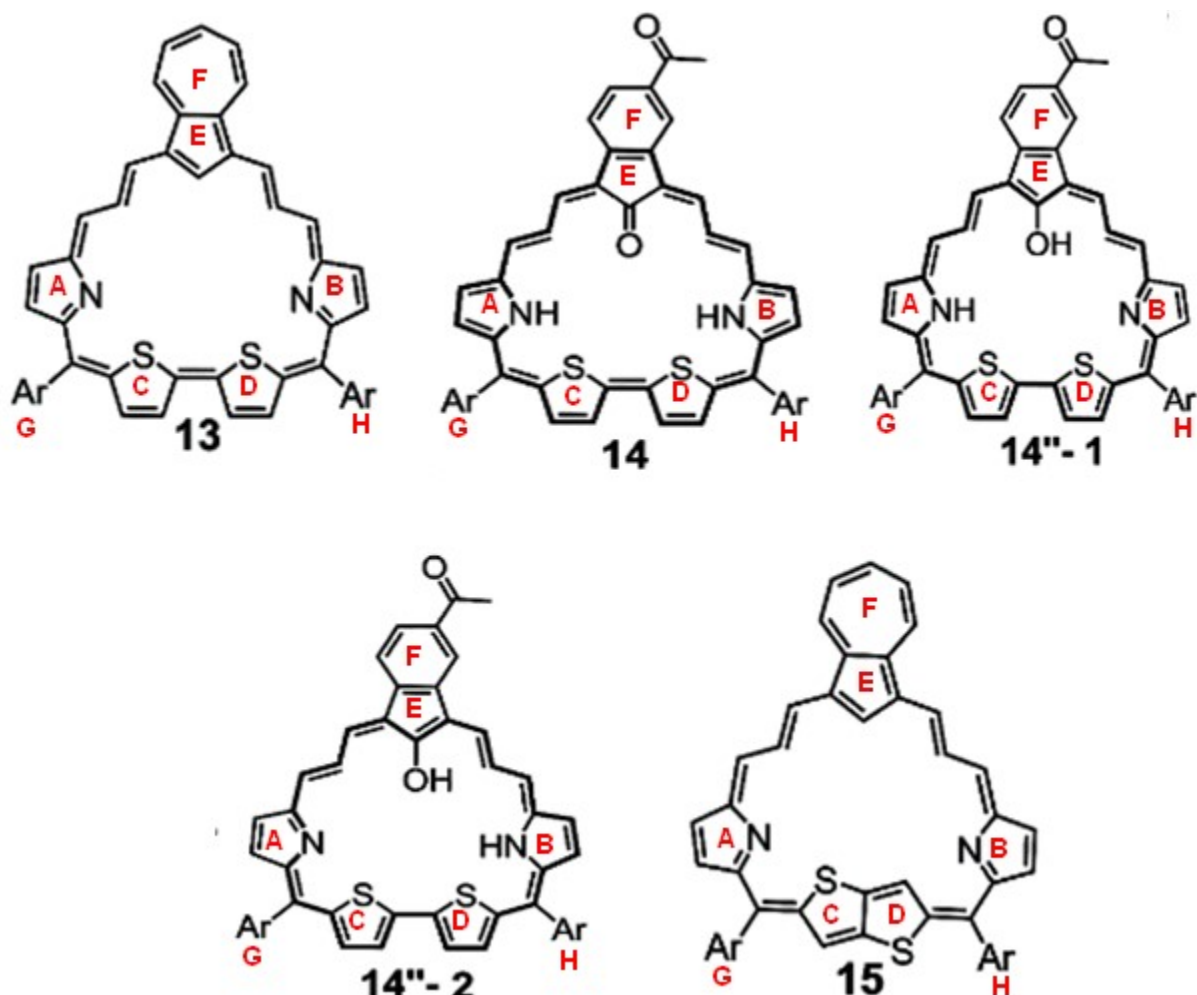


Fig. S73 Representation of individual rings used to calculated NICS, HOMA and *H* indices

Table S6. The calculated NICS (0), NICS (1) and  $\Sigma$ NICS (1) values of each ring centre for **13**, **14**, **14"-1**, **14"-2** and **15**.

Ring		<b>13</b>	<b>14</b>	<b>14"-1</b>	<b>14"-2</b>	<b>15</b>
Imino-type pyrrole -1 [A]	NICS(0)	-1.33	-	0.58	-0.16	-3.29
	NICS(1)	-5.06	-	-3.60	-3.79	-6.56
Imino-type pyrrole -2 [B]	NICS(0)	-1.33	-	-	-	-
	NICS(1)	-5.06	-	-	-	-
Amino-type pyrrole -1 [A]	NICS(0)	-	-11.12	-15.86	-16.55	-3.26
	NICS(1)	-	-9.33	-12.95	-14.00	-5.40
Amino-type pyrrole -2 [B]	NICS(0)	-	-11.04	-	-	-
	NICS(1)	-	-9.31	-	-	-
Thiophene-1 [C]	NICS(0)	-11.77	-8.00	-22.00	-19.35	-6.05
	NICS(1)	-9.97	-6.24	-19.08	-16.58	-4.00
Thiophene-2 [D]	NICS(0)	-11.77	-7.97	-19.80	-21.23	4.53
	NICS(1)	-9.85	-6.22	-16.42	-18.01	4.15
Azulene-5-memebered ring [E]	NICS(0)	-15.58	23.43	13.97	14.75	-16.09
	NICS(1)	-17.11	15.24	7.18	8.43	-17.45
Azulene-6-memebered ring [F]	NICS(0)	-	3.17	-0.57	-0.20	-
	NICS(1)	-	-0.48	-3.65	-3.28	-
Azulene-7-memebered ring [F]	NICS(0)	4.78	-	-	-	-7.82
	NICS(1)	0.70	-	-	-	-9.47
Mesitylene-1 [G]	NICS(0)	-7.72	-8.42	-6.54	-6.70	-9.93
	NICS(1)	-8.94	-9.88	-8.13	-8.28	-11.18
Mesitylene-2 [H]	NICS(0)	-7.72	-8.00	-6.72	-6.54	-9.84
	NICS(1)	-8.94	-6.24	-8.28	-8.08	-11.13
	$\Sigma$ NICS(1)	-64.21	-60.41	-121.87	-119.57	-61.03

Table S7. Harmonic oscillator model of aromaticity (HOMA) values of each ring for **13**, **14**, **14"-1**, **14"-2** and **15**

	<b>13</b>	<b>14</b>	<b>14"-1</b>	<b>14"-2</b>	<b>15</b>
Imino-type pyrrole-1 [A]	0.3118	-	0.4081	0.4172	0.2908
Imino-type pyrrole-2 [A]	0.3118	-	-	-	0.3065
Amino-type pyrrole-1 [B]	-	0.8610	0.7007	0.7692	-
Amino-type pyrrole-2 [B]	-	0.8638	-	-	-
Thiophene-1 [C]	0.4137	0.3619	0.5933	0.5300	0.1964
Thiophene-2 [D]	0.4137	0.3607	0.6035	0.5300	0.3060
Azulene-5-memebered ring [E]	0.3094	-0.7096	0.1108	0.1065	0.2351
Azulene-6-memebered ring [F]	-	0.9204	0.9227	0.9249	-
Azulene-7-memebered ring [F]	0.7018	-	-	-	0.6322
Mesitylene-1 [G]	0.9364	0.9367	0.9352	0.9371	0.9350
Mesitylene-2 [H]	0.9364	0.9367	0.9375	0.9359	0.9357

Table S8.  $H$  values for **13**, **14**, **14"** and **15** at RCP

	<b>13</b>	<b>14</b>	<b>14"-1</b>	<b>14"-2</b>	<b>15</b>
Imino-type pyrrole-1 [A]	0.010	-	0.010	0.010	0.011
Imino-type pyrrole-2 [B]	0.010	-	-	-	0.011
Amino-type pyrrole-1 [A]	-	0.012	0.012	0.012	
Amino-type pyrrole-2 [B]	-	0.012	-	-	-
Thiophene-1 [C]	0.009	0.009	0.009	0.009	0.009
Thiophene-2 [D]	0.009	0.009	0.009	0.009	0.009
Azulene-5-memebered ring [E]	0.010	0.010	0.010	0.010	0.010
Azulene-6-memebered ring [F]	-	0.009	-	-	0.004
Azulene-7-memebered ring [F]	0.004	-	0.009	0.009	-
Mesitylene-1 [G]	0.009	0.009	0.009	0.009	0.009
Mesitylene-2 [H]	0.009	0.009	0.009	0.009	0.009
Centre	0.00004	0.00009	0.00010	0.00010	0.00013

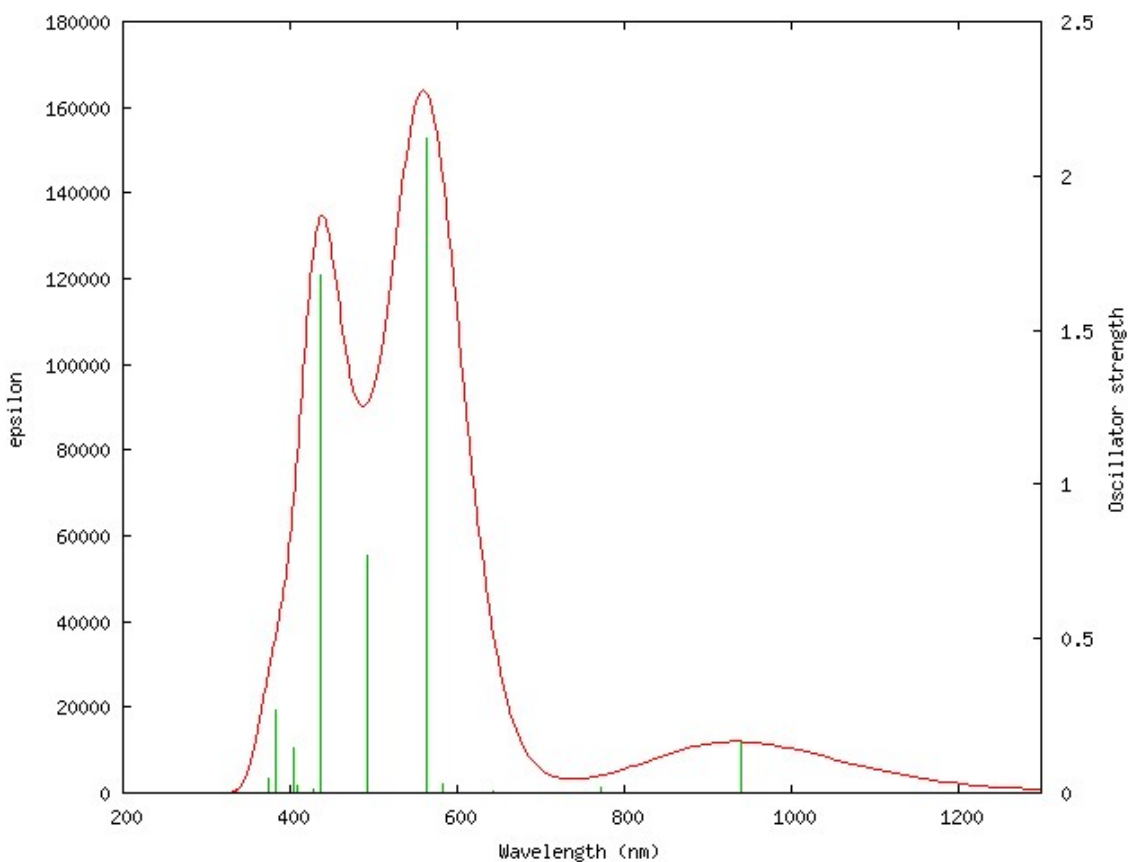


Fig. S74 Computed absorption spectrum of **13** in solvent phase ( $\text{CH}_2\text{Cl}_2$ ) using TD-DFT method at the B3LYP/6-31G(d,p) level

Table S9. Computed absorption maxima ( $\lambda_{\max}$  nm), Electronic excitation energies (E, eV), and Oscillator strength (f) of **13** in solvent phase ( $\text{CH}_2\text{Cl}_2$ ) using TD-DFT method at the B3LYP/6-31G (d, p) level.

No.	Cal. $\lambda_{\max}$ (nm)	Oscillator Strength f	E (eV)	Main Contributing Configurations
1	940.3	0.161	1.31	HOMO→LUMO (94%)
2	772.7	0.020	1.60	HOMO-1→LUMO (46%), HOMO→ LUMO +2 (49%)
3	719.1	0.003	1.72	HOMO→ LUMO +1 (96%)
4	643.6	0.005	1.93	HOMO -1→ LUMO +1 (97%)
5	582.3	0.028	2.13	HOMO-1→ LUMO +2 (50%), HOMO→ LUMO +3 (48%)
6	564.3	2.121	2.20	HOMO -1→LUMO (55%), HOMO→LUMO +2 (46%)
7	493.2	0.768	2.51	HOMO -2→LUMO (32%), HOMO -1→LUMO +2 (32%), HOMO→LUMO +3 (33%)
8	447.8	0.001	2.77	HOMO-3→LUMO (35%), HOMO-1→LUMO +3 (62%)
9	437	1.677	2.84	HOMO-2→LUMO (62%), HOMO-1→LUMO+2 (12%), HOMO→LUMO+3 (17%)
10	429	0.010	2.89	HOMO-3→LUMO (57%), HOMO-1→ LUMO+3 (25%)
11	427.8	0.000	2.90	HOMO-4→LUMO (98%)
12	426.4	0.000	2.91	HOMO-5→LUMO (98%)
13	408.8	0.023	3.03	HOMO-6→LUMO (93%)
14	408.1	0.000	3.04	HOMO-7→LUMO (98%)
15	404	0.147	3.07	HOMO-8→LUMO (87%)
16	383.7	0.004	3.23	HOMO-3→LUMO+2 (78%)
17	383.6	0.269	3.23	HOMO-9→LUMO (44%), HOMO-2→LUMO+1 (26%), HOMO-2→LUMO+2 (24%)
18	374.4	0.000	3.31	HOMO-3 →LUMO+1 (54%), HOMO→LUMO+4 (33%)
19	373.5	0.036	3.32	HOMO-3→LUMO+1 (29%), HOMO→LUMO +4 (51%)
20	373.3	0.047	3.32	HOMO-2→LUMO+1 (48%), HOMO-2 → LUMO+2 (38%)

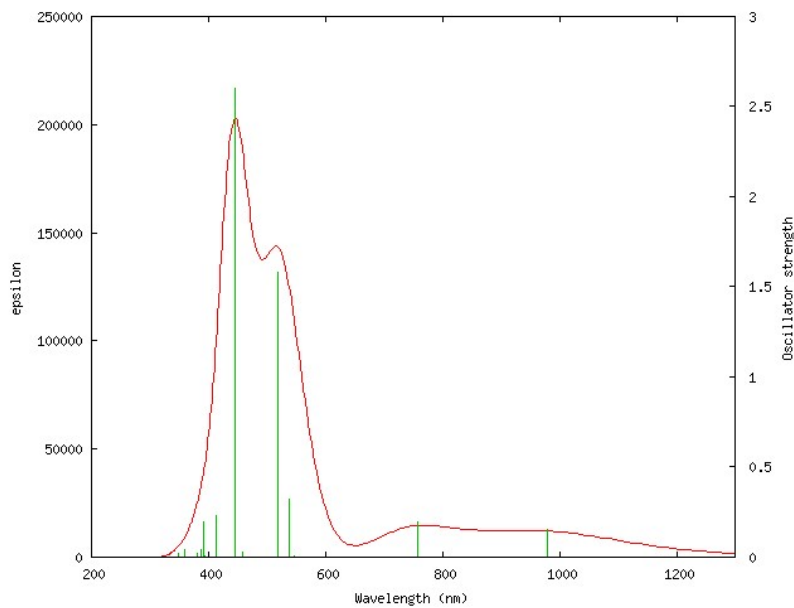


Fig. S75 Computed absorption spectrum of **14** in solvent phase ( $\text{CH}_2\text{Cl}_2$ ) using TD-DFT method at the B3LYP/6-31G(d,p) level

Table S10. Computed absorption maxima ( $\lambda_{\max}$  nm), Electronic excitation energies (E, eV), and Oscillator strength ( $f$ ) of **14** in solvent phase ( $\text{CH}_2\text{Cl}_2$ ) using TD-DFT method at the B3LYP/6-31G(d,p) level.

No.	Cal. $\lambda_{\max}$ (nm)	Oscillator Strength $f$	E (eV)	Main Contributing Configurations
1	980.26	0.156	1.26	HOMO→LUMO (95%)
2	756.83	0.193	1.64	HOMO-1→LUMO (18%), HOMO→LUMO+1 (82%)
3	547.56	0.004	2.26	HOMO-1→LUMO+1 (60%), HOMO→LUMO+2 (27%)
4	538.89	0.322	2.30	HOMO-2→LUMO (34%), HOMO→LUMO+2 (45%)
5	518.91	1.581	2.39	HOMO-1→LUMO (66%), HOMO→LUMO+1 (16%)
6	457.69	0.027	2.71	HOMO-2→LUMO+1 (86%)
7	445.21	2.600	2.78	HOMO-2→LUMO (42%), HOMO-1→LUMO+1 (33%), HOMO→LUMO+2 (18%)
8	423.57	0.000	2.93	HOMO-5→LUMO+1 (83%)
9	413	0.233	3.00	HOMO-1→LUMO+2 (19%), HOMO→LUMO+3 (65%)
10	408	0.000	3.04	HOMO-5→LUMO (84%)
11	394.54	0.004	3.14	HOMO-4→LUMO (90%)
12	394.44	0.001	3.14	HOMO-3→LUMO (90%)
13	391.26	0.195	3.17	HOMO→LUMO+3 (17%), HOMO→LUMO+4 (64%)
14	386.46	0.042	3.21	HOMO-8→LUMO (25%), HOMO-1→LUMO+2 (43%), HOMO→LUMO+5 (19%)
15	380.84	0.000	3.26	HOMO-6→LUMO (98%)
16	380.8	0.000	3.26	HOMO-7→LUMO (97%)
17	379.77	0.021	3.26	HOMO-8→LUMO (15%), HOMO→LUMO+5 (70%)
18	358.42	0.042	3.46	HOMO-2→LUMO+2 (85%)
19	354.65	0.000	3.50	HOMO-9→LUMO (63%), HOMO-9→LUMO+1 (14%), HOMO-9→LUMO+2 (13%)
20	349.4	0.018	3.55	HOMO-10→LUMO (28%), HOMO-8→LUMO+1 (20%), HOMO-3→LUMO+1 (44%)

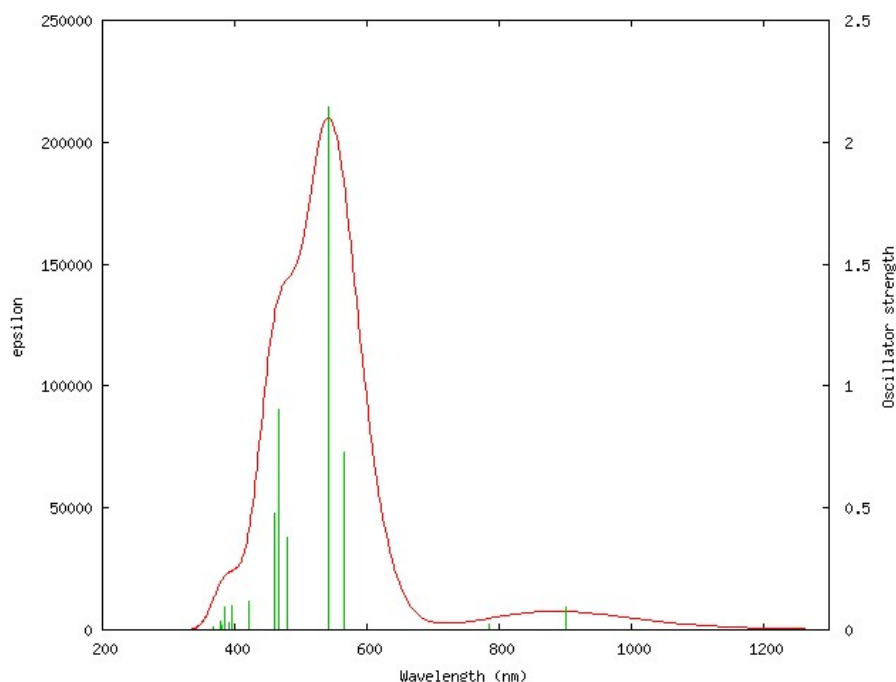


Fig. S76 Computed absorption spectrum of **14**-**1** in solvent phase ( $\text{CH}_2\text{Cl}_2$ ) using TD-DFT method at the B3LYP/6-31G(d,p) level

Table S11. Computed absorption maxima ( $\lambda_{\max}$  nm), Electronic excitation energies (E, eV), and Oscillator strength ( $f$ ) of **14"-1** in solvent phase ( $\text{CH}_2\text{Cl}_2$ ) using TD-DFT method at the B3LYP/6-31G(d,p) level.

No.	Cal. $\lambda_{\max}$ (nm)	Oscillator Strength $f$	E (eV)	Main Contributing Configurations
1	902.3	0.093	1.37	HOMO-1→LUMO+1 (22%), HOMO→LUMO (73%)
2	784.6	0.025	1.58	HOMO-1→LUMO (37%), HOMO→LUMO+1 (58%)
3	564.9	0.727	2.19	HOMO-2→LUMO (24%), HOMO-1→LUMO+1 (49%), HOMO→LUMO (12%)
4	541.3	2.145	2.29	HOMO-1→LUMO (53%), HOMO-1→LUMO+1 (10%), HOMO→LUMO+1 (35%)
5	480.9	0.380	2.58	HOMO-2→LUMO (53%), HOMO→LUMO+2 (32%)
6	466	0.906	2.66	HOMO-2→LUMO (16%), HOMO-2→LUMO+1 (41%), HOMO-1→LUMO+1 (10%), HOMO→LUMO+2 (20%)
7	459.9	0.479	2.70	HOMO-2→LUMO+1 (41%), HOMO→LUMO+2 (41%)
8	421	0.115	2.95	HOMO-3→LUMO (44%), HOMO-1→LUMO+2 (45%)
9	417.8	0.001	2.97	HOMO-4→LUMO (97%)
10	407.9	0.002	3.04	HOMO-3→LUMO (30%), HOMO-8→LUMO (16%), HOMO-1→LUMO+2 (33%), HOMO→LUMO+4 (14%)
11	398.3	0.000	3.11	HOMO-6→LUMO (96%)
12	395.6	0.098	3.13	HOMO-3→LUMO+1 (74%)
13	392.5	0.027	3.16	HOMO-5→LUMO (86%)
14	384.6	0.093	3.22	HOMO-8→LUMO (21%), HOMO→LUMO+3 (63%)
15	382.1	0.000	3.24	HOMO-7→LUMO (98%)
16	380.9	0.016	3.26	HOMO-5→LUMO+1 (64%)
17	379.5	0.014	3.27	HOMO-8→LUMO (10%), HOMO-4→LUMO+1 (79%)
18	379	0.038	3.27	HOMO-8→LUMO (30%), HOMO-5→LUMO+1 (29%), HOMO→LUMO+4 (12%), HOMO-4→LUMO+1 (11%)
19	369.5	0.000	3.36	HOMO-7→LUMO+1 (98%)
20	366.9	0.011	3.38	HOMO-8→LUMO+1 (15%), HOMO-6→LUMO+1 (66%)

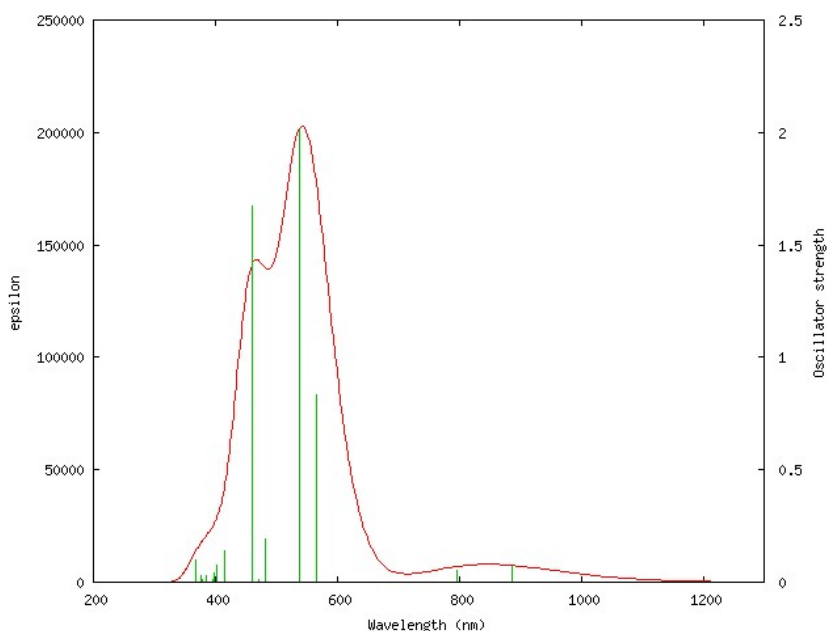


Fig. S77 Computed absorption spectrum of **14"-2** in solvent phase ( $\text{CH}_2\text{Cl}_2$ ) using TD-DFT method at the B3LYP/6-31G(d,p) level

Table S12. Computed absorption maxima ( $\lambda_{\max}$  nm), Electronic excitation energies (E, eV), and Oscillator strength ( $f$ ) of **14"-2** in solvent phase ( $\text{CH}_2\text{Cl}_2$ ) using TD-DFT method at the B3LYP/6-31G(d,p) level.

No.	Cal. $\lambda_{\max}$ (nm)	Oscillator Strength $f$	E (eV)	Main Contributing Configurations
1	886.355	0.071	1.40	HOMO-1→LUMO+1 (19%), HOMO→LUMO (62%), HOMO→LUMO+1 (11%)
2	797.167	0.054	1.56	HOMO-1→LUMO (28%), HOMO→LUMO (14%), HOMO→LUMO+1 (53%)
3	565.488	0.835	2.19	HOMO-2→LUMO (22%), HOMO-1→LUMO+1 (47%), HOMO-1→LUMO (13%), HOMO→LUMO (11%)
4	538.988	2.013	2.30	HOMO-1→LUMO (51%), HOMO-1→LUMO+1 (14%), HOMO→LUMO+1 (30%)
5	482.707	0.193	2.57	HOMO-2→LUMO (44%), HOMO→LUMO+2 (49%)
6	470.222	0.012	2.64	HOMO-2→LUMO+1 (88%)
7	459.470	1.674	2.70	HOMO-2→LUMO (29%), HOMO-1→LUMO+1 (13%), HOMO→LUMO+2 (43%)
8	414.882	0.138	2.99	HOMO-3→LUMO (18%), HOMO-1→LUMO+2 (68%)
9	412.055	0.000	3.01	HOMO-4→LUMO (98%)
10	403.145	0.077	3.08	HOMO-3→LUMO (63%), HOMO→LUMO+4 (15%)
11	398.314	0.044	3.11	HOMO-3→LUMO+1 (75%)
12	395.002	0.010	3.14	HOMO-5→LUMO (82%)
13	393.311	0.001	3.15	HOMO-6→LUMO (87%)
14	385.676	0.026	3.21	HOMO-4→LUMO+1 (19%), HOMO→LUMO+3 (68%)
15	385.484	0.006	3.22	HOMO-4→LUMO+1 (80%), HOMO→LUMO+3 (16%)
16	382.877	0.000	3.24	HOMO-7→LUMO (96%)
17	377.952	0.013	3.28	HOMO-6→LUMO+1 (13%), HOMO-5→LUMO+1 (69%)
18	376.712	0.028	3.29	HOMO-8→LUMO (57%), HOMO-5→LUMO+1 (11%), HOMO→LUMO+4 (23%)
19	371.630	0.003	3.34	HOMO-6→LUMO+1 (83%), HOMO-5→LUMO+1 (15%)
20	368.855	0.098	3.36	HOMO-10→LUMO (25%), HOMO-8→LUMO+1 (55%)

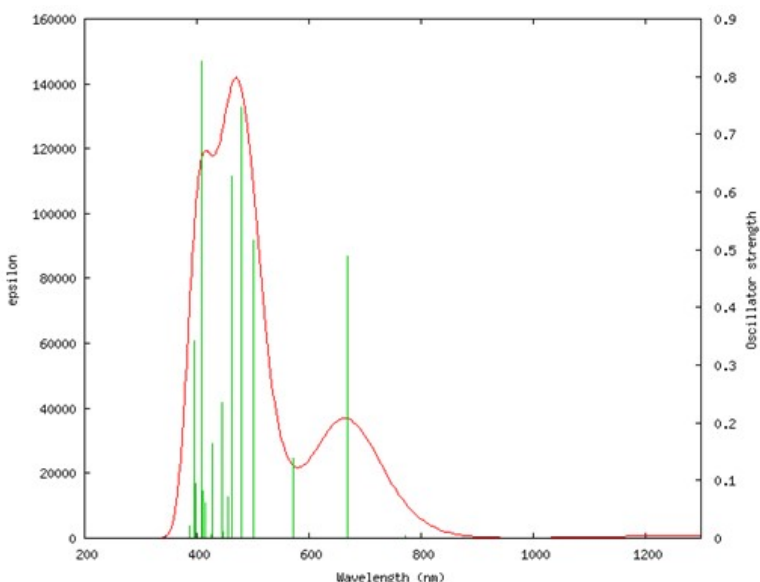


Fig. S78 Computed absorption spectrum of **15** in solvent phase ( $\text{CH}_2\text{Cl}_2$ ) using TD-DFT method at the B3LYP/6-31G(d,p) level

Table 13 Computed absorption maxima ( $\lambda_{\max}$  nm), Electronic excitation energies (E, eV), and Oscillator strength ( $f$ ) of **15** in solvent phase ( $\text{CH}_2\text{Cl}_2$ ) using TD-DFT method at the B3LYP/6-31G (d, p) level.

No.	Cal. $\lambda_{\max}$ (nm)	Oscillator Strength $f$	E (eV)	Main Contributing Configurations
1	1368.0	0.013	0.91	HOMO→LUMO (99%)
2	772.0	0.004	1.61	HOMO→LUMO+2 (96%)
3	669.5	0.488	1.85	HOMO-2→LUMO (10%), HOMO→LUMO+1 (88%)
4	572.4	0.139	2.17	HOMO-1→LUMO (76%), HOMO→LUMO+3 (22%)
5	500.7	0.517	2.48	HOMO-3→LUMO (47%), HOMO-2→LUMO (44%)
6	480.0	0.748	2.58	HOMO-3→LUMO (47%), HOMO-2→LUMO (39%)
7	463.4	0.627	2.68	HOMO-2→LUMO+1 (20%), HOMO-1→LUMO (11%), HOMO→LUMO+3 (54%)
8	455.5	0.071	2.72	HOMO-1→LUMO+2 (85%)
9	447.8	0.011	2.77	HOMO-5→LUMO (20%), HOMO-4→LUMO (73%)
10	444.7	0.038	2.79	HOMO-5→LUMO (72%), HOMO-4→LUMO (18%)
11	444.4	0.235	2.79	HOMO-1→LUMO+1 (79%)
12	428.9	0.164	2.89	HOMO-8→LUMO (75%), HOMO-7→LUMO (12%)
13	425.5	0.000	2.91	HOMO-6→LUMO (90%)
14	425.0	0.006	2.92	HOMO-8→LUMO (14%), HOMO-7→LUMO (78%)
15	416.2	0.062	2.98	HOMO-2→LUMO+2 (45%), HOMO→LUMO+4 (42%)
16	410.4	0.082	3.02	HOMO-10→LUMO (80%)
17	408.7	0.826	3.03	HOMO-2→LUMO+1 (62%), HOMO→LUMO+3 (10%)
18	398.9	0.094	3.11	HOMO-11→LUMO (72%), HOMO-9→LUMO (12%)
19	396.3	0.341	3.13	HOMO-11→LUMO (14%), HOMO-9→LUMO (70%)
20	387.3	0.022	3.20	HOMO-2→LUMO+2 (46%), HOMO→LUMO+4 (36%)



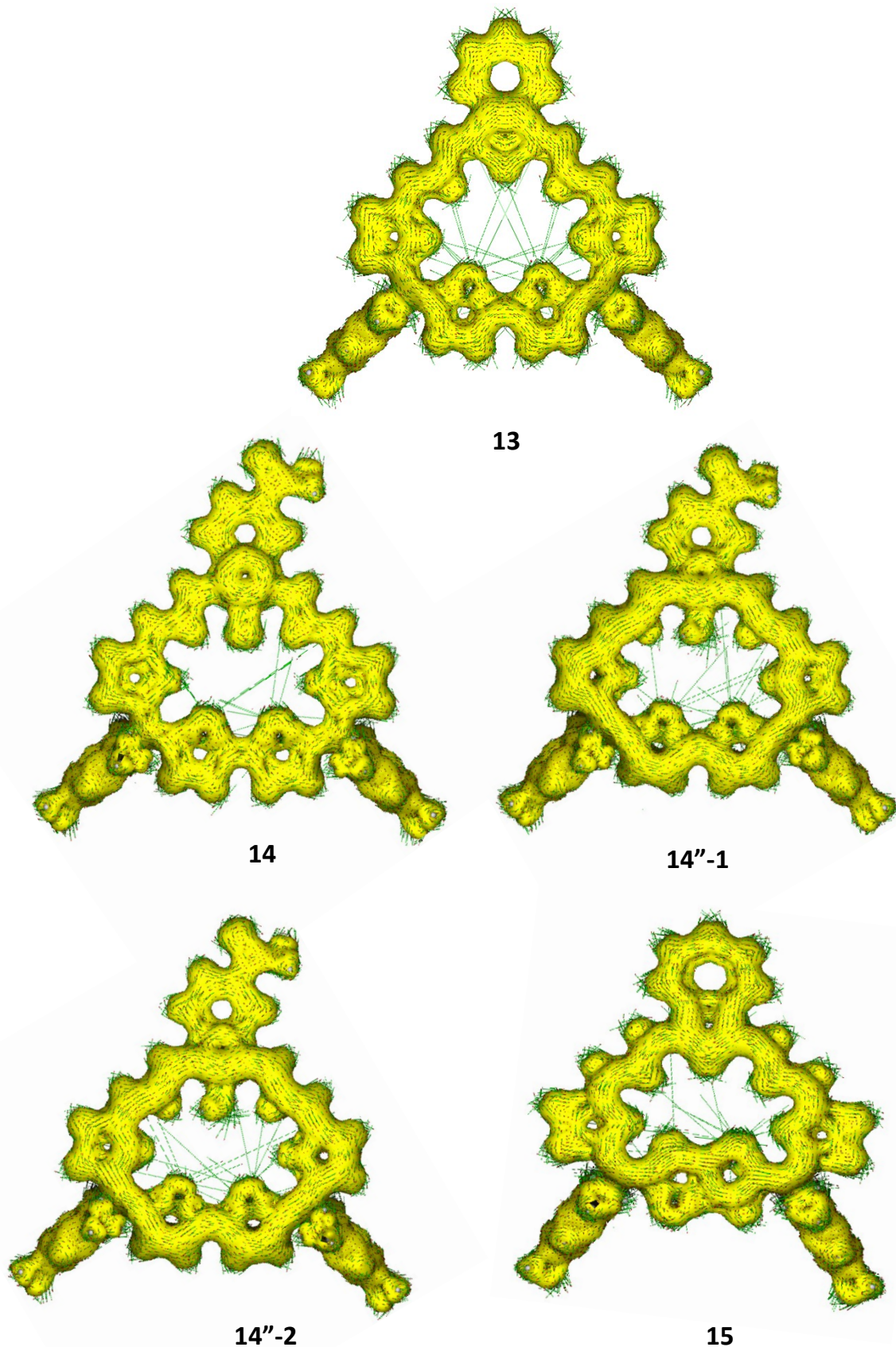


Fig. S79 The Anisotropy of Induced Current Density (AICD) plot of **13**, **14**, **14"-1**, **14"-2** and **15** at B3LYP-6-31G(d,p) level of theory. A continuous clock-wise ring current along the macrocycle indicating the aromatic nature of macrocycles in **13**, **14**, **14"-1**, **14"-2** and continuous anti clock-wise ring current along the macrocycle indicating the anti-aromatic nature of macrocycle in **15**

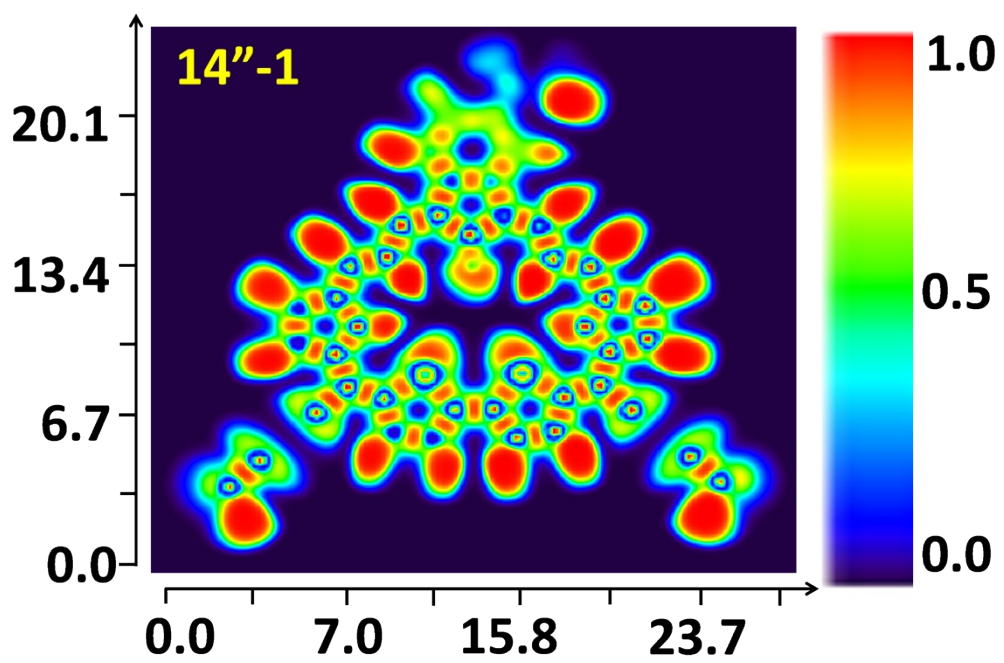


Fig. S80 Colour-filled map of the electron localization function of **14''-1** at the B3LYP/6-31G (d,p) level

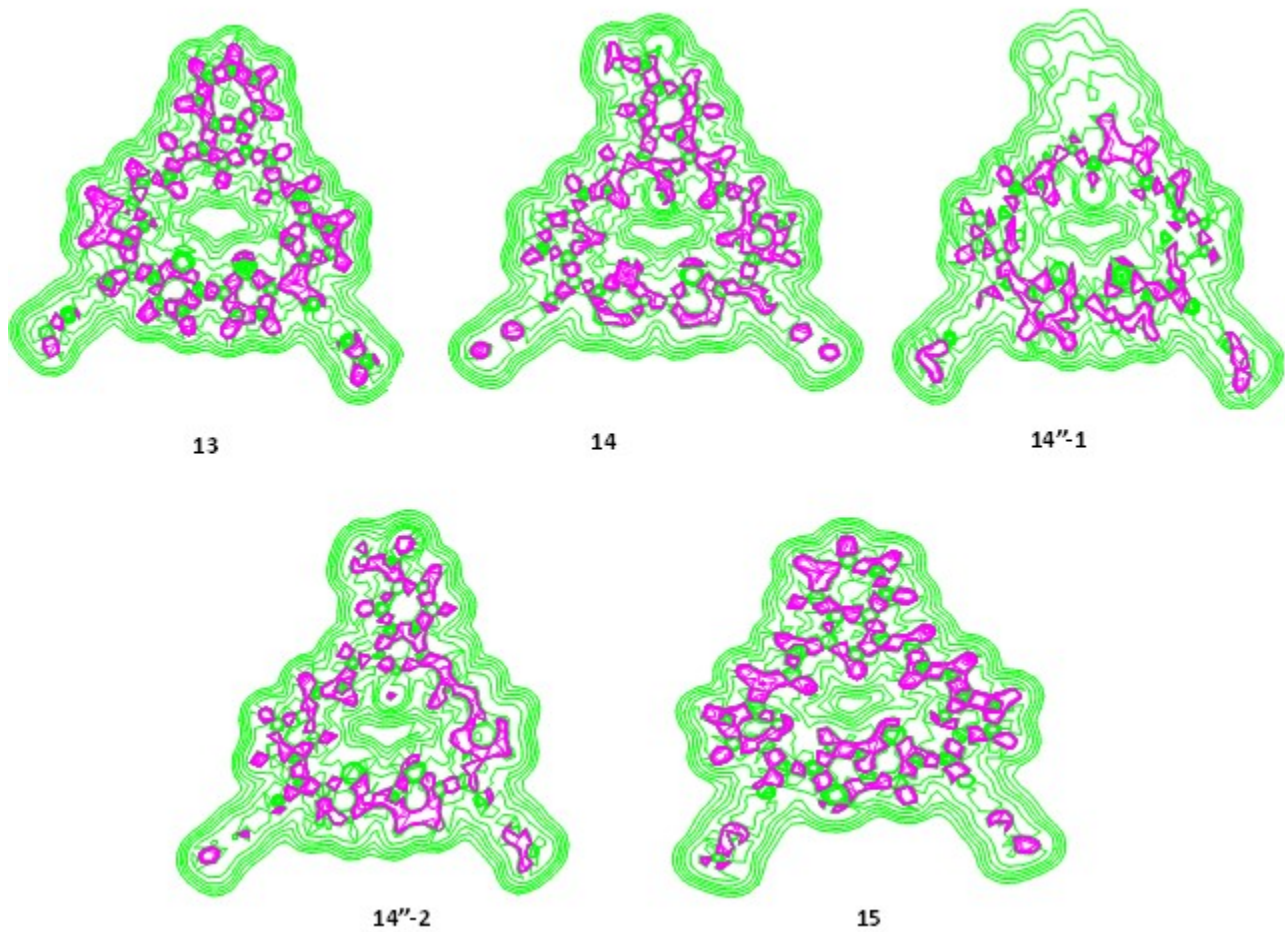


Fig. S81 The Contour line diagram of the Laplacian of electron density along the macrocycle plane. Solid green lines indicate charge depletion [ $\nabla^2 \rho(r) > 0$ ] and solid gray lines indicate charge concentration [ $\nabla^2 \rho(r) < 0$ ]

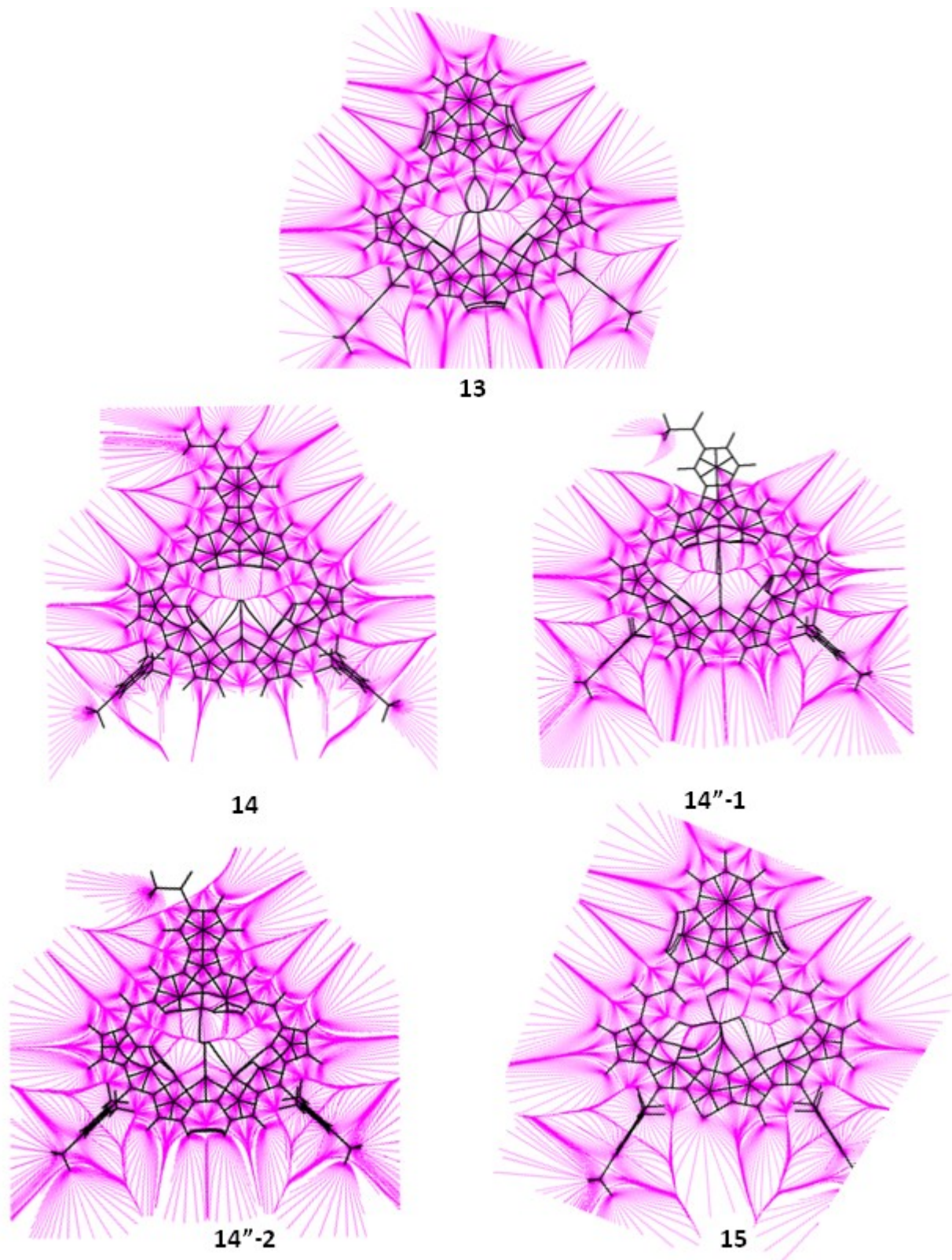
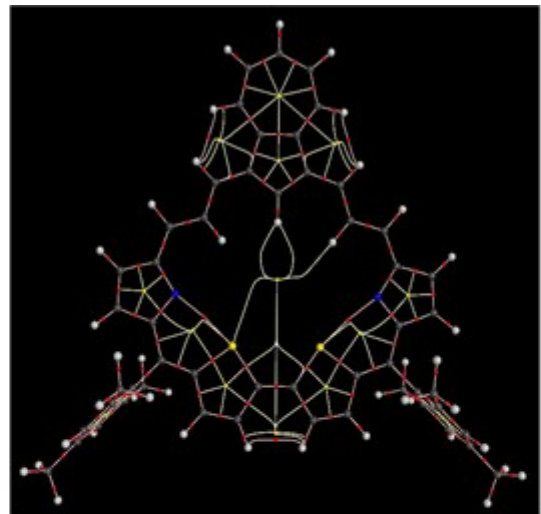
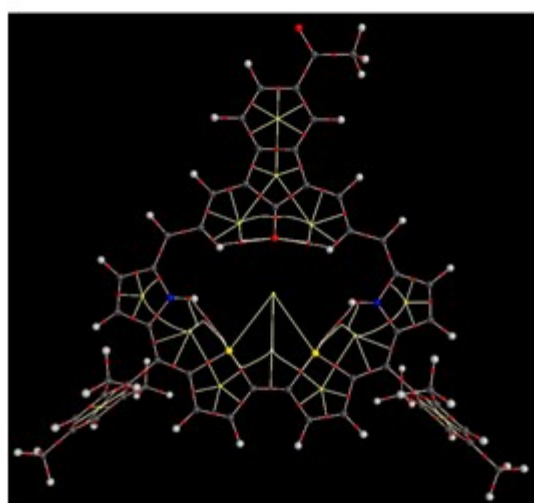


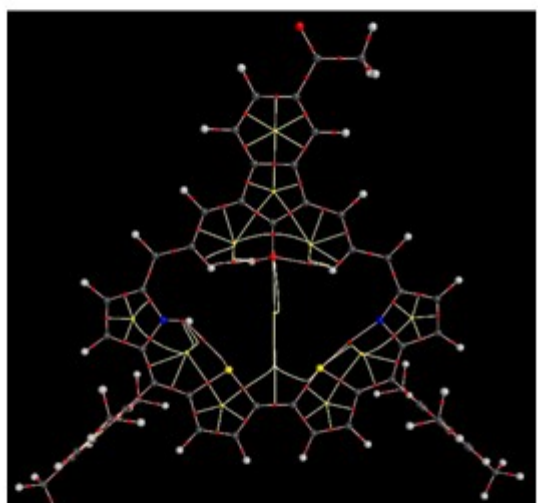
Fig. S82 The Gradient vectors of the macrocycles computed at B3LYP/6-31G (d,p) level



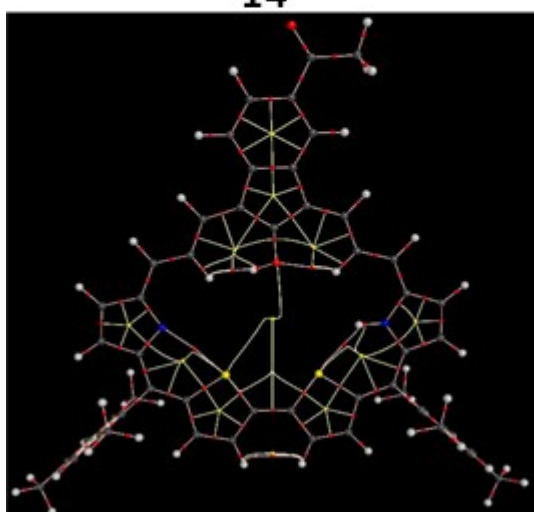
13



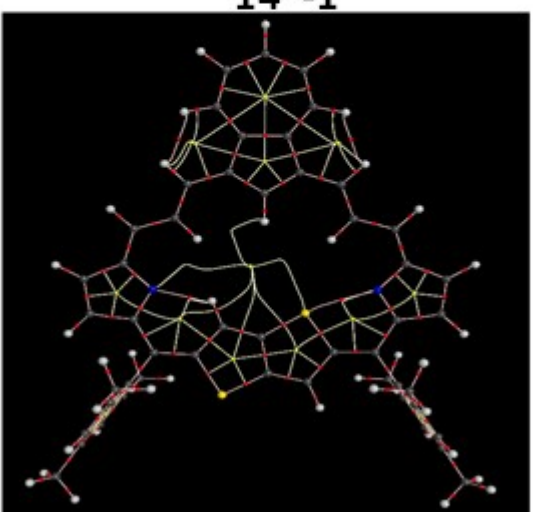
14



14''-1



14''-2



15

Fig. S83 Molecular graph of **13**, **14**, **14"-1**, **14"-2** and **15**. Solid lines indicate bond paths and large circles correspond to attractors, small red ones to bond critical points (BCPs), yellow ones to ring critical points (RCPs)

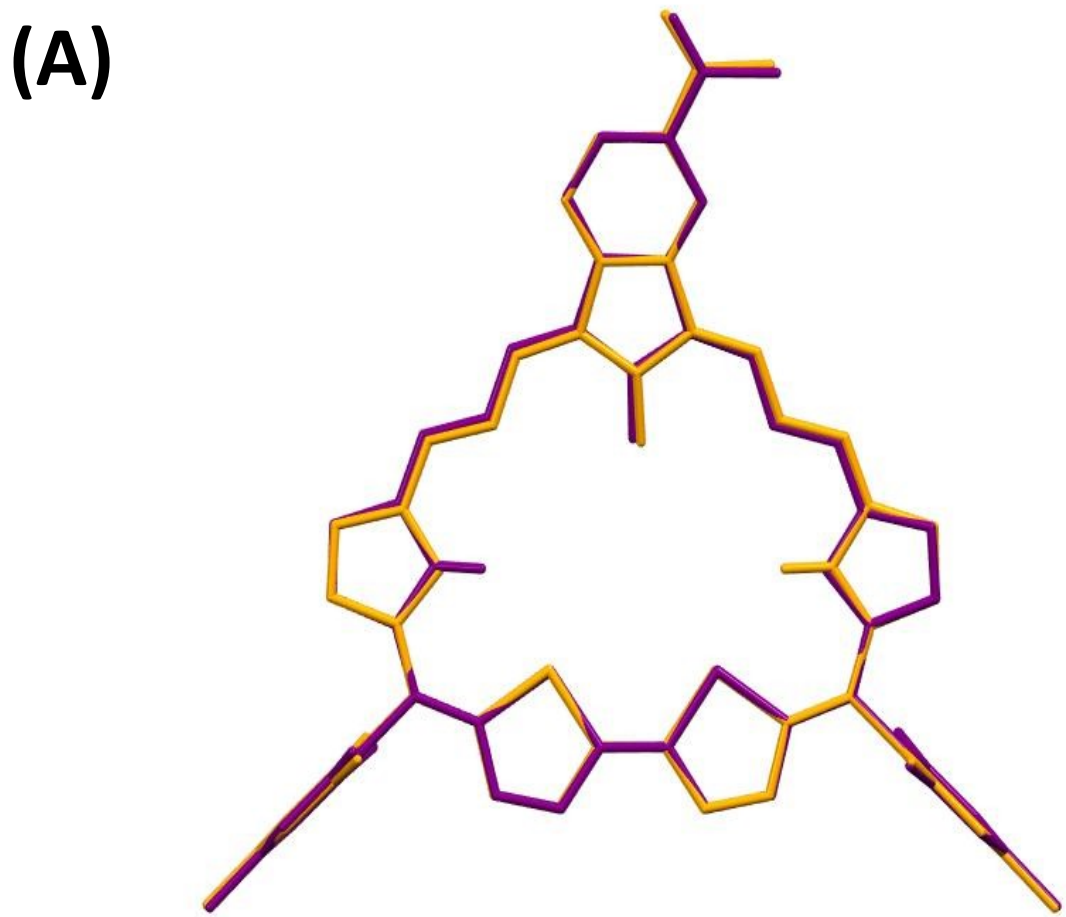


Fig. S84 Structure overlay between **14"-1** (purple) and **14"-2** (yellow) of optimized structures (A: top view, B: side view)

## 5. X,Y,Z Coordinates

### Cartesian Coordinates

13

16	-1.740594000	-1.128681000	0.000166000	6	5.627443000	-2.696953000	0.000196000
7	-4.031609000	0.723946000	-0.000479000	6	7.722282000	-4.592322000	0.000605000
6	-0.696590000	-2.565997000	0.000623000	6	7.191072000	-4.106714000	1.198454000
6	-1.497270000	-3.746963000	0.000954000	1	7.595581000	-4.464079000	2.143057000
1	-1.068816000	-4.741133000	0.001262000	6	6.153379000	-3.168683000	1.221600000
6	-2.842130000	-3.513432000	0.000782000	6	7.190613000	-4.107732000	-1.197464000
1	-3.594420000	-4.291710000	0.000954000	1	7.594768000	-4.465901000	-2.141916000
6	-3.211671000	-2.130942000	0.000319000	6	6.152914000	-3.169733000	-1.221015000
6	-4.523347000	-1.672837000	0.000000000	6	5.616750000	-2.673726000	-2.544719000
6	-5.627429000	-2.696976000	0.000133000	1	6.147760000	-3.139157000	-3.379315000
6	-7.722258000	-4.592357000	0.000370000	1	4.550050000	-2.895656000	-2.655278000
6	-7.191061000	-4.106844000	1.198263000	1	5.722514000	-1.587687000	-2.638155000
1	-7.595576000	-4.464288000	2.142833000	6	5.617715000	-2.671562000	2.545089000
6	-6.153372000	-3.168809000	1.221495000	1	6.149053000	-3.136277000	3.379875000
6	-7.190582000	-4.107667000	-1.197655000	1	5.723493000	-1.585442000	2.637562000
1	-7.594726000	-4.465761000	-2.142140000	1	4.551061000	-2.893418000	2.656245000
6	-6.152888000	-3.169659000	-1.221122000	6	8.821028000	-5.629080000	0.000813000
6	-5.616709000	-2.673548000	-2.544781000	1	8.408226000	-6.645860000	0.000260000
1	-6.147743000	-3.138876000	-3.379419000	1	9.457705000	-5.538064000	-0.884403000
1	-4.550018000	-2.895516000	-2.655366000	1	9.456825000	-5.538637000	0.886712000
1	-5.722423000	-1.587495000	-2.638112000	6	4.901865000	-0.294389000	-0.000616000
6	-5.617728000	-2.671785000	2.545028000	6	6.291536000	0.180463000	-0.001200000
1	-6.149036000	-3.136609000	3.379773000	1	7.172651000	-0.445764000	-0.001243000
1	-5.723569000	-1.585680000	2.637606000	6	6.221282000	1.534502000	-0.001631000
1	-4.551061000	-2.893590000	2.656157000	1	7.035299000	2.248547000	-0.002107000
6	-8.820998000	-5.629120000	0.000485000	6	4.800822000	1.868746000	-0.001336000
1	-8.408191000	-6.645898000	-0.000154000	6	4.302600000	3.159325000	-0.001526000
1	-9.457671000	-5.538033000	-0.884727000	1	5.033782000	3.966569000	-0.002007000
1	-9.456800000	-5.538757000	0.886388000	6	2.936295000	3.516132000	-0.001091000
6	-4.901864000	-0.294408000	-0.000456000	1	2.217358000	2.701424000	-0.000612000
6	-6.291537000	0.180438000	-0.000928000	6	2.519075000	4.822726000	-0.001171000
1	-7.172650000	-0.445793000	-0.000984000	1	3.296702000	5.584340000	-0.001556000
6	-6.221290000	1.534478000	-0.001276000	6	1.163189000	5.275592000	-0.000803000
1	-7.035310000	2.248520000	-0.001673000	6	0.737814000	6.648711000	-0.000008000
6	-4.800830000	1.868728000	-0.001009000	1	-0.000025000	3.399374000	-0.002011000
6	-4.302618000	3.159313000	-0.001166000	6	1.260178000	9.117220000	0.001325000
1	-5.033809000	3.966549000	-0.001583000	6	-0.000007000	9.718010000	0.001826000
6	-2.936317000	3.516132000	-0.000784000	6	-1.260217000	9.117214000	0.001690000
1	-2.217373000	2.701431000	-0.000324000	6	1.580669000	7.754799000	0.000594000
6	-2.519110000	4.822733000	-0.000914000	6	-1.580713000	7.754819000	0.000932000
1	-3.296748000	5.584337000	-0.001297000	1	2.107987000	9.797323000	0.001582000
6	-1.163233000	5.275614000	-0.000664000	1	-0.000015000	10.805879000	0.002429000
6	-0.0000015000	4.481910000	-0.001211000	1	-2.108008000	9.797340000	0.002252000
6	-0.737855000	6.648707000	0.000073000	1	2.645730000	7.537461000	0.000466000
16	1.740604000	-1.128675000	0.000055000	1	-2.645773000	7.537472000	0.001062000
7	4.031606000	0.723958000	-0.000735000				
6	0.696605000	-2.565994000	0.000634000				
6	1.497290000	-3.746957000	0.001075000				
1	1.068838000	-4.741129000	0.001509000	14			
6	2.842148000	-3.513421000	0.000912000	S	-0.27400200	2.35550900	-0.16835400
1	3.594441000	-4.291696000	0.001184000	N	-3.39817200	2.10357100	-0.07781900
6	3.211684000	-2.130930000	0.000332000	H	-2.59178900	1.53891100	0.14347100
6	4.523357000	-1.672821000	-0.000027000	C	1.39430300	2.91850000	0.05084700
			C	1.38880100	4.33829100	0.21111100	

H	2.30419000	4.90060700	0.34802000	C	6.40783600	-1.16240100	2.54917400
O	-1.55722700	-2.28260700	0.00823300	H	7.08577400	-1.17784400	3.40638500
C	0.15197200	4.91497800	0.18467000	H	5.66158600	-0.37966600	2.72123200
H	-0.02219100	5.97668900	0.30275800	H	5.86871200	-2.11551500	2.52746400
C	-0.94284800	4.00600500	0.00431900	C	6.54645000	-0.51024000	-2.50069500
C	-2.28067200	4.36098000	-0.03926800	H	7.27869400	-0.43514200	-3.30872600
C	-2.60615600	5.83166400	0.02217600	H	5.91183800	-1.38047600	-2.69672500
C	-3.23572900	8.58146900	0.13155200	H	5.89853900	0.37160600	-2.55056300
C	-2.93954000	7.95915200	-1.08401100	C	10.81333600	-0.44749500	0.19390400
H	-2.95775400	8.54577700	-1.99986800	H	11.09918600	0.59954100	0.35518600
C	-2.62193700	6.59877100	-1.16179200	H	11.24197100	-1.02989800	1.01497400
C	-3.21619300	7.80119800	1.29102200	H	11.28714100	-0.77298700	-0.73690000
H	-3.44941400	8.26411900	2.24737500	C	4.50697200	-2.30636800	-0.12564400
C	-2.90829500	6.43721300	1.26038100	C	5.27377000	-3.48381400	-0.28143500
C	-2.90415800	5.63870700	2.54393100	H	6.34895700	-3.50329100	-0.37382300
H	-3.12415200	6.27924600	3.40180800	C	4.40421600	-4.57103200	-0.30422900
H	-1.93416800	5.16101400	2.71737500	H	4.66472700	-5.61395400	-0.41970500
H	-3.65179800	4.83873300	2.51876000	C	3.09180200	-4.08589000	-0.16425100
C	-2.30740400	5.97661200	-2.50346400	C	1.87704600	-4.82463600	-0.12687300
H	-2.45906700	6.69729400	-3.31114800	H	2.00128200	-5.90556300	-0.16538700
H	-2.94130400	5.10618300	-2.70072400	C	0.61089000	-4.31026100	-0.05708900
H	-1.26943300	5.62993200	-2.55234200	H	0.43541400	-3.23922300	-0.03926700
C	-3.54297800	10.05899600	0.19445300	C	-0.54582800	-5.13880500	-0.02304200
H	-2.63130300	10.64682300	0.35972300	H	-0.37265700	-6.21596600	-0.03589900
H	-4.23011900	10.29068700	1.01374200	C	-1.84391400	-4.70163900	0.01374700
H	-3.99313600	10.41434100	-0.73716800	C	-3.04827500	-5.53257700	0.03752500
C	-3.41117300	3.48604300	-0.13451900	C	-3.19337100	-6.92181200	0.05959000
C	-4.76381500	3.86094400	-0.29621000	H	-2.32274800	-7.57158500	0.06248300
H	-5.10706800	4.87988200	-0.39083500	C	-4.47081700	-7.47443500	0.07926400
C	-5.53779500	2.70291500	-0.32204900	H	-4.61633500	-8.54899900	0.09705000
H	-6.61015000	2.63621200	-0.44224300	C	-6.95293800	-7.32800500	0.10064600
C	-4.67958900	1.59923100	-0.17750900	O	-7.04558600	-8.54813900	0.12000600
C	-5.01760100	0.21610200	-0.13935300	C	-8.20679800	-6.46667600	0.09946300
H	-6.08565600	0.00885400	-0.18039700	H	-8.23198100	-5.80552700	0.97267200
C	-4.14588000	-0.83394200	-0.06606200	H	-8.24849500	-5.83189400	-0.79246800
H	-3.07194200	-0.67730400	-0.04547400	H	-9.07766000	-7.12228600	0.11742800
C	-4.58460400	-2.19017500	-0.03082400	<b>14"-1</b>			
H	-5.66397400	-2.35036200	-0.04621900				
C	-3.77565600	-3.29224800	0.01006700				
C	-2.28717800	-3.28162800	0.01275500	S	0.58437800	-2.25301000	0.00251800
C	-4.19742200	-4.69838600	0.03565100	N	3.50428600	-1.82389200	-0.13546100
C	-5.46976100	-5.25923600	0.05587700	C	-1.03049100	-2.95040200	0.15339200
H	-6.34582800	-4.61844400	0.05556900	C	-0.95233800	-4.35696800	0.23651500
C	-5.61681100	-6.65882000	0.07775800	H	-1.82563200	-4.99060600	0.32619100
S	2.48085000	0.34021000	-0.16504100	O	1.31762100	2.35587900	-0.60334500
N	3.18582200	-2.71076200	-0.06984200	C	0.33487300	-4.84676900	0.17175800
H	2.40384600	-2.11132000	0.14755400	H	0.58353300	-5.89947500	0.21351100
C	2.51160900	2.10142600	0.05116100	C	1.33896600	-3.85954600	0.04272400
C	3.86620900	2.52638900	0.20973000	C	2.71861300	-4.13466100	-0.02815700
H	4.12482000	3.56943700	0.34436600	C	3.13054200	-5.58295000	0.00460100
C	4.79095000	1.52268400	0.18404400	C	3.92382200	-8.29137600	0.06062900
H	5.85560700	1.67864800	0.30073000	C	3.64614000	-7.64787800	-1.14830900
C	4.25610400	0.20347200	0.00672400	H	3.74229000	-8.20146400	-2.07978900
C	4.99977200	-0.96418400	-0.03418200	C	3.25045700	-6.30709900	-1.20012400
C	6.50003100	-0.82973400	0.02609400	C	3.80337600	-7.55233000	1.24055800
C	9.31186400	-0.60012500	0.13266500	H	4.02304600	-8.03079000	2.19250000
C	8.62831000	-0.50953800	-1.08271900	C	3.41161300	-6.20941000	1.23709400
H	9.19246400	-0.35305900	-1.99950700	C	3.30640000	-5.45274100	2.54174700
C	7.23544500	-0.61742500	-1.15909400	H	3.53796300	-6.10351600	3.38888200
C	8.56286700	-0.81264100	1.29343600	H	2.30096700	-5.04556100	2.69166000
H	9.07527700	-0.89194800	2.24970200	H	3.99712500	-4.60335600	2.56747000
C	7.16949400	-0.93049300	1.26417300	C	2.97000500	-5.65605100	-2.53549700

H	3.11436400	-6.36692900	-3.35315900	C	-1.03704000	4.30340400	-0.30391800
H	3.63017200	-4.79980700	-2.70915300	H	-0.84637800	3.25942100	-0.06704800
H	1.94346700	-5.27867000	-2.59189900	C	0.05435000	5.16397000	-0.38190800
C	4.31828500	-9.74913100	0.09313300	H	-0.16567800	6.22464300	-0.49760500
H	3.43728400	-10.39701600	0.18374000	C	1.41264800	4.80682300	-0.30099000
H	4.97016600	-9.96862300	0.94399300	C	2.53634500	5.73979000	-0.12440000
H	4.84311700	-10.04234500	-0.82097100	C	2.57164800	7.12840800	-0.01525400
C	3.73572100	-3.16466500	-0.11276000	H	1.66156100	7.71917000	-0.07111300
C	5.16751700	-3.45398500	-0.15636100	C	3.80097000	7.76078700	0.16975000
H	5.61500500	-4.43790100	-0.15262700	H	3.86751000	8.84008400	0.25188800
C	5.78739100	-2.24508500	-0.19482200	C	6.26825900	7.77622300	0.46513500
H	6.84966700	-2.03816000	-0.22996000	O	6.27444600	8.99735100	0.54666300
C	4.72771100	-1.24427100	-0.18081900	H	0.51854900	2.55687500	-1.11147900
C	4.96047600	0.14956500	-0.19258900	H	-2.60614700	1.98048300	0.14817100
H	6.00384300	0.46325500	-0.18476700	C	7.57192500	6.99877200	0.57103400
C	3.98067000	1.12460600	-0.20552100	H	7.54660100	6.29911700	1.41375900
H	2.94546600	0.80692900	-0.23521200	H	7.75662700	6.41190200	-0.33542600
C	4.28914300	2.49304200	-0.16367900	H	8.38746000	7.70784400	0.71487700
H	5.34542600	2.75152800	-0.08813800				
C	3.39139000	3.55617400	-0.18130700				
C	1.98193400	3.51568900	-0.35722900				
C	3.73374300	4.98419000	-0.03394200	S	-0.46221900	2.26234400	-0.08707500
C	4.95122000	5.61766900	0.16479000	N	-3.58268500	1.90150300	-0.10159300
H	5.86445000	5.03666800	0.24473300	H	-2.75423300	1.36722200	0.11011300
C	4.99350600	7.02393200	0.26181000	C	1.17826600	2.89182900	0.13203400
S	-2.40041400	-0.48273900	-0.08130200	C	1.11186100	4.29768000	0.27027300
N	-3.42910700	2.47348400	-0.16114400	H	1.99886000	4.90258500	0.41033600
C	-2.24248600	-2.22337700	0.18803200	O	-1.49234600	-2.20833200	-0.41942300
C	-3.52076700	-2.76684900	0.40815700	C	-0.15609000	4.82930000	0.22145000
H	-3.67174300	-3.82215000	0.59808800	H	-0.37107200	5.88519100	0.32022600
C	-4.55813500	-1.85302800	0.37929900	C	-1.19767900	3.88048600	0.04344300
H	-5.59574600	-2.11505600	0.53935100	C	-2.56436300	4.18925600	-0.02727200
C	-4.16760900	-0.51891300	0.12926500	C	-2.93361400	5.65066800	0.01067900
C	-5.04926500	0.57953500	0.02157800	C	-3.63770400	8.38439900	0.07635300
C	-6.52333900	0.27371600	0.09558600	C	-3.33012700	7.74948700	-1.12999900
C	-9.28746000	-0.28966900	0.23291700	H	-3.36784200	8.31983100	-2.05546700
C	-8.59399400	-0.37994500	-0.97713900	C	-2.97575300	6.39731000	-1.18598200
H	-9.13206000	-0.66733900	-1.87776400	C	-3.59053900	7.62527800	1.24886700
C	-7.22458300	-0.10920400	-1.06796600	H	-3.83121500	8.09830500	2.19837100
C	-8.57349000	0.09139000	1.37220600	C	-3.24427100	6.26997700	1.24004400
H	-9.09451100	0.17209400	2.32365800	C	-3.21178800	5.49531900	2.53799200
C	-7.20436000	0.37505500	1.32745400	H	-3.42591000	6.14950500	3.38698900
C	-6.48251000	0.78642700	2.59071800	H	-2.23406200	5.03172600	2.70536200
H	-7.14695400	0.72373700	3.45630400	H	-3.95083900	4.68684000	2.54104000
H	-5.61334200	0.14913200	2.78302100	C	-2.65168400	5.76071700	-2.51843400
H	-6.11302700	1.81565100	2.52492000	H	-2.77790100	6.47815500	-3.33326900
C	-6.52452800	-0.22231500	-2.40315900	H	-3.29831400	4.90056300	-2.72094200
H	-7.23356200	-0.48204300	-3.19337800	H	-1.61990300	5.39449000	-2.54797400
H	-6.03543000	0.71691800	-2.68176500	C	-3.98484200	9.85385400	0.11533700
H	-5.74471900	-0.99111700	-2.38332300	H	-3.08777900	10.46911500	0.25904800
C	-10.75908500	-0.62033300	0.31218500	H	-4.66894300	10.08215400	0.93806000
H	-10.91474800	-1.68383500	0.53276000	H	-4.45470400	10.17919800	-0.81750800
H	-11.25586300	-0.04980300	1.10252700	C	-3.64465200	3.28251600	-0.12157600
H	-11.26875500	-0.40756500	-0.63219000	C	-5.02893800	3.60898700	-0.24842200
C	-4.70259800	1.92860800	-0.15581300	H	-5.40862300	4.61729200	-0.31459800
C	-5.59497200	3.02394500	-0.39936500	C	-5.75459200	2.43597800	-0.28038400
H	-6.66666600	2.92119100	-0.47962900	H	-6.82627600	2.33191100	-0.37941000
C	-4.85322500	4.17254800	-0.53530600	C	-4.84995400	1.34659100	-0.18183600
H	-5.22040600	5.16825700	-0.74292600	C	-5.12870800	-0.02828700	-0.17288500
C	-3.47435700	3.84584100	-0.37413400	H	-6.18236500	-0.29791500	-0.18417500
C	-2.37161300	4.69459100	-0.44172300	C	-4.17484500	-1.03441800	-0.15731700
H	-2.58899300	5.74272200	-0.63170500	H	-3.12537100	-0.76461700	-0.19177500

				<b>15</b>
C	-4.47829100	-2.39948000	-0.11081400	
H	-5.53242700	-2.66983300	-0.05592900	
C	-3.55990900	-3.44873400	-0.11631000	16
C	-2.14625300	-3.38240000	-0.24003100	7
C	-3.88729300	-4.88306900	-0.01012100	6
C	-5.10261700	-5.53561200	0.13372700	1
H	-6.02593700	-4.96834500	0.19497800	6
C	-5.12952800	-6.94397100	0.19964800	6
S	2.43303600	0.35883500	0.00038300	6
N	3.33168700	-2.45918600	-0.14861500	6
C	2.35128800	2.12106900	0.14142800	6
C	3.65594800	2.66181000	0.26543100	1
H	3.84294700	3.72349000	0.36551200	6
C	4.65485900	1.72060400	0.23595300	6
H	5.70898800	1.95439200	0.31229500	1
C	4.20939200	0.37928500	0.08883900	6
C	5.05706800	-0.73120000	0.00935400	6
C	6.53992900	-0.47379800	0.06895300	1
C	9.32440400	-0.01996000	0.18004500	1
C	8.64010800	0.00061000	-1.03815300	1
H	9.19312300	0.19029900	-1.95552900	6
C	7.26087300	-0.22005900	-1.11691000	1
C	8.59052500	-0.27806600	1.34100300	1
H	9.10430500	-0.30705200	2.29943700	1
C	7.21069400	-0.50581200	1.30984000	6
C	6.46536600	-0.78840400	2.59450100	1
H	7.14205400	-0.75641300	3.45233500	1
H	5.66626500	-0.05939300	2.76553100	1
H	5.99134900	-1.77538000	2.57291000	6
C	6.57051300	-0.19413800	-2.46175800	6
H	7.28780200	-0.00190100	-3.26385700	1
H	6.07113500	-1.14543100	-2.67340200	6
H	5.79952600	0.58259300	-2.50393600	1
C	10.80870500	0.25314100	0.24329900	6
H	11.00999100	1.32195100	0.38912200	6
H	11.27900300	-0.28081400	1.07447900	1
H	11.31092100	-0.04784500	-0.68090400	6
C	4.62889900	-2.07573600	-0.12682700	1
C	5.52505500	-3.22187900	-0.27103300	6
H	6.60514200	-3.18263000	-0.28275500	1
C	4.71973200	-4.31042000	-0.39003200	6
H	5.00791400	-5.34660500	-0.51491300	6
C	3.35416500	-3.81502600	-0.30195100	6
C	2.21266200	-4.62693900	-0.35594200	16
H	2.37398800	-5.69088900	-0.52279200	7
C	0.90399700	-4.17617300	-0.20938400	6
H	0.80068600	-3.12030100	0.02658500	6
C	-0.20505400	-5.01919200	-0.27839500	6
H	0.00897600	-6.08113300	-0.39592700	1
C	-1.56118300	-4.67065900	-0.20358100	6
C	-2.67839800	-5.62098500	-0.08002800	6
C	-2.69911600	-7.01189200	-0.00443700	6
H	-1.78042900	-7.59015100	-0.04636800	6
C	-3.92517100	-7.66358900	0.12884400	6
H	-3.97966900	-8.74520000	0.18519000	1
C	-6.39995800	-7.71612800	0.34663700	6
O	-6.39318600	-8.93868300	0.40086100	6
H	-0.60617600	-2.38263400	-0.76772100	1
C	-7.71652300	-6.95720500	0.42904900	6
H	-7.72606800	-6.27533400	1.28648900	6
H	-7.88142100	-6.35405500	-0.47054300	1
H	-8.52654600	-7.67941900	0.53305300	1

1	1.619141000	5.031655000	-2.653518000	1	-2.875878000	2.012267000	-0.060211000
6	2.384045000	4.675140000	2.557664000	6	-4.999100000	2.146052000	0.003580000
1	2.906913000	5.075606000	3.430197000	1	-5.828290000	2.851514000	0.027867000
1	1.341148000	5.006652000	2.606476000	6	-5.344477000	0.744564000	0.017539000
1	2.370100000	3.583368000	2.641757000	6	-6.676052000	0.212746000	0.035090000
6	6.059553000	7.258657000	0.255653000	1	-3.380713000	-0.266980000	0.011023000
1	6.970618000	6.648380000	0.296287000	6	-9.181068000	0.532408000	0.052899000
1	6.148012000	7.914377000	-0.615797000	6	-9.677278000	-0.772143000	0.072408000
1	6.049703000	7.885426000	1.152461000	6	-8.980151000	-1.981408000	0.079893000
6	0.021839000	4.461743000	-0.056376000	6	-7.847028000	0.959722000	0.036303000
6	-0.329388000	5.887670000	-0.000056000	6	-7.595133000	-2.191557000	0.069164000
1	0.370015000	6.712315000	0.032724000	1	-9.926506000	1.323189000	0.050247000
6	-1.690280000	5.942180000	0.002488000	1	-10.761953000	-0.858730000	0.083250000
1	-2.317748000	6.823704000	0.040984000	1	-9.590466000	-2.880451000	0.095957000
6	-2.159672000	4.560204000	-0.046123000	1	-7.718399000	2.039452000	0.021882000
6	-3.447990000	4.068665000	-0.025249000	1	-7.296488000	-3.237190000	0.078806000
1	-4.275731000	4.774763000	0.012039000				
6	-3.738816000	2.670479000	-0.032690000				